Evaluation of Critical and Essential Concrete Highway Bridges in a Moderate Seismic Hazard

by

Jordan L. Panzer

A thesis submitted to the Graduate Faculty of
Auburn University
in partial fulfillment of the
requirements for the Degree of
Master of Civil Engineering

Auburn, Alabama
May 3, 2014

Approved by

Justin D. Marshall, Ph.D., P.E., Chair, Assistant Professor of Civil Engineering
J. Brian Anderson, Ph.D., P.E., Associate Professor of Civil Engineering
Robert W. Barnes, Ph.D., P.E., Associate Professor of Civil Engineering

Abstract

The task of this thesis is to determine if the response of critical and essential bridges designed using the AASHTO LRFD Bridge Design Specifications would meet performance requirements when subjected to the moderate seismic hazard present in the state of Alabama. The design procedures for these concrete superstructure bridges involve a displacement-based design found in the AASHTO Guide Specifications for LRFD Seismic Bridge Design. Displacement-based design procedures in bridges can provide an economical and efficient design. However, a caveat to using the displacement-based design procedures of the Guide Specifications relates to its inapplicability for critical or essential bridges. This thesis will provide an analysis of designed bridge behavior in the state, and determine if this behavior is acceptable for bridges classified as critical or essential. Recommendations and conclusions relating to design will also be provided for bridges subject to Alabama's moderate hazard.

Acknowledgements

I would like to thank the Alabama Department of Transportation for providing valuable bridge plans and designs for use in this project, as well as connection details that aided in the complicated modeling procedure undertaken in this project. This project would have been all the more difficult without these valuable documents.

I would like to thank those involved in the maintenance and updating of resources like PEER and the USGS, resources that provide valuable records of ground motions and hazard maps that help to further our knowledge of seismic behavior and phenomena.

I would like to thank Dr. Justin Marshall for his leadership and knowledge throughout this project, without his guidance this undertaking would not have been possible. He has helped many students learn to become better engineers and I am no exception.

I would like to thank the civil engineering faculty of Auburn University for always being available to answer questions especially Dr. Anderson, who provided valuable insight on all manner of geotechnical phenomena pertaining to this project.

I would like to thank all of my friends and peers that I have come to know these past six years, their support and guidance has helped me grow as a person, co-worker, and engineer. Without them I do not know if I could have accomplished any of this.

Lastly I would like to thank my family, who has always supported me in life and school. They motivate me to work hard and are a constant source of guidance. I am grateful for everything they have given me.

Table of Contents

List of Tables

List of Figures

Chapter 1: Introduction

1.1 Problem Statement

The evaluation and determination of geologic seismic behavior and hazard is a constantly updating process. New research and updated geologic analysis technologies results in greater understanding of seismic hazards, resulting in updated codes and specifications. Recent research has resulted in an increased understanding of the seismicity of the Southeast United States. This region has been known to have a relatively low seismicity, resulting in its classification as a moderate seismic hazard zone. Alabama is one of the states in this region that has had its seismic hazard modified recently. These modifications make their way into the seismic design specifications in the form of increased seismic loads and increased seismic design categories.

The Alabama Department of Transportation (ALDOT) is currently using the 17th edition of the American Association of State Highway and Transportation (AASHTO) Standard Specifications (Standard Specifications for Highway Bridges, 2002) for the design of precast prestressed concrete bridges for the state. Originally these specifications were designed using allowable stress design (ASD) theory and have been updated to incorporate principles of Load and Resistance Factor Design (LRFD). These specifications, however, have not been updated since 2002. As a result of this lack of updating, ALDOT has been forced to adopt a new bridge design specification. The new design specifications selected were the AASHTO LRFD Design Specifications (LRFD

Bridge Design Specifications, 2009), these specifications are based on LRFD principles and regularly updated with the help of new research. Major changes in the recent specifications revolve around the area of seismic design, prompting an update to ALDOT's seismic design criteria.

1.2 Problem Overview

In an effort to update seismic bridge design procedures, the Alabama Department of Transportation (ALDOT) has investigated the use of the AASHTO Guide Specifications for LRFD Seismic Bridge Design (AASHTO, 2011). This document uses displacement-based criteria in the seismic design of highway bridges. The document was created for use in any region of the United States, and has been tailored to account for the most seismically active zones. A downside to using this document is its exclusion of criteria for performance of "critical" and "essential" bridges. These bridge classifications are determined based on the bridge's role as a transportation lifeline after a major destructive event.

ALDOT requested that a study and analysis be performed on various highway bridges designed according to the guide specifications. These analyses assess the behavior and performance of each of these bridges during seismic events that are scaled to the hazard present in Alabama. Results of these analyses provide a recommendation as to whether or not the Guide Specifications can be used as a design tool for critical and essential bridges in the state of Alabama. The following document provides an overview of the work done leading up to the bridge analysis, as well as the analysis itself and the conclusions and recommendations obtained from the results of the analysis. The next

chapter of this thesis provides a background for recent seismic bridge damage found around the world, as well as the bridge behaviors seen during seismic events. This chapter also provides information regarding seismic hazards in Alabama. The third chapter of this thesis provides an overview of the methodology and procedure used in the analyses performed for the presented research. Modeling decisions and hazard evaluation/selection are also presented in this chapter. The fourth chapter of this thesis presents the results taken from the analyses performed, as well as indicated some of the key pieces of data that relate to bridge performance during seismic events. The final chapter of this thesis provides conclusions and recommendations obtained from analysis of the observed results of this research.

Chapter 2: Literature Review

2.1 Bridges in Seismic Events

2.1.1 Function of Bridges

Bridges serve a variety of important purposes in the realm of transportation infrastructure. Bridges provide a transportation connection between two points that could not be connected using standard roadways. They are planned and engineered far in advance of construction. They are often the most expensive sections of transportation systems per mile, and are likely to control the capacity of the transportation system (Barker & Puckett, 2007). In order for a transportation system to function, all of its collective parts must function, thus if a bridge fails, the entire system fails.

Highway systems provide transportation for all ground vehicles and are used by both civilian and military ground vehicles. They provide transportation for goods, services, people and emergency services. In the event of the failure of these systems, the flow of these aforementioned items would be drastically reduced, if not halted completely. This fact illustrates the importance of preserving the functionality of these systems and their respective components.

2.1.2 Bridge Components

Typical components that are present in most bridges include girders, deck, abutments, foundations and bents/piers. The focus of this paper is on structural concrete

highway bridges, which consist of all the aforementioned components. Starting from the ground up, these bridges consist of a foundation system, connecting the soil beneath the bridge with the substructure of the bridge. This substructure consists of abutments, elements that connect roadway to the bridge, as well as vertical columns and the beams, called bent caps, which span horizontally between and connect their tops. These "Column-Bent Cap" frames are called "Bents" and serve to support the superstructure of the bridge. Standard Highway Bridge superstructures consist of reinforced concrete decking that rests on girders. These superstructures are broken into spans, sections of superstructure that are supported on either end by substructure.

In the case of the bridges in this research, a few more details can be included in the description of bridge components. The prestressed concrete girders are simply supported at each end and rest on elastomeric bearing pads. These bearing pads rest on the surface of abutments and bent caps. These pads allow for movement of the girders relative to the substructure. Girders are also given lateral stability and stiffness with the addition of cast in place reinforced concrete web walls. Both the bent caps and the columns that support them consist of cast in place reinforced concrete. These are the main components that are focused on in this paper.

2.1.3 Seismic Events

Among the many events that threaten to damage and possibly cause the failure of bridge systems, earthquakes and other seismic related phenomena have the capacity to do significant damage in many areas throughout the United States and around the world. Chen & Duan define earthquakes in *Bridge Engineering Seismic Design* as

> *"naturally occurring broad-banded vibratory ground motions that are due to a number of causes, including tectonic ground motions, volcanism, landslides, rockbursts, and man-made explosions, the most important of which are caused by the fracture and sliding of rock along tectonic faults within the Earth's crust."*

Ground motion is a primary result of earthquakes, but it is not the only impact worth mentioning. Tsunamis, like the one that occurred off the coast of Japan as a result of the 2011 Tōhoku Earthquake, can cause damage on par or greater than the resulting ground motions of earthquakes. Fissures, like those caused in Taiwan during the Chi-Chi event (September 21st, 1999), open in the soil and rock near the site of an earthquake as a result of displacement that occurs along faults, deep underground. These fissures can cause massive displacement differentials in any structure that rests above them, often resulting in large scale damage. Liquefaction is also an important event that can result in certain soil types during an earthquake. "*Liquefaction* has been widely used to describe a range of phenomena in which the strength and stiffness of a soil deposit are reduced due to the generation of pore water pressure. It occurs most commonly in loose, saturated sands" (Chen & Duan, 2000). These occurrences are difficult to account for because they are hard to accurately predict in both frequency and scale.

Earthquake ground motions also trigger other destructive events. Landslides and lateral spreading can cause damage to structures and roadways, and are produced by ground motions in certain soil conditions. Man-made disasters can also result from damage caused by ground motions, an example being the radiation leak of the Fukashima

nuclear reactor that occurred as a result of the 2011 Tōhoku Earthquake. Fires are also a common result of widespread damage in populated areas affected by large ground motions. Structural collapse can also occur in severe ground motions, resulting in massive economic costs as well as the possibility of human casualties.

Earthquakes present a large economic and safety hazard for many urban areas around the world. Regions affected by severe seismic events usually require emergency aid as well as viable ways of transporting civilians away from the areas that have become unsafe or unfit for habitation. The importance of having functioning transportation systems is highlighted in situations like this. Bridges and roadways are not immune to damage however, and steps must be taken to ensure their survival and function after seismic events.

2.1.4 Seismic Behavior of Bridges

Bridges react to ground motions in much the same way as buildings and other structures. Ground motions transfer forces into the foundation of the bridge due to the bridges natural inertial resistance to movement. These foundation forces transfer through the substructure of the bridge and eventually reach the connection between super and substructure. The forces are then transferred through the interface of the super and substructure. The result of these forces is deformation of the effected components of the bridge. This movement can be defined by a combination of displacements, velocities and accelerations.

In the case of simple highway girder bridges, some generalized behavior can be described. Due to the super-to-substructure connection consisting of friction bearing pads, it can be assumed that the superstructure slides with respect to the substructure.

The overall system behaves like two separate systems interfacing with one another at the bearing pad locations. The superstructure behaves like a stiff beam (simply supported), while the substructure behaves like a rigid frame consisting of columns and beams. The largest proportion of mass is located in the superstructure, giving it more inertial response to ground motion accelerations.

Bridges, like all structures, have certain characteristics that can be used to predict seismic behavior. Mass distribution gives an indication as to how the structure will respond to forces in the form of motion. Stiffness helps to predict the distribution of forces throughout the structure. A fundamental structural period, a parameter that dictates dynamic behavior, can be established using a relation of both of these parameters. The fundamental structural period represents a time interval of structure oscillation. If a loading function was applied to a structure whose period is similar to that of the fundamental structural period, the structure experiences a buildup of energy, often with little way of dissipating that energy. These loading cases can continue until either the stiffness or the mass of the system changes, or the properties of the loading conditions change. Cases like these can cause certain ground motions to become more damaging to certain bridges. Many highway bridges have fundamental periods within the range where earthquakes motions contain significant energy. This explains the existence of dissimilar bridges having very different responses to the same ground motion and it also highlights the importance of bridges having the ability to dissipate energy during a ground motion through the use of targeted damage zones.

2.1.5 Seismic Damage to Bridges

Seismic damage in bridges can be divided into two classes, *primary* and *secondary* damage. Primary damage is described as bridge damage caused directly by earthquake ground shaking or deformation. Secondary damage is described as bridge damage that was caused by other failures or damage that resulted from ground shaking or deformation (Chen & Duan, 2000). An example of primary damage would be a span becoming unseated as a result of ground motions, and the resulting girder damage caused by the spans impact with the ground would be considered secondary damage.

This section has emphasis placed on three critical examples of primary damage that are typically associated with earthquake bridges failures: 1) Foundation Failure, 2) Span Unseating and 3) Column Failure. Each of these failures have been documented in earthquakes around the world, and are a primary concern in bridge design, especially in regions with moderate to high seismic hazards.

Foundation failure is a broad title meant to encompass any failure of soils or foundation elements. According to Chen and Duan, reports of foundation failures during earthquakes are not very common, except for cases involving liquefaction. They do speculate that underground foundation failures may remain undetected, keeping a significant number of failures unreported. Despite being rarely reported, foundation failures remain a critical failure mode of bridges, whose importance should not be overlooked. "Foundation damage associated with liquefaction-induced lateral spreading has probably been the single greatest cause of extreme distress and collapse of bridges" (Chen & Duan, 2000). Examples of foundation failure and lateral spreading, resulting from 2010 Maule Earthquake can be seen in the following figures presented by Yen et al.

(2011). Figure 2.1 displays a bridge abutment that has displaced enough to have separated from one of its support piles. Figure 2.2 contains a photograph taken of the settlement of a bridge foundation; this bridge, the eastern approach to Llacolen bridge, is discussed later in this section due to a span unseating. Examples of foundation settlement that did not result in bridge collapse can be found in Figure 2.3 and Figure 2.4. An example of lateral spreading can be seen in Figure 2.5, which can cause additional foundation loading pressures.

Figure 2.1: Overview of damage to south abutment of Tubul bridge (Yen, et al. 2011)

Figure 2.2: Ground settlement and lateral movement of eastern approach to Llacolen bridge (Yen, et al. 2011)

Figure 2.3: Column settlement under approach to Juan Pablo II bridge (Yen, et al. 2011)

Figure 2.4: Differential settlement underneath first span over water at northern end of Juan Pablo II bridge (Yen, et al. 2011)

Figure 2.5: Lateral spreading and ground failure at old Ramadillas bridge (Yen, et al. 2011)

Unseating of spans is a commonly observed phenomenon in bridges that fail during earthquakes. This behavior is especially prevalent in simply supported bridges with shorter spans and seat widths. Unseating refers to the girders of a span becoming displaced to a large enough degree resulting in a complete loss of vertical support provided by the bent cap that they are resting on. This situation results in a massive loss in vertical strength and overall stability for the span, and can cause other elements of a bridge to become damaged or fail. If enough of the girders experience unseating, a total collapse of the span may occur.

Earthquakes that occurred in California during the 80s and 90s highlighted this downside of simply supported, simple span bridges and resulted in design changes away from these types of bridges. These types of failures have also been observed around the world in recent years. The Baihwa Bridge, a reinforced concrete bridge with a 500 meter

long viaduct and a height of 30 meters was constructed in 2004 in China, experienced a span unseating and collapse during the 2008 Wenchuan Earthquake. This unseated slab can be seen in Figure 2.6. Reconnaissance indicated that a lack of sufficient support length along with insufficient restrainers was observed for this bridge, as well as other damaged bridges in the region (Lin, et al. 2008). An eastern approach span of the Llacolen Bridge and multiple spans of the Tubul Bridge in Concepción, Chile experienced span unseating during the 2010 Maule Earthquake as seen in Figure 2.7 and 2.8 (Yen, et al. 2011).

Figure 2.6: The unseated slab of Baihwa Bridge (Lin, et al. 2008)

Figure 2.7: Unseating of simply supported span in eastern approach to Llacolen Bridge (Yen, et al. 2011)

Figure 2.8: Unseated spans of the Tubul Bridge (Yen, et al. 2011)

Modern seismic design practices in bridge engineering seek to allow displacement and inelasticity to absorb and dissipate energy from ground motions. Columns are designed to contain areas of high ductility that will form plastic hinges during ground motions. These plastic hinge zones rely on strong connecting elements (e.g., bent caps, foundations) to allow yielding to the hinge zone without failure of other elements. If this behavior does not occur properly a non-ductile column or connection failure could result.

Column failure is the last damage case discussed in this Chapter. Failure of a load carrying member, such as a column, can result in severe damage to total failure of a bridge. Column failure is often the primary cause of bridge collapse (Chen & Duan, 2000). In regions of high seismicity it is important to design and detail reinforced concrete columns with ductility and inelastic deformation in mind. Most damage to columns can be attributed to inadequate detailing, resulting in limited deformation capacity and energy dissipation. Detailing inadequacies can produce many different failures within a column, including a combination of flexural, shear, splice or anchorage failures (Chen & Duan, 2000). Proper detailing is meant to provide both flexural strength, as well as shear strength to a column. A flexural failure of a column occurs when the column rotational capacity is exceeded, either by strong ground motions or

excessive deflections of the bridge. Flexural failures can be identified by broken or elongated rebar seen at hinge zones, as well as rebar completely uncoupled from any concrete. An example of a flexural column failure can be seen in Figure 2.7 as a result of the 2011 Christchurch Earthquake, this particular column first experienced shear failure that weakened it, resulting in a flexural failure due to rebar buckling (Wotherspoon, et al. 2011). A shear failure occurs in a column when the shear resistance of the column is exceeded; a difficult failure to design for given that the shear strength of a column can be diminished during a bridges response to a ground motion. Another factor that makes designing for shear failure difficult is the fact that the shear forces resisted by a column relate directly to the stiffness of the bridge, thus a stronger column will be subjected to a larger shear force. Shear failures are identified by steep diagonal cracking throughout the center or "core" of a reinforced concrete column. These cracks extend throughout the entire diameter of the core, and in some cases completely dilate the core into discrete blocks of concrete (Chen & Duan, 2000). An example of shear failure can be seen in Figure 2.8, in the case of a column supporting the Juan Pablo II Bridge in Concepción, Chile.

Figure 2.9: Moorehouse Avenue Overbridge pier flexural buckling failure (Wotherspoon, et al. 2011)

Figure 2.10: Shear failure in column at north end of Juan Pablo II Bridge (Yen, et al. 2011)

2.2 Modeling and Analysis Method

The focus of this project involved analyzing the behavior of specific bridges modeled using computer software. The software chosen was CSIBridge 15, a structural design and analysis program with the capability of nonlinear dynamic response history analysis (Computer and Structures Inc., 2012). Given the need for an accurate model of

bridge behavior during ground motions, as well as accurate analysis of nonlinear elements, the Time-History Analysis method was selected for use in this project. This method requires accurate bridge information (Structural and Geotechnical) from design documents, as well as an accurate suite of scaled ground motions meant to simulate earthquake events.

2.3 Ground Motion Selection

Time history analyses of nonlinear structures require an input of acceleration data in order to function. Many factors are involved in the selection of acceleration data, chief among them being probable hazard associated with the location of the structure being analyzed. Section 5.4.4 of AASHTO's guide specifications states the requirements for a Nonlinear Time History Method Analysis (NTHM). AASHTO requires at least three ground motions be used for NTHM, with less stringent performance requirements being placed on analysis involving seven or more (AASHTO, 2011). For this particular project a range of seven to ten ground motions were selected for two different hazard levels, a design-level hazard, meant to represent the hazard of a 1,000 year event (ten selected ground motions), and a maximum credible earthquake (MCE) hazard, meant to represent the seismic hazard of a 2,500 year event (seven selected ground motions). The probabilistic exceedance of these levels are 7% in 75 years and 2% in 50 years, respectively. The selection process is similar to the process used by Rodriguez-Marek (Rodriguez-Marek, 2007).

2.3.1 Selection and Scaling

Ground motions have a variety of unique characteristics that need to be accounted for when selected for a Time History Analysis. Each ground motion needs to have similar parameters to that of the chosen hazard. Parameters like Peak Ground Acceleration (PGA), distance from the fault and site class are all used in selection of ground motions. Accepted ground motions are then scaled according to response factors discussed in the next chapter.

2.4 Modeling Considerations

Accuracy of bridge models is an important aspect of displacement-based and performance-based design. Mass and stiffness make up the majority of calculation parameters used during nonlinear time history analysis, and taking account of these parameters and how they behave is paramount. Changes in stiffness are the primary nonlinear behaviors that are accounted for in bridge models for these types of analysis. Without these behaviors, accurate results cannot be recorded.

2.5 Summary

This chapter reviewes the functions of bridges, and the role they play during a seismic event. Seismic bridge behavior and damage is been highlighted in this chapter in an effort to focus attention on key design concepts, as well as provide an overview on the complexities of seismic bridge analysis. The practices and guidelines set forth by AASHTO and other design aids take into account many different scenarios and factors in an attempt to ensure both survival and function of bridges under seismic loads. The

methodology and philosophies outlined in this chapter continue to be used throughout the remainder of this project and thesis.

Chapter 3: Analysis Procedure

3.1 Introduction

The first part of this thesis is the overview of information that has been selected for use in the project detailed within. The factors that led to the selection of ground motions, bridges, model connection designs and material behavior are all discussed, as well as simplifications that were chosen to expedite the analysis process. Information was selected using research and procedures from projects performed in the past, as well as engineering judgment.

3.2 Selection of Bridges

All bridges analyzed in this project were selected from a list of existing highway bridges in the state of Alabama. The seismic design details used in the analysis have been updated to the most recent edition of AASHTO's Guide Specifications in order to analyze designs according to current code, as well as anticipate future bridge design in the state. The bridge selection process revolved around three major factors: seismic hazard (based on location), soil condition and bridge geometry. Seven highway bridges were considered for this analysis, but only five were chosen based on the aforementioned factors.

3.2.1 Seismic Hazard

The geography of Alabama is not constant throughout, although some generalizations can be made for the purpose of this project. The southern portion of the state tends to rest on deep layers of sandy soils. These regions also tend to have little exposure to seismic activity. The hazard originates in the Northwest region of Alabama (New Madrid Fault Zone), or in the mountainous region at the border of Alabama, Georgia and Tennessee (East Tennessee Seismic Zone). Bridges in South Alabama tend to face a greater wind hazard than a seismic hazard. This information, in combination with soil conditions, led to the elimination of most of the southern bridge designs. Bridges that were selected for use in this project tended to be located in the northern section of the state where the foundation conditions were similar to what would be expected in the areas of highest seismicity. Selected bridges outside of this region still displayed characteristics consistent with bridges in the region.

3.2.2 Soil/Geologic Conditions

Geotechnical data became a defining factor in the selection of applicable bridges. Soil classifications at site locations can play a major role in overall earthquake hazard and structural performance. Soil information was included along with the bridge plans provided by ALDOT for this project. This soil information was used in the bridge selection process because it not only correlated to the bridge's location in the state, but also correlated to the foundation types used in the bridges.

Geological properties helped create expected soil conditions throughout the state in regions without specific data. Basic generalizations were determined for different

regions of the state, and helped classify bridges, as well as estimate which bridges could be designed in specific regions. The more mountainous regions of Alabama tended to have a soil layer between ten to thirty feet deep, resting on a hard rock layer. Foundations for these particular bridges consisted of drilled shafts that founded the bridge to the rock layer. Other locations in northern Alabama consisted of deeper soil layers, but still utilized similar foundation systems. Regions in central Alabama with similar soil conditions included bridges with pile group foundations, these bridges were also considered to be constructible in areas of higher seismicity, and thus were not dismissed in the selection process. The bridges selected were bridges that could be constructed in higher hazard regions of Alabama, which also contained foundations that are suitable for soil found in these regions.

3.2.3 Bridge Geometry

A bridge's geometry contributes significantly to the seismic behavior. A bridge with tall columns and long spans will have a lower stiffness compared to a bridge with shorter spans and shorter columns. In addition to component lengths, component dimensions are also a factor in bridge response. For the purpose of this project it was important to collect a range of bridge geometry in order to realistically account for a spectrum of possible bridge designs. Bridge configurations that included steel girders or concrete girders with changing thicknesses were not considered for this project. Bridges that did not include bearing pad supports were also excluded from this project due to significant analysis effort being placed on bearing pad behavior and the girder-to-cap connection.

3.2.4 Final Selection

A total of five bridge designs were selected for use in this project, all meeting the conditions required. A list of these bridges and their locations can be seen in Table 3.1. A map of the bridge locations can be seen in Figure 3.1. The Little Bear Creek Bridge was selected due to its location in the North West corner of the state, as well as its usage of two different girder sizes and bearing pad sizes along its three spans. These discontinuities provided unique dynamic behavior, like a tendency for a structure to deviate from its first mode shape. The soil conditions at this particular site consisted of a relatively shallow soil layer, as to be expected in this region of the state.

Table 3.1: Bridge Locations

Number	Bridge	Location
1	Little Bear Creek	Russellville
2	Scarham Creek	Albertville
3	Norfolk Southern RR	Gadsden
4	Oseligee Creek	Lanett
5	Bent Creek Road	Auburn

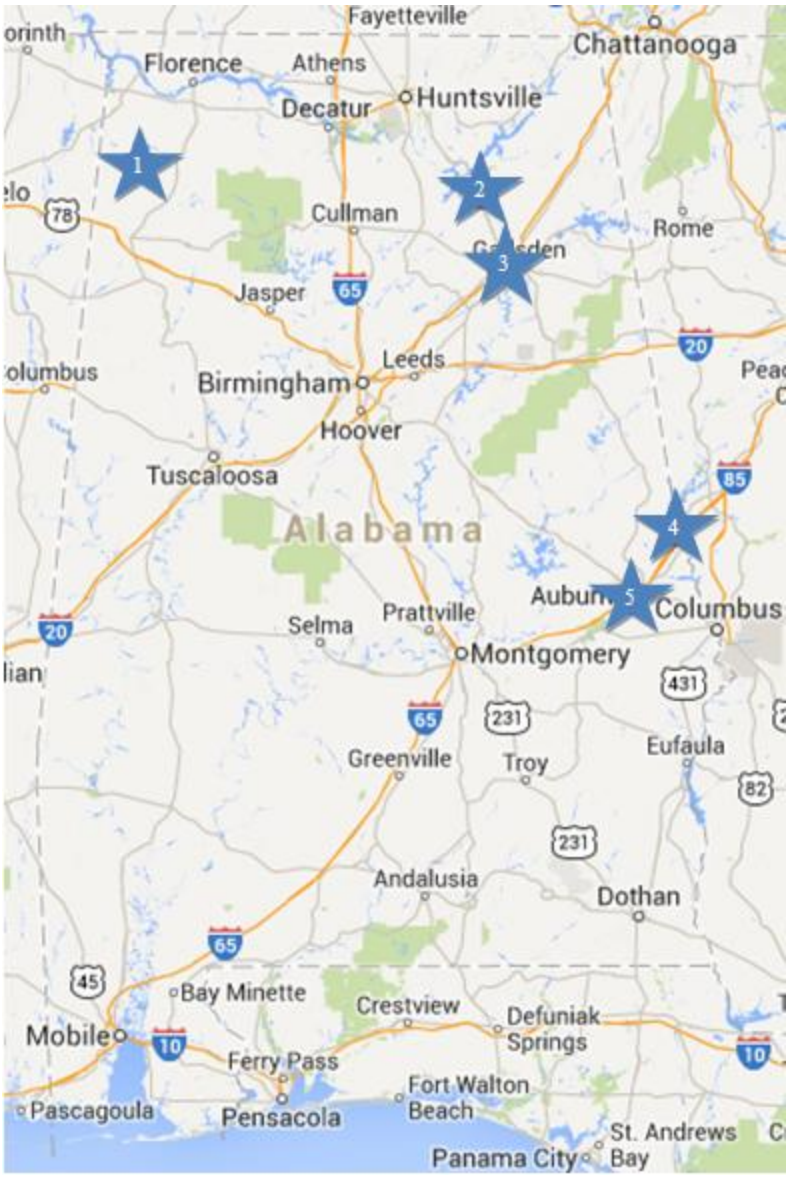

Figure 3.11: Bridge Locations

The Scarham Creek Bridge was the second bridge selected for this project. The Scarham Bridge contained the tallest and largest bent columns, making it one of the more flexible bridges. Concrete struts were used in the bent design in an effort to reduce the unbraced length of the columns. These struts presented a unique opportunity for dynamic element observation, since they appeared to have been overdesigned for the purpose of stability and safety. Overdesigns like these can actually become harmful to earthquake

response if members are not detailed accordingly, so this condition made this particular bridge an important one to analyze. The site conditions remain typical for the region, and the bridge is supported by drilled shaft foundations.

The third bridge that was selected was the Norfolk Southern Railroad Bridge, a section of I-59 that spans above railroad tracks. The geometry of the Norfolk Bridge represents a typical highway bridge. It consists of two similar spans supported by a typical three column bridge bent. The soil conditions present at this location resulted in the bridge being supported on a driven pile group footing foundations. This was the first bridge selected with these foundations, as well as being the first bridge selected that uses rectangular columns instead of circular columns.

The first bridge selected outside of the northern area of Alabama was the Oseligee Creek Bridge. This bridge consists of three evenly spaced 80 ft. spans that are supported by two column bents. The foundation of the bridge consists of driven pile foundations that extend all the way to bedrock. Soil at this location was determined to have poor strength, and showed susceptibility to scour. The geometry of this bridge was an important factor in the selection of this bridge, but its soil conditions may cause it to behave differently than expected.

The last and largest bridge selected for these analyses was the Bent Creek Bridge, located in Lee County. This bridge contains two bridge spans supported by fifteen girders each and a single five column bridge bent. The mass and stiffness associated with this bridge made it an attractive option for analysis within this project. The bridge itself is not located in a region of seismicity, but it was deemed plausible that this design could be reused in a more seismic region of Alabama. Some of the drawbacks regarding a

bridge this size involve modeling concerns. This is the second bridge to be supported on a pile footing foundations.

3.3 Selection of Ground Motions

After the selection of bridges is performed, a determination of seismic hazard and the ground motions that represent them must be performed. A total of ten scaled ground motions (GMs) were selected for the worst design-level hazard present in the state of Alabama. The procedure used to select these ground motions involved the following tasks:

1. Perform a probabilistic seismic hazard analysis (PSHA) for each hazard location.
2. Collect GMs that contain values and properties similar to those highlighted by the PSHA.
3. Obtain a design spectra for the locations from the PSHA based on a Uniform Hazard Spectrum (UHS) with a probability of exceedance of 7% in 75 years.
4. Select 7-12 GMs with a spectral shape that best match the UHS.
5. Apply scaling to the ground motions from (3) to fit the target spectra obtained from (2).

3.3.1 Probable Seismic Hazard Analysis (PSHA)

The PSH analyses for this project were performed using the tools provided by the United States Geological Survey (USGS) (https://geohazards.usgs.gov/deaggint/2008/). Details regarding the specifics of the procedures and calculations used by these tools can be found at the USGS website (USGS 2013). A PSHA requires some information to run,

including site location, shear wave velocity of the top 30 meters of a soil (V_{s30}), and a seismic event return period for the hazard. A V_{s30} of 760 m/s, corresponding to a site class of B, was selected for Alabama, and a return period of 1000 years was selected, being input as a 5% exceedance probability in the next 50 years (similar return period correlating to the 7% exceedance in the next 75 years as specified in AASHTO). The results of a PSHA analysis can be seen in the form of a deaggregation plot which allows the user to see the contributions from faults and other sources projected onto a 3–dimensional plot. The horizontal axis of the plot represents event magnitude; the vertical axis of the plot represents distance between event epicenter and location. The height of each bar represents the portion of contribution an event has towards the hazard of a location. Figure 3.2 displays the deaggregation plot for Muscle Shoals, Alabama.

From a PSHA performed for four different locations in Alabama, it was determined that the two locations that had the highest seismic hazards were the northeast and northwest corners of the state, with a probabilistic peak ground acceleration (PGA) of 0.09095g and 0.07557g, respectively. It can be observed in Figure 3.3 that Bridgeport experiences a bimodal distribution meaning that the hazard is defined primarily by a magnitude 5-5.5 earthquake at a distance of 50 km (30 miles) or a magnitude 7.5-8 at a distance of 350 km (210 miles). Using this information, a bin of about 40 earthquakes was selected using the Pacific Earthquake Engineering Research (PEER) Center database, a collection of ground motions recorded around the world. These ground motions were then sorted by various parameters such as distance from fault, event magnitude, ground conditions, response spectrum behavior and PGA.

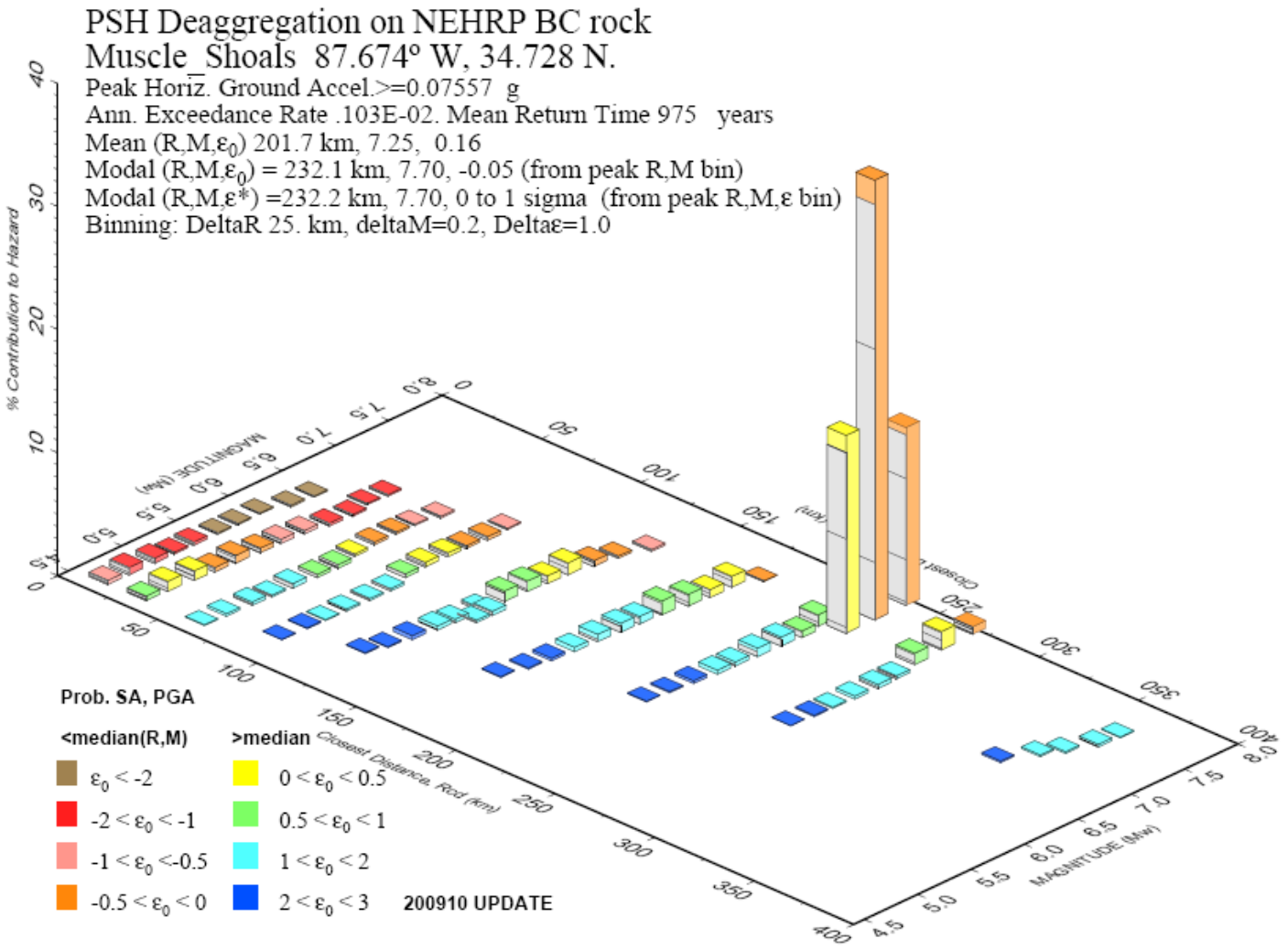

Figure 3.2: Deaggregation Plot for Muscle Shoals, AL

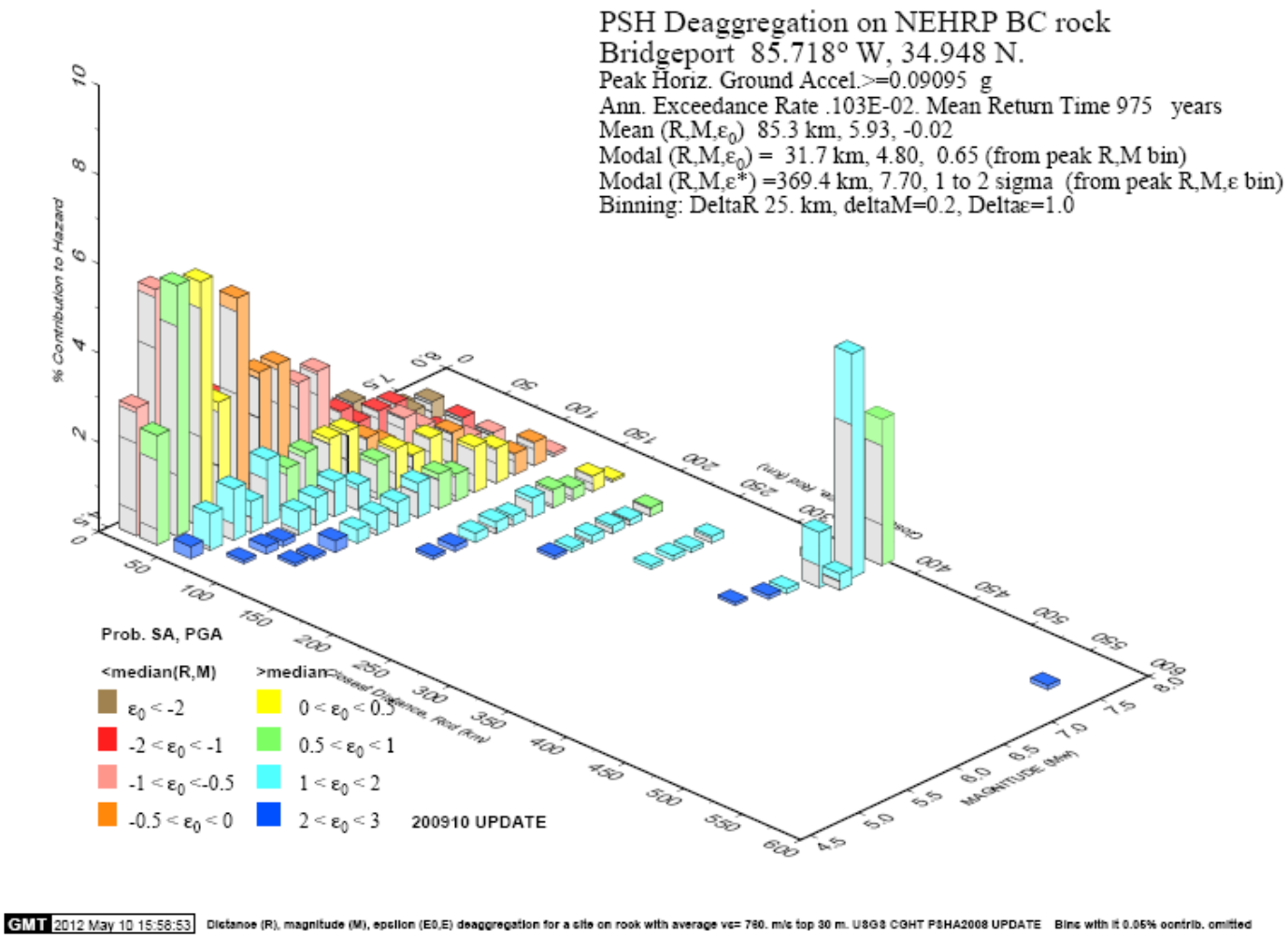

Figure 3.3: Deaggregation Plot for Bridgeport, AL

3.3.2 Uniform Hazard Spectrum (UHS)

A UHS was calculated for the two most critical locations in Alabama in the form of a Design Response Spectrum (DRS). These DRSs were calculated using maps and equations present in Section 3.4 of AASHTO's Guide Specifications. The two locations selected for the creation of a UHS were Bridgeport, Alabama and Muscle Shoals, Alabama. Both locations were assumed to have soil corresponding to a site class C. Table 3.2 provides the site data obtained from AASHTO's ground motion maps. Natural bridge periods were assumed to be in the range of zero to three seconds, and the UHS was plotted accordingly. The target spectra for the bridges are displayed in Figure 3.4 and Figure 3.5 which shows that the hazard spectra for the two sites and the resulting average response from the ground motions selected in the next section of this chapter. It can be observed that the DRS for each site remain similar to the other, despite the geographic distance between the two sites. The DRS for Muscle Shoals shows a greater hazard for bridges of higher periods, while the Bridgeport site shows slightly larger hazard for stiffer bridges. This behavior can be explained by the expected event distance between event epicenter and site location, with close proximity events typically producing motions with higher frequencies. These higher frequencies motions tend to produce higher responses in stiff structures; however these high frequency motions dissipate energy as they travel. Longer frequency motions tend to travel longer distances and produce higher responses in flexible structures. Due to the different hazards present for the state, both DRS's were used in the ground motion scaling process.

Table 3.2: Hazard Map Data

Hazard Location	Values from map (g)			Site coefficients			Final Acceleration Values		
	PGA	S_s	S_1	F_{PGA}	F_a	F_v	A_s	S_{DS}	S_{D1}
Bridgeport, AL	0.111	0.221	0.068	1.2	1.2	1.7	0.1332	0.2652	0.1156
Florence, AL	0.089	0.213	0.078	1.2	1.2	1.7	0.1068	0.2556	0.1326

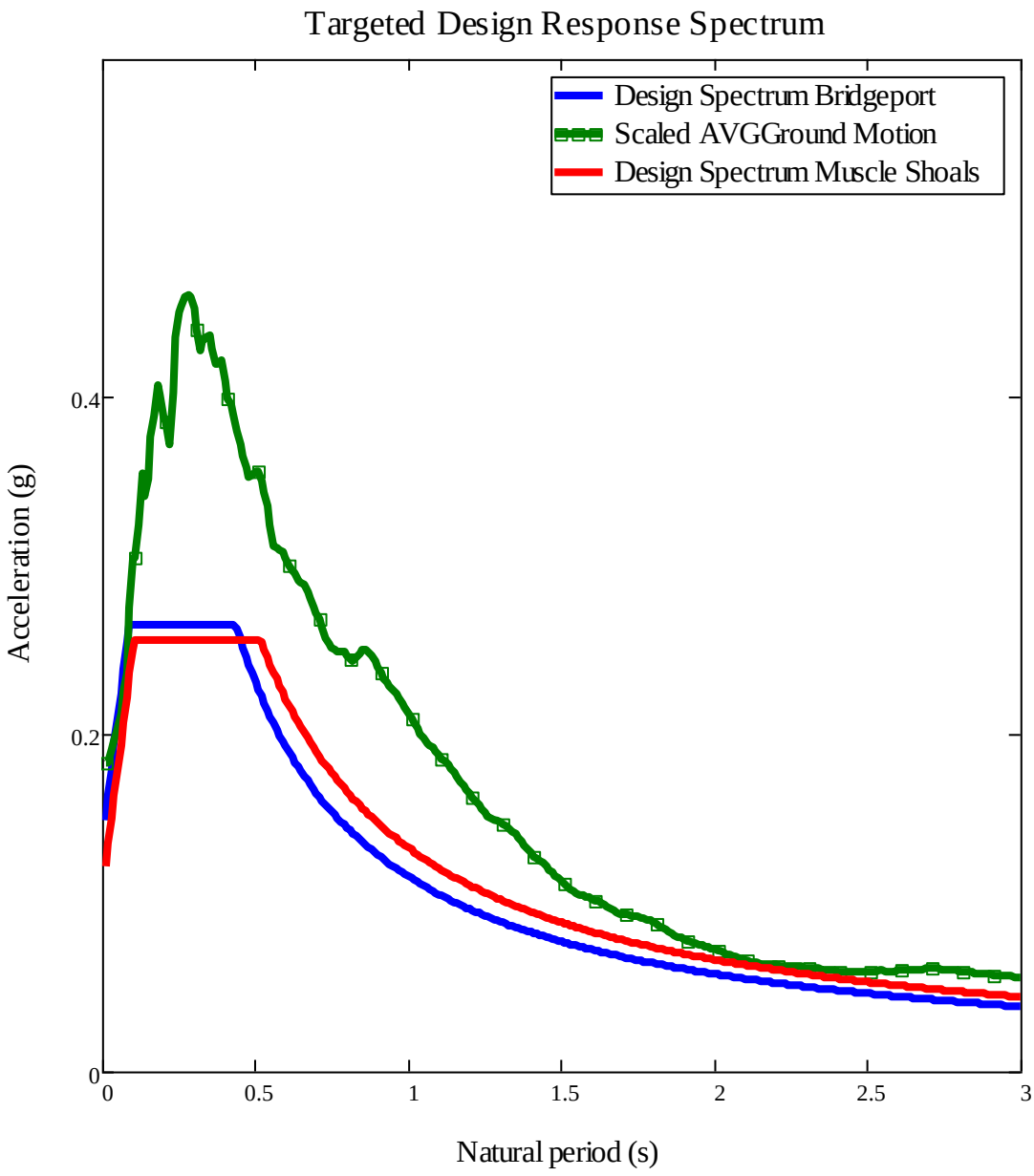

Figure 3.4: Targeted Design Spectrum

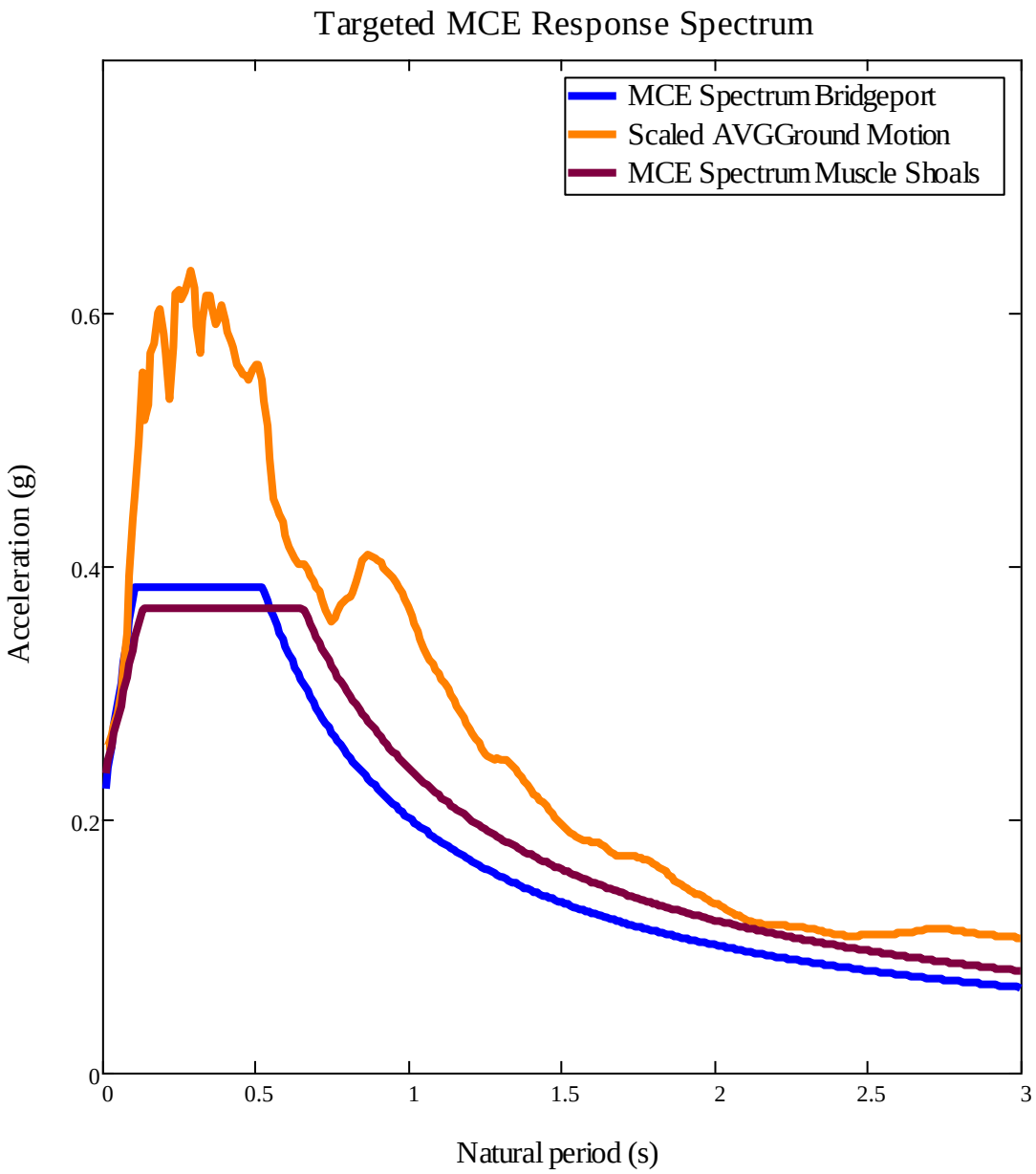

Figure 3.5: Targeted MCE Spectrum

3.3.3 Ground Motion

Initially a set of 40 ground motions were selected for possible use in this project and needed to be reduced to a set size of 7-12. The initial constraints that led to the selection of these initial 40 included the following:

1. A PGA between 0.007 and 0.020g

2. A site V_{s30} that did not correlate to a site class of A, E or F.
3. An event magnitude between 5.5 and 7.5
4. Exclusion of any subduction zone events

After an initial 40 were selected, properties of the GMs were analyzed in order to create a diverse suite of motions. The first parameter used to eliminate motions was simply to limit the number of motions used from each event. Oversaturation of a ground motion data set with many GMs taken from a single event can bias expected behaviors, as well as harm performance criteria of certain bridges that may have a unique response to the over selected event. It was decided to limit the ground motions a single event could contribute to two. This condition provided a decent reduction in the set of ground motions.

The next parameter included in GM elimination was the analysis of response spectrum produced by each GM. The behavior of each motion's RS was examined, especially between a natural period of 0.5 and 3 seconds. Values for these criteria were not specifically defined, and ground motions were eliminated based on engineering judgment. The main factor involved in this selection process was the compilation of a diverse response spectrum. Similar responses resulted in ground motions being eliminated, as well as responses deemed too weak or two severe to be feasibly incorporated into this analysis. Any GM that needed to be scaled by a factor less than 0.5 or greater than 2 was also eliminated. Table 3.3 displays some of the properties associated with the ten GMs selected for this analysis. The RS of each selected GM can be seen in Figure 3.6 and Figure 3.7, as well as their average and the DRSs for the two hazard sites in Alabama. Ground motions that represent the hazard present in Alabama

can be difficult to acquire, due to a scarcity of recorded ground motions in geological conditions found in the Eastern United States.

Table 3.3: Ground Motion Data

NGA Event #	Event	Year	Station	Magnitude	Mechanism	Rupture distance (km)	V_{s30}(m/s)
68	San Fernando 1	1971	LA - Hollywood Stor FF	6.61	Reverse	22.8	317
70	San Fernando 2	1971	Lake Hughes #1	6.61	Reverse	27.4	425
186	Imperial Valley	1979	Niland Fire Station	6.53	Strike-Slip	36.9	208
333	Coalinga-01	1983	Parkfield - Cholame 8W	6.36	Reverse	51.8	257
512	N. Palm Springs	1986	Anza - Tule Canyon	6.06	Reverse-Oblique	52.1	685
832	Landers	1992	Amboy	7.28	Strike-Slip	69.2	271
1741	Little Skull Mnt.	1992	Station #2 NTS Control Point	5.65	Normal	24.7	660
1147	Kocaeli-Turkey 1	1999	Ambarli	7.51	Strike-Slip	69.6	175
1165	Kocaeli-Turkey 2	1999	Izmit	7.51	Strike-Slip	7.2	811
1107	Kobe	1999	Kakogawa	6.9	Strike-Slip	22.5	312

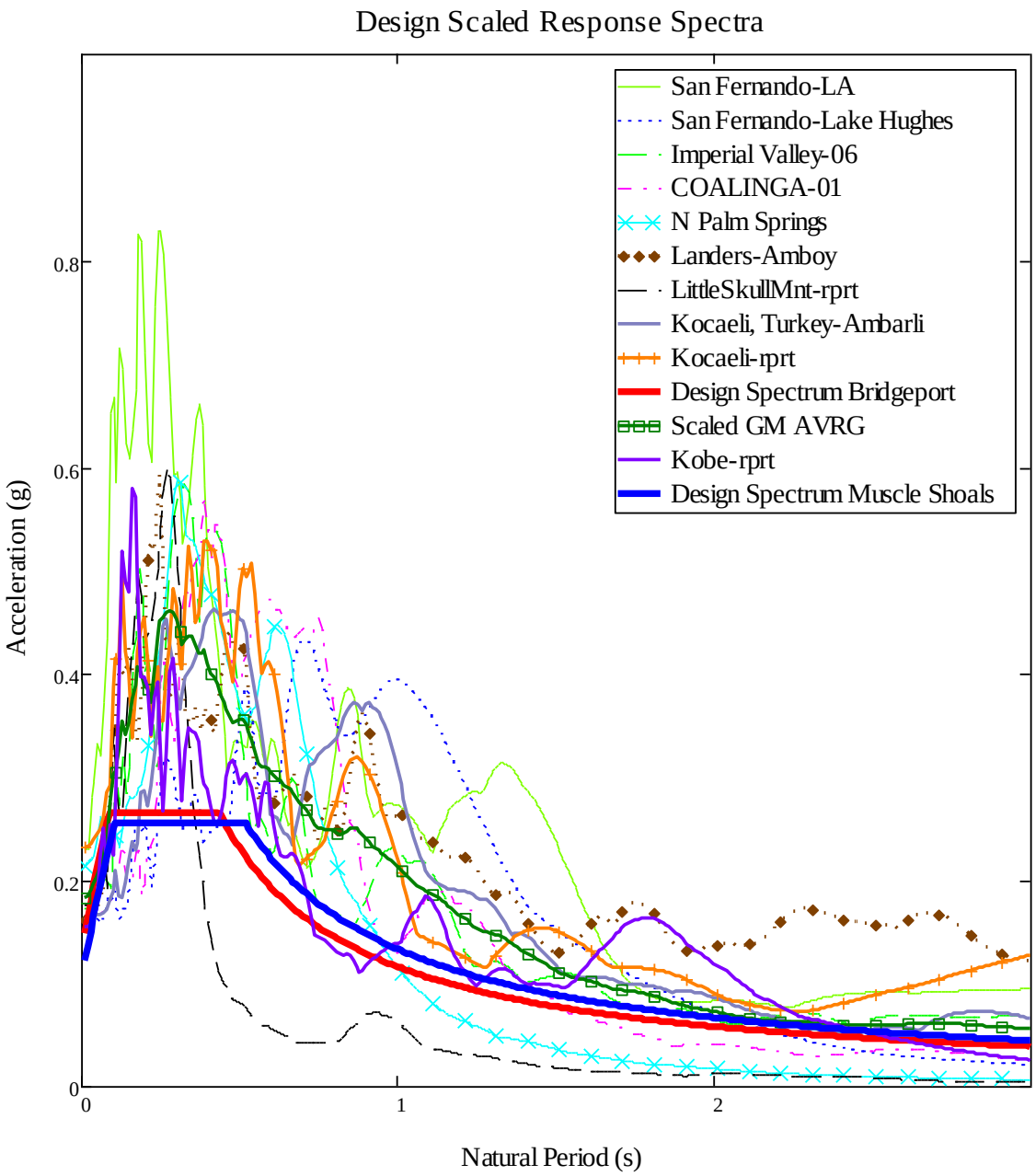

Figure 3.6: Design-Level Response Spectra

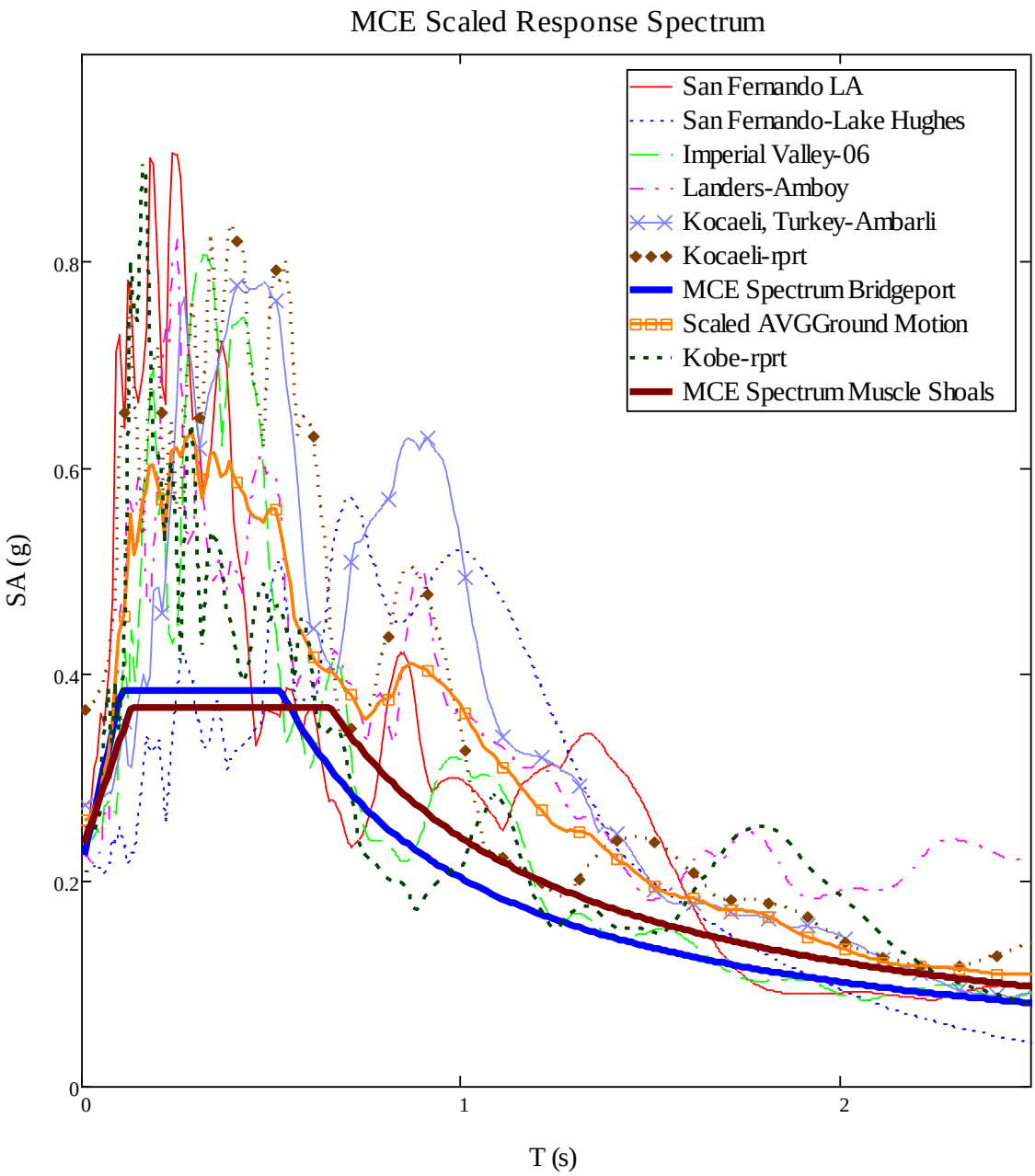

Figure 3.7: MCE-Level Response Spectra

An additional two ground motions were also initially included in the selected GMs, but have subsequently been eliminated. These ground motions were synthetic ground motions created as a prediction of future ground motions associated with a large scale New Madrid fault event. These GMs used soil conditions and behavior associated

with Memphis, and the GMs indicated behavior associated with large columns of sand, a geotechnical feature that is not associated with the regions being analyzed in this project. A list of the final ground motions selected as well as their associated scaling factors can be seen in Table 3.4.

Table 3.4: Ground Motion Scaling

Ground Motion	Design-Level Scale Factor	MCE-Level Scale Factor
San Fernando 1	1.10	1.20
San Fernando 2	1.10	1.45
Imperial Valley	1.59	2.20
Coalinga-01	1.70	-
N. Palm Springs	1.95	-
Landers	1.40	1.95
Little Skull Mnt.	1.50	-
Kocaeli- Turkey 1	0.65	1.10
Kocaeli- Turkey 2	0.95	1.50
Kobe	0.62	0.95

3.4 Selection of Modeling Elements

Computer models of existing structures, especially ones used for complicated analysis, require a balance of accuracy in geometry, behavior, and functionality. A model that includes every detail of a structure may be considered accurate, but not practical for the purpose of analysis. A structure simplified so much as to neglect important aspects of behavior may also be deemed impractical for analysis. It is with these ideas in mind that the models for this project were designed.

3.4.1 Superstructure Modeling

The bridge models were initially constructed using information taken from plans provided by ALDOT. This information helps to build the initial geometry of the entire bridge using the Bridge Designer toolbar found in CSI Bridge. This process includes the specifications of bridge spans, bents, abutments, deck geometry, girder geometry, bent cap dimensions, bent column dimensions and span support conditions. Each parameter was imported into the bridge builder as the provided designs had indicated. Once this is done a modeling option is presented that will determine the complexity of the model's superstructure. The first options present are a three dimensional meshed superstructure composed of smaller elements, representing each component of the deck, web walls and girders. A second option is that of a spine model, a model that calculates the stiffness of the overall superstructure, and simplifies it into a single beam element. The spine model also neglects inelastic behaviors that may be associated with large or deep elements. Typically elements of simply supported spans behave elastically in dynamic motions, elements like bridge decks and girders. Attempts at using the complex mesh model resulted in slow analysis with an eventual failure. This led to acceptance of the simplified spine model. The overall performance of the spine model may not contain the accuracy present in the meshed three-dimensional model, but the meshed model also accounts for and records information that would not be used at the conclusion of the analysis. Superstructure behavior was also not a cause for concern in this analysis compared to the behavior of the substructure and connections. Thus it was acceptable to use a spine approximation for modeling of the bridges in this project.

Bridges that are designed as simply supported typically contain expansion joints at support locations. These joints consist of a small gap between spans that allows for the expansion and contractions due to thermal and long term displacements as well as rotations at the end of the spans. For modeling considerations these elements needed to have their behavior represented due to their importance in longitudinal motions. This was accomplished by placing gap elements between span elements. These gap elements are specified as linear elements that only activate after they have compressed a certain distance. Once the springs are activated they function like a compression spring with a stiffness of 5000 kips/in. This stiffness is meant to transfer a large force for a small amount of compressive displacement over the entire span element. A similar procedure was also performed for the expansion joint located at the abutments.

3.4.2 Substructure Model

A primary focus of this project is the observation and analysis of substructure behavior under the effects of a design-level GMs. With this in mind special precautions were taken to ensure accurate modeling and behavioral considerations pertaining to the substructure of each bridge, beginning with the foundation. The analytical models incorporate geotechnical properties of each bridge in the form of multi-linear foundations. These foundation springs have been calculated using a static pushover analysis detailed in work done by Kane (2013). Stiffness associated with each of the six degrees of freedom is modeled at each foundation location. These multi-linear springs do not contain a specific failure limit, due to the behavior of the spring elements in CSIBridge. The foundation displacements must be noted for final analysis in order to

determine whether the displacements and rotations exceeded those generated in the soil-structure interaction model.

Columns represent the next aspect of the bridge models that needed to be carefully modeled. Column behavior in bridges is highly dependent on accurate detailing of the column and its connections to other elements. For this analysis it was assumed that detailing in the columns is consistent with that specified by AASHTO. Accurate detailing within columns results in ductile plastic hinging at points determined by AASHTO. These hinges and their behavior are accounted for in the bridge models using the "define hinge function". Hinges are placed within the columns at select points and with defined lengths. Hinges are specified to account for multiple directions of behavior, as well as different controlling behavior limits. Shear hinges behave in the directions of shear and act as a sudden, non-ductile failure. Shear hinges were considered later on in this project, but for a different element. The behavior needed for plastic hinges in columns results from a ductile interacting flexural-axial hinge. This hinge type accounts for rotational and axial behavior within the element. This hinge type was selected for the purpose of this analysis; however this particular hinge type is subdivided further by which directional movement it should include as well as which method is used for behavior determination. A biaxial direction was selected due to its more accurate application in a model that is subjected to dynamic GMs in two different global directions. The selection of behavioral analysis method for the column is a more complex issue that required supplementary study and testing.

The first option that was applicable for hinge analysis was the use of a Caltrans specified hinge. This particular hinge type uses a simplification to determine various

capacities of a plastic hinge in an effort to alleviate design computations as well as provide a conservative estimation of hinge behavior. The backbone curve for a Caltrans Hinge can be seen in Figure 3.8 and can be observed to display a linear elastic behavior at low rotations, followed by a sequence of inelastic behaviors meant to represent yielding and eventual failure of a hinge. It is recommended that significant hysteresis should be avoided when using Caltrans Hinges in dynamic analysis (Computers & Structures inc. 2012). An analysis was performed on a simple reinforced concrete moment frame using Caltrans Hinges. The frame was loaded with a lateral force and results were measured to determine the applicability of the Caltrans Hinge compared to the second hinge analysis option, the Fiber Hinge.

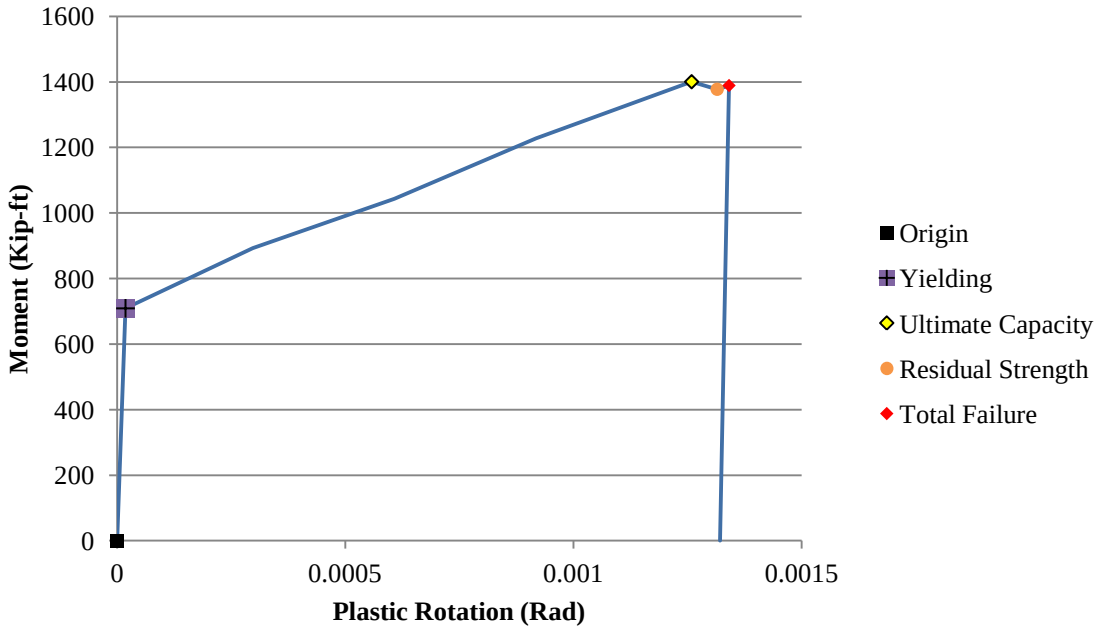

Figure 3.8: Idealized Caltrans Hinge

A Fiber Hinge analysis is a type of finite element analysis used in the determination of hinge behaviors and capacities. It operates under the theory that a real structural element can be modeled as a collection of smaller individual elements, and that

the smaller the individual elements get, the more accurate the behavior of the collection of elements becomes. The fiber hinge model is the more complex option among the two hinge analyses. Sections of the cross section of a member are divided into sections of concrete and steel. Each section is analyzed based on the material properties and location of each fiber in order to determine cross-section behavior and capacities at given loading conditions. Figure 3.9 displays a backbone curve resulting from a fiber hinge analysis. "The fiber-hinge model is more accurate in that the nonlinear material relationship of each fiber automatically accounts for interaction, changes in moment-rotation curve, and plastic axial strain. A trade-off is that fiber application is more computationally intensive" (Computers & Structures inc., 2012).

An analysis was performed on a simple reinforced concrete moment frame using plastic hinges. The frame was loaded with a lateral force and results were compared to that of the Caltrans Hinge. The resulting capacities were similar, indicating that both hinges estimated similar strengths; however, the displacements indicated that the fiber hinge was a much more rotationally flexible hinge. It was determined that both hinge types were viable and later testing would show that fiber hinges resulted in more favorable numerical analysis behavior.

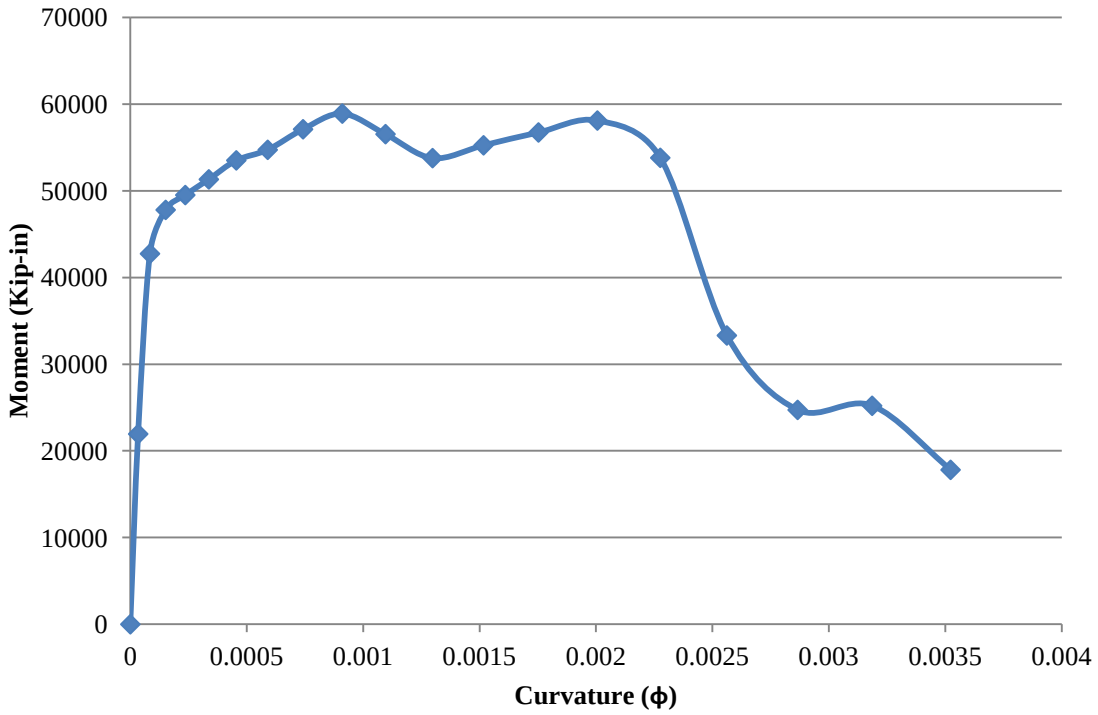

Figure 3.9: Fiber Analysis Backbone Curve

In order to use a plastic hinge in modeling, characteristics of the hinging element need to be specified in detail. A typical frame element in CSI Bridge and SAP 2000 can be specified with just cross-section geometry, concrete strength, reinforcement layout and steel properties. An accurate hinge will require a more in-depth property specification. The Section Designer tool was used to create columns in the modeling for this project. Column designs included specification of longitudinal and shear reinforcement as well as spacing and clear cover distances. Concrete was subdivided into confined and unconfined sections to be analyzed using the Mander-Confined and Mander-Unconfined concrete properties. An axial load was also specified on the columns in the creation of a backbone curve for each section. These properties help to establish nonlinear behavior where nonlinear behavior is expected.

Bent caps and abutments, the last remaining substructure elements, were modeled as elastic frame elements. They are assumed to have adequate detailing and design strength to avoid any nonlinear hinging that may cause instabilities in the bridge structure. The size of these elements depth and stiffness should allow them to resist moments transferred from the bent columns, allowing the use of this assumption. Abutments were also assumed to be supported with fixed foundation connections for the purpose of this project. This property was determined when the geotechnical behavior of these elements was not considered a major concern for this project.

3.4.3 Connection Modeling

In addition to substructure behavior, connection behavior between the super- and substructure was also a primary focus in this analysis. Special attention was paid to the behavior occurring in this region, and the impact each of these behaviors contributed to that of the overall bridge. As stated in Section 2.1.2, the bridges in this project all contain a girder-to-elastomeric bearing pad connection at the end of each span. This connection detail can be seen in Figure 3.10. Each of these bearing pads is made from layers of elastomeric material interspersed with thin steel plates (steel shims). These shims act to reduce bulging of the elastomeric material when subjected to vertical loads by limiting the thickness of each individual layer of elastomeric material. It is with this in mind that all bearing pads are initially selected, meaning that the overall thickness of a single bearing pad is determined from the amount of vertical load that it is designed to resist. Additional design is performed in regards to rotational capacity of the girders along with bearing pad dimensions allowing for enough longitudinal girder expansion/contraction.

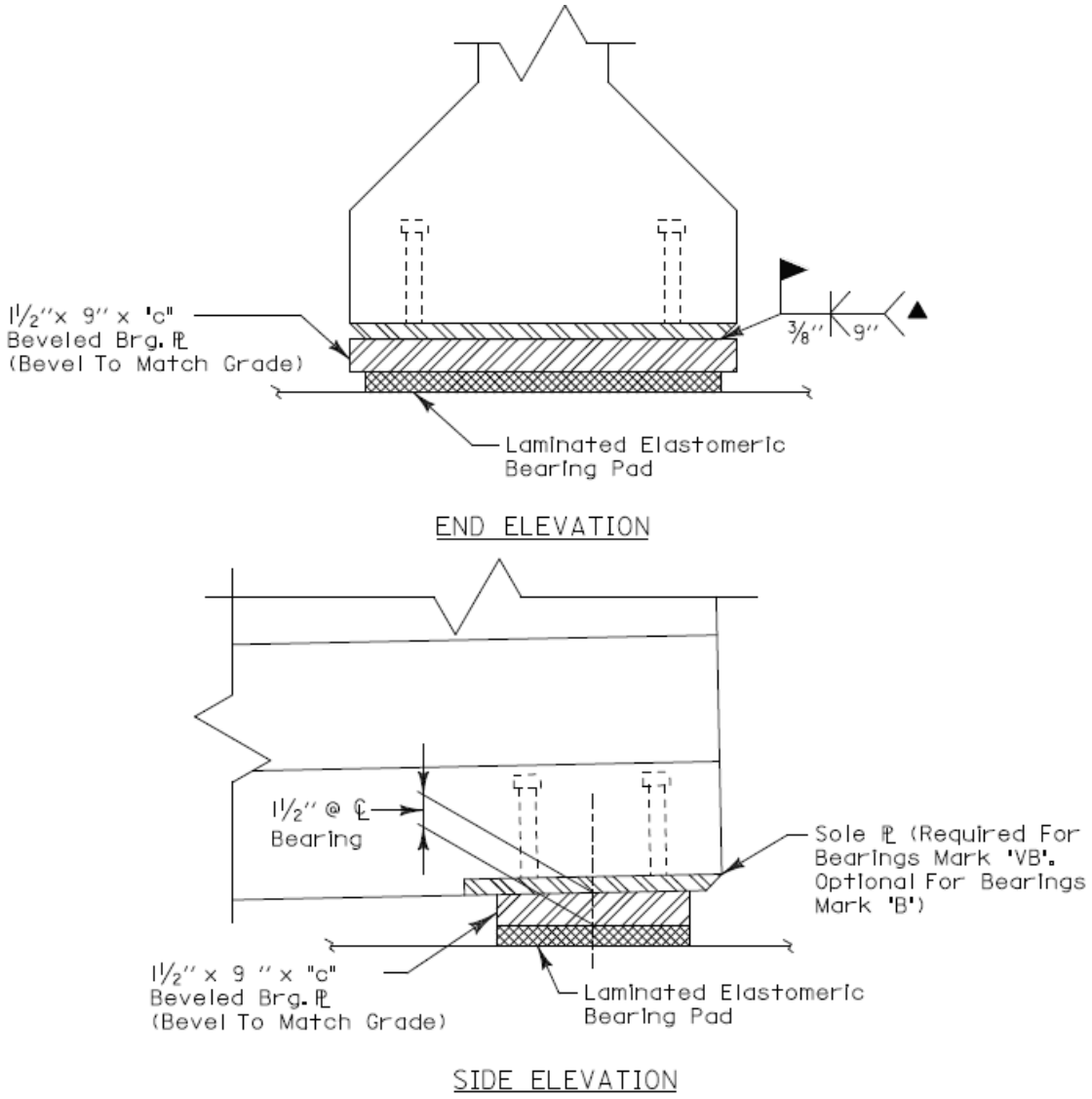

Figure 3.10: Example Bearing Pad Configuration (Alabama DOT, 2012)

Elastomeric bearing pad thickness results in more flexible behavior during lateral shearing, regardless of the number of steel shims. An elastomeric bridge bearing's deformation in a lateral direction can be determined according to Equation 3.1. The dimensions of each bearing pad are extrapolated from bridge design drawings, and a Shear Modulus (G) of 135 psi was selected from values found in a Caltrans design memo (Caltrans, 1994). The deflection equation will eventually change at larger forces, but can be used for the purpose of modeling because the shear experienced in these bearing pads

are limited to a ceiling value determined by eventual slipping between the bearing pad and the girder. A force-displacement relationship for a bearing in shear can be seen in Figure 3.11, with a plateau being reached at the point of slipping.

Equation 3.1

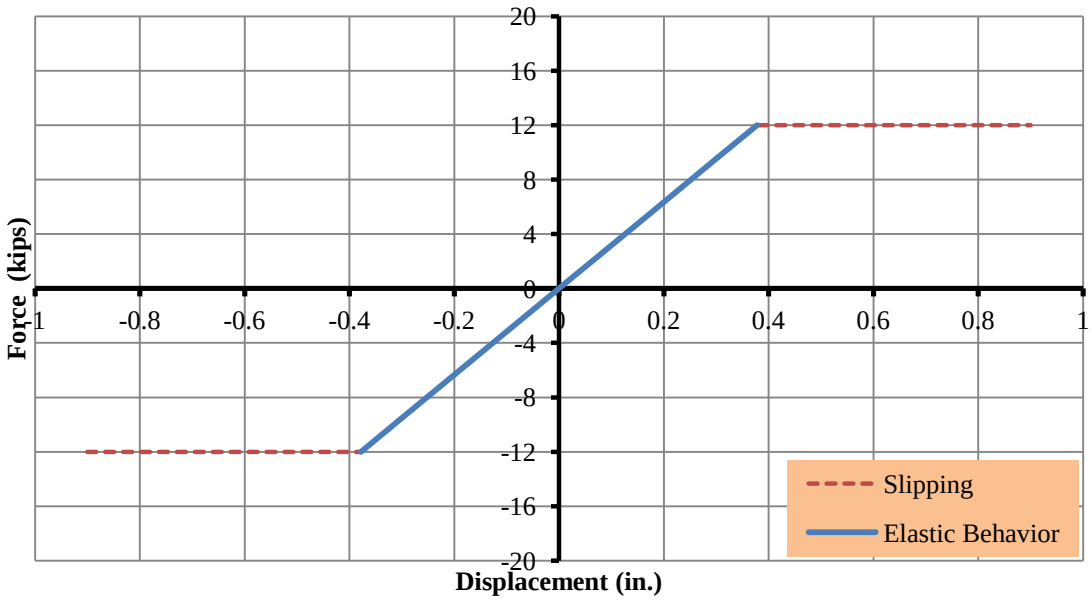

Figure 3.11: Example Bearing Pad Force-Displacement Relationship

Research performed on a connection detail in use by the Illinois DOT, similar the one used by ALDOT, observed a friction coefficient between 0.2 and 0.5 in its bearing pad-steel plate friction connection; however, cyclical loading resulted in reduced values due to degradation of the rigidness of the bearing pad surface (Steelman, et al. 2012). Dynamic friction coefficients of 0.2 and 0.4 were selected for a lower and upper bound in this analysis. The process of implementation can be found later in this chapter. All of these factors contributed to the creating of force-displacement plots for each bearing bad in use for this project, and these plots were implemented into the model using multi-

elastic plastic kinetic link elements. The "kinetic" distinction of these link elements refers to the behavior these links exhibit during unloading. A plastic link element recognizes unloading of a link and follows a different stiffness than the one used in the loading process. The manner of which an unloading stiffness is determined varies depending on the type of plastic link, with "kinetic" most closely describing the behavior of a friction connection.

Each bridge model is meant to be loaded in a longitudinal direction (direction of travel) and a transverse direction (perpendicular to direction of travel). The connection that resists motion in the longitudinal direction consists solely of a bearing pad, but there is an additional connection detail in the lateral direction that is also considered in the model. Figure 3.12 displays a view of ALDOT's typical connection, consisting of both a bearing pad and a clip angle with anchor bolts meant to limit movement in the lateral direction. This clip angle system consists of steel clip angles fastened to the girder via small threaded inserts and fastened to either abutments or bent caps via anchor bolts. For the purpose of this analysis it is assumed that the small threaded inserts that transfer longitudinal or tensile forces from girder to clip angle are not sufficiently embedded within the girder to provide any real resistance. This configuration results in a single-level longitudinal connection system; however, the anchor bolt provides the clip angles with sufficient stiffness to resist transverse forces when the movement is towards the angle. The overall failure of this clip angle system is determined to occur when the anchor bolts have experienced nominal shear strength capacity. This limit state was deemed conservative, and also selected above a failure state of the clip angles themselves due to the girders eventual collision with the anchor bolt in the event of a clip angle

failure. Equation 3.2 was used to determine the shear capacity of an anchor bolt, assuming adequate embedment was provided for the bolt.

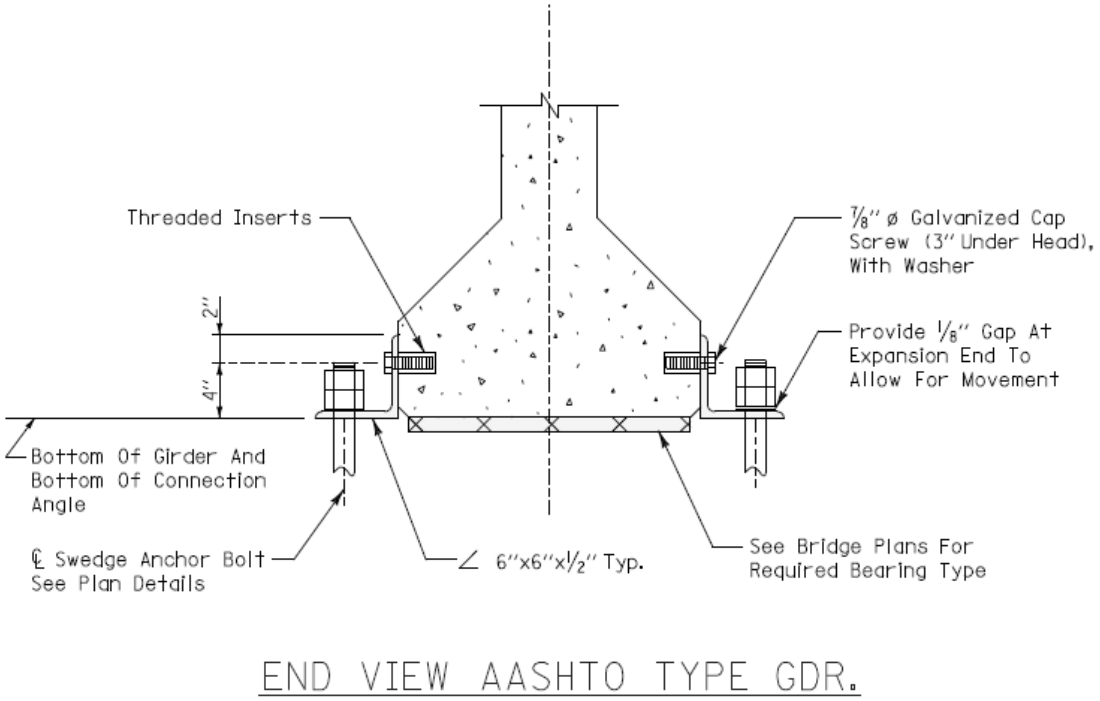

Figure 3.12: Clip Angle Connection Detail

Equation 3.2

Modeling the anchor bolt's contribution to the total bridge model connection proved to be a difficult challenge. Several options were attempted that appeared accurate in both behavior and geometry. The first option was the creation a frame element that acted as a fuse element, failing in shear. The frame element would act in parallel with the bearing pad link, and contain a shear hinge. This initial option was modified to incorporate two frame elements acting in parallel with one another, and connected to the bearing pad link via gap links. These gap links allow only one frame element to be

loaded in shear for each direction of transverse movement. Theoretically this system would mimic the real life behavior of the bridge during transverse movement in an accurate way. The implementation of this modeling option proved to behave differently than anticipated. Shear hinging resulted in the element being split into two different elements causing instabilities in the analysis, as well as the frame elements collecting additional forces and moments despite releases being implemented into the system as a measure of preventing that behavior from occurring.

The second option implemented for modeling the transverse restrainer connection was the use of multi-linear elastic links in place of frame elements. These elements require force displacement data in order to implement. Initial shear stiffness equations of anchor bolts resulted in an incredibly stiff system. Implementing the calculated shear stiffness values into elastic links created a system with large stiffness changes, resulting in numerical instability within models. These stiffness equations were then modified to account for displacements within the clip angle configuration, resulting in the selection of an overall displacement of 0.55 inches between loading and failure of all clip angle systems. This displacement was also meant to create a constant between all bridge models. The resulting model functioned, but still resulted in some numerical instability during some of the ground motions. It was also observed that this model did not accurately replicate shear failure behavior in the model, and a new link element was selected, the multi-linear plastic link element. This new link element has the capability to apply failure and strength degradation that is expected with the behavior of this connection; as well as continue to function after loss of strength, instead of causing a numerical instability. A "kinematic" plastic hinge was initially selected, but its behavior

did not match up with the expected behavior of the system. A "Pivot" plastic link model was selected instead, based on its behavior matching that of the expected behavior of the system. The Pivot link requires additional inputs in order to shape the unloading and reloading properties of the link; all Pivot factors for this link were set to zero in order to achieve desired behavior. The implementation of this link resulted in reduced numerical failures in many of the bridge analyses, and was selected as the best option for modeling the clip-angle connection.

The implementation of connection elements into the bridge models required an additional step. A simplification was made to combine connection elements together to form a single connection element in place of multiple connection models. This simplification was made in order to reduce overall complexity of the models. It was assumed that the bridge deck remains nearly rigid in its plane during ground motions, allowing the use of this simplification. Bridges that contain bents with more than two columns use an altered version of this simplification, multiple simplified connections at each column location.

The final step in the modeling process for each bridge is the creation of behavioral limits. The focus of the analysis in this project is centered on bridge behavior, but certain information cannot be accurately known. This fact resulted in the creation of two different versions of each bridge model, a lower limit model and an upper limit model. The principal difference between each of these models is the friction coefficient between bearing pad and girder surface. The lower bound model assumes slipping to occur at a friction coefficient of 0.2. The upper bound model assumed a coefficient of 0.4. The actual behavior of the bridge should fall somewhere between these two models. Another

important range of uncertainty occurs in the prediction of system damping present within each bridge model. A method for determining and specifying a damping factor was established and implemented based on Rayleigh damping. The theory behind this damping method can be found in (Chopra 2007). A model analysis was performed for each bridge model, with certain elements altered to remain stiff or flexible, and natural periods were recorded at the first and third mode shape for movement in lateral and longitudinal directions. These natural periods were correlated to a damping factor of 2% and entered into a CSI table that calculated Raleigh damping factors. These factors are applied to the model during the analysis procedure.

3.5 Analysis Method

The Time-History Analysis method was selected for use in this project. This method of analysis functions by running a model, composed of stiffness and mass properties, through a series of subsequent analyses. These analyses involve the application of a single acceleration value to the model and then calculating the models response to that acceleration using the equations of motion. The resulting model is then subjected to a subsequent acceleration that represents the next acceleration value of a given time history. This process is repeated until the model has experienced the entire acceleration time history. A Hilber-Hughes-Taylor Time Integration Method was used in order to apply each ground acceleration history to the models. Time history analysis results are recorded as a response history.

3.5.1 Pre-Analysis Procedure

Before the Nonlinear Time History Analysis was preformed, certain steps were taken to ensure accurate results. The bridge models were preloaded with self weigh loading in order to account for p-delta effects. A nonlinear Time History Analysis is able to incorporate p-delta effects into its analysis; thus this loading step results in the consideration of p-delta behaviors. An additional 20 seconds of zero acceleration was added to the end of each GM used in analysis, in order to observe the free vibration of each bridge after an event. This allowed for the observation and recording of residual response in each bridge. With these steps preformed analysis was then able to be performed.

3.5.2 Post-Analysis Procedure

After analysis was complete, steps needed to be taken to ensure completed results. All analyses were examined to have run through the entirety of their associated ground motions. If the examined results did not result in a complete analysis, their associated model was examined for adequate modal behavior. If this check did not indicate a reason for failure, the nonlinear analysis parameters were altered and the analysis was performed again. This process was iterated until a completed response was generated or consistent incomplete analyses were observed. A final alteration of the time integration method was considered and applied for a few cases that did not result in complete analysis.

3.6 Overview of Bridge Models

The following section will include the details used to create each bridge model, and an overview of the modifications and features of each bridge. Simplifications will be

explained and justified. Expected behavior is also included in the description of each bridge as well as the bridge's natural periods taken from modal analysis.

3.6.1 Little Bear Creek Bridge

This bridge carries the two lanes of State Road 24 over Little Bear Creek in Franklin County. It is a three span bridge with spans of unequal lengths. The outer span lengths are 85 feet and the interior span is 130 feet. The outer spans support the 7 inch concrete deck with six Type III Girders and the interior span supports the deck with six BT-72 Girders. Each of the six Type III girders rests upon 20.5" x 9" bearing pads. These bearing pads were calculated to slip after an average (0.3 friction coefficient) displacement of 0.567" correlating to a shear of 18.15 kips per bearing pad. The clip-angle/anchor bolt configuration for the transverse connection contained anchor bolts with a diameter of 1.25". These bolts were modeled with a shear capacity of 45 kips. Each of the six BT-72 girders rests upon 24.5" x 9" bearing pads. These bearing pads were calculated to slip after an average (0.3 friction coefficient) displacement of 1.185" correlating to a shear of 33 kips per bearing pad. The clip-angle/anchor bolt configuration for the transverse connection contained anchor bolts with a diameter of 1.5". These bolts were modeled with a shear capacity of 61 kips. A simplification was also modeled for this bridge using a redesigned clip-angle/anchor bolt configuration for the transverse connection at each span which contained anchor bolts with a diameter of 1.75". These bolts were modeled with a shear capacity of 78 kips. The two bridge piers are 40' x 5' x 7' and supported by two circular columns 4.5 feet in diameter with 3 inches of concrete cover. The columns are reinforced longitudinally with 24 #11 bars and transversely with #5 hoops uniformly spaced at 10 inches from the bottom of the hinge

zone to the top of the foundation, and spaced at 6 inches inside the hinge zone. The average clear height of Bent 2 is 12.06 feet and 16.88 feet for Bent 3. All columns are supported on drilled shafts 5 feet in diameter. The concrete cover of the drilled shafts is 6 inches but the longitudinal reinforcement in the drilled shaft still aligns with the longitudinal reinforcement of the column.

This bridge model contains a single girder connection to represent six girder connections. The selection of a single connection representing six total connections results in a miscalculation of the gravity moments imparted into the bent columns in a conservative fashion. A non-rectangular member was selected to model the bent caps, and a gap link was established to model possible impact stiffness between the deeper girder and this abutment. Plastic hinges were modeled at the top and bottom column locations. The CSiBridge model for this bridge can be seen in Figure 3.13.

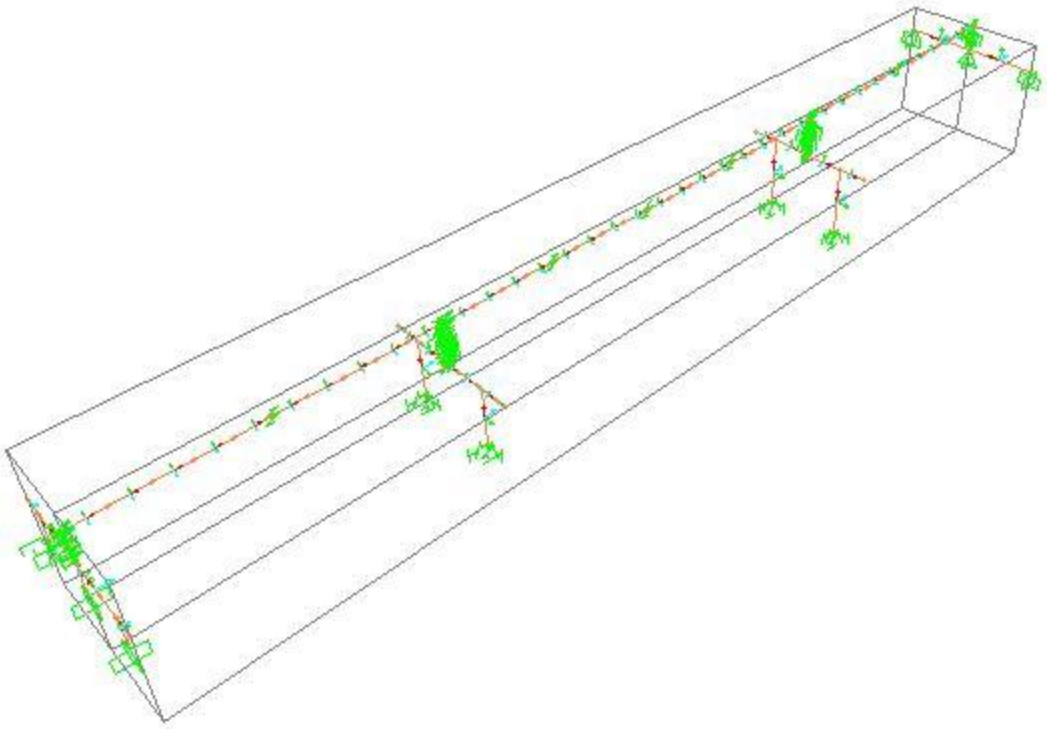

Figure 3.13: Little Bear Creek Bridge Model

The overall model of this bridge was found to be moderately stiff in the context of the other bridges modeled due to shorter columns and stiff foundations. Differences in mass between spans could result in secondary mode shapes dictating dynamic behavior in the transverse direction. Modal analysis of the model revealed a first mode natural period of 0.470 seconds in the transverse direction and 0.818 seconds in the longitudinal direction. The third mode natural periods of the fixed version of this bridge resulted in a natural period of 0.140 seconds in the transverse direction and 0.164 seconds in the longitudinal direction. The "fixed version" bridge model is a version of the bridge model in which all bearing pad connections and all expansion joints are fixed, and these connections do not allow movement along any degree of freedom. This ultra stiff bridge model attempts to maximize the possible stiffness of the bridge's geometry, resulting in the lowest possible natural period obtainable from the bridge. The third mode natural

period of the "fixed version" of the bridge represents the lowest acceptable natural period the bridge could obtain, and this number is used as a stiffness boundary for the calculation of damping. Foundation behavior for this structure could result in hinging forming in the foundations, but that cannot be predicted in this particular model which specifies hinges in the column only.

3.6.2 Oseligee Creek Bridge

The Oseligee Creek Bridge is a two lane bridge that carries County Road 1289 over Oseligee Creek in Chambers County. It is a three span bridge with equal span lengths of 80 feet. The 7 inch concrete deck is supported by four Type III girders. Each of the four girders rests upon 20.5" x 9" bearing pads. These bearing pads were calculated to slip after an average (0.3 friction coefficient) displacement of 0.66" correlating to a shear of 21 kips per bearing pad. The clip-angle/anchor bolt configuration for the transverse connection contained anchor bolts with a diameter of 1.75". These bolts were modeled with a shear capacity of 60.9 kips. The two bridge piers are 30' x 4' x 5' and supported by two circular columns 3.5 feet in diameter with 3 inches of concrete cover. The columns are reinforced longitudinally with 12 #11 bars and transversely with #4 hoops uniformly spaced at 12 inches from the bottom of the hinge zone to the rock line, with the hinge zone being reinforced with #4 ties at 6 inch spacing. The average clear height of Bent 2 is 17.93 feet and 25.83 feet for Bent 3. All columns are supported on drilled shafts 3.5 feet in diameter with concrete cover of 3 inches.

This bridge model contains a single connection to represent four girder connections. The selection of a single connection representing four total connections results in miscalculated gravity moments imparted into the bent columns in a

conservative fashion. Plastic hinges were modeled at the top and bottom column locations. The CSIBridge model for this bridge can be seen in Figure 3.14.

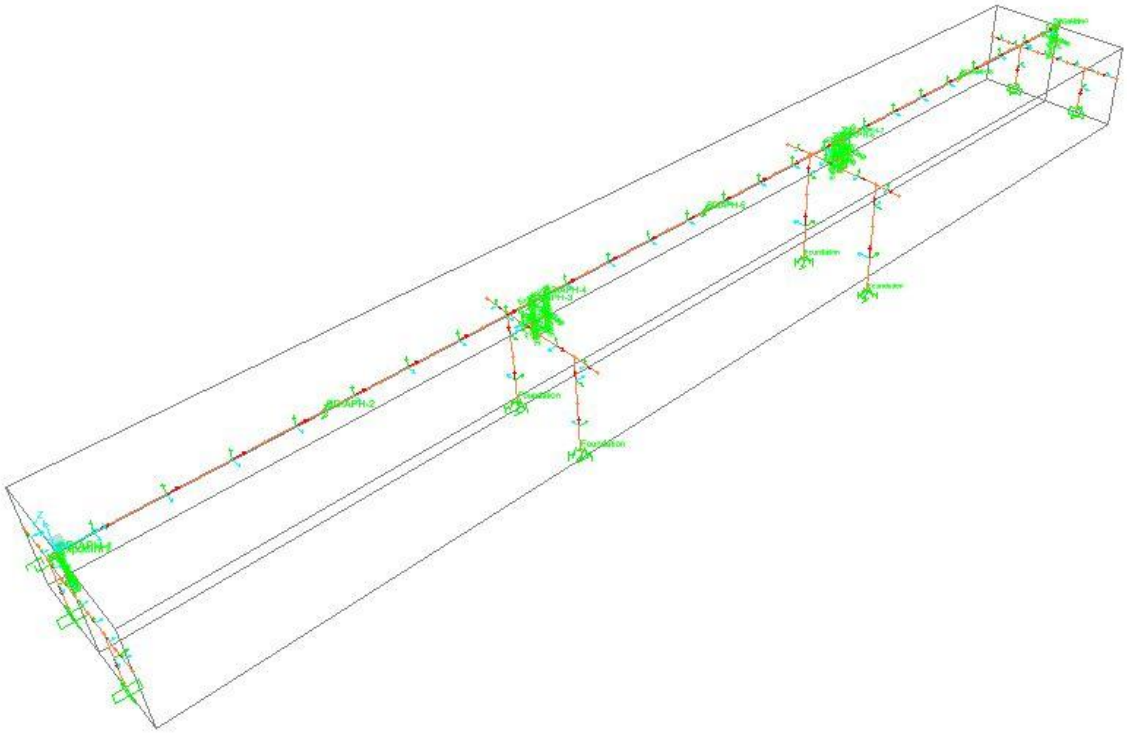

Figure 3.14: Oseligee Creek Bridge Model

The overall model of this bridge was found to be moderately flexible in the context of the other bridges modeled due to a 100% scour condition that was selected by geotechnical analysis of the bridge. Initial modal analysis of this bridge shows stiff bridge behavior, however bridge geometry of the model results in more flexible behavior after hinge formation. This behavior combined with second order effects could result in column buckling, however a bridge with these conditions helps to diversify the overall bridge suit. Modal analysis of the model revealed a first mode natural period of 0.689 seconds in the transverse direction and 1.066 seconds in the longitudinal direction. The third mode natural periods of the fixed version of this bridge resulted in a natural period of 0.154 seconds in the transverse direction and 0.262 seconds in the longitudinal

direction. The combination of tall, flexible substructure and short span lengths could result in dissimilar behaviors in super and substructure, resulting in possible higher forces at the connection location. Foundation behavior for this could result in hinging forming in the foundations, but that cannot be predicted in this particular model which specifies hinges in the column only. Large foundation rotations could result due to second order effects as well as large moments occurring in the substructure.

3.6.3 Norfolk Southern Railroad Bridge

The bridge over Norfolk Southern Railroad is the southbound I-59 bridge in Etowah County, a two-lane bridge that crosses over a Norfolk Southern railroad line and a state highway. It is a two-span bridge with unequal span lengths of 125 feet and 140 feet. Nine modified BT-54 girders support a 6 inch concrete deck that is 46.75 feet wide. Each of the nine girders rests upon 24.5" x 9" bearing pads. These bearing pads were calculated to slip after an average (0.3 friction coefficient) displacement of 1.132" correlating to a shear of 31.5 kips per bearing pad. The clip-angle/anchor bolt configuration for the transverse connection contained anchor bolts with a diameter of 1.375". These bolts were modeled with a shear capacity of 48 kips. The only bridge pier is 53' x 4.5' x 4' and supported by three square columns 3.5 feet in width. The columns are reinforced longitudinally with twelve #11 bars and transversely with #4 ties uniformly spaced at 9 inches from the bottom hinge zone to the top hinge zone, with a spacing of 4 inches inside each hinge zone. The average clear height of the columns is 25.25 feet. The bridge is supported on driven piles. The pile cap is 8.5' x 8' x 4.5' and each pile cap is supported by 7 HP 12x53 steel piles.

This bridge model contains three girder connections to represent nine girder connections. The selection of multiple connections representing nine total connections results in the miscalculation of gravity moments imparted into the bent columns in a conservative fashion. Plastic hinges were modeled at the top and bottom column locations. The CSiBridge model for this bridge can be seen in Figure 3.15.

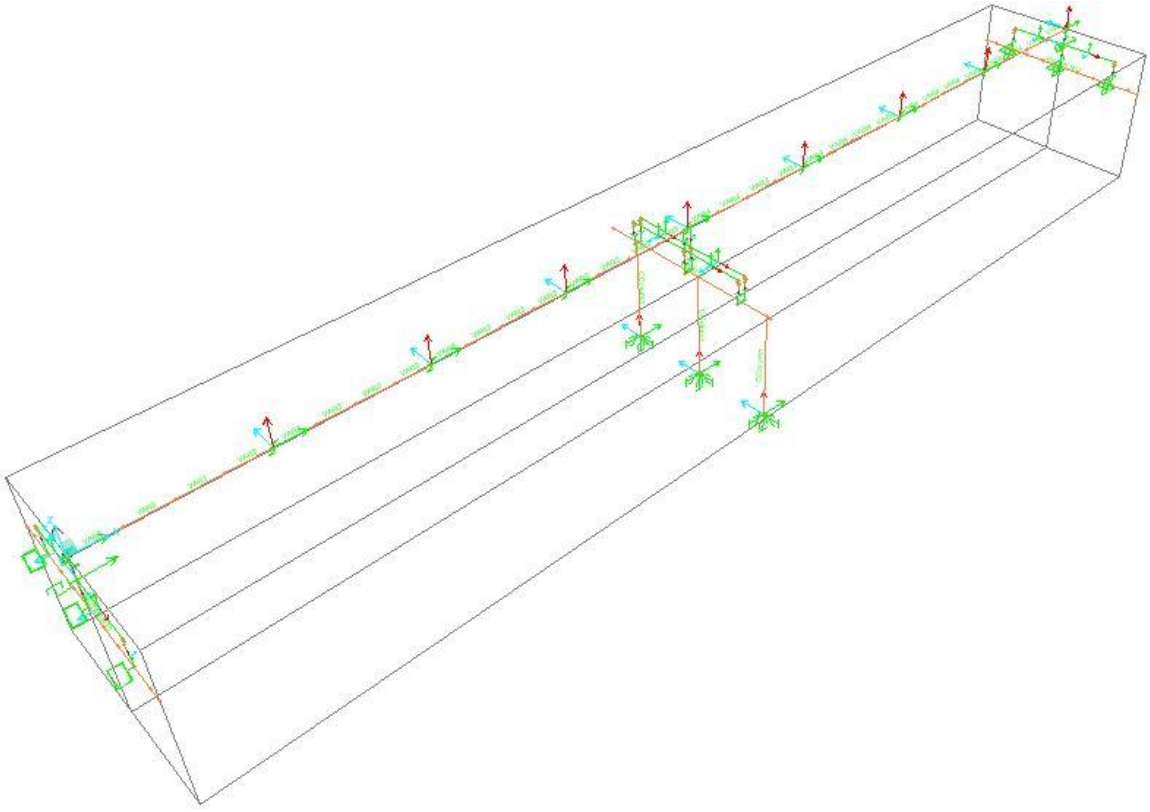

Figure 3.15: Norfolk Creek Bridge Model

The overall model of this bridge was found to be initially stiff due to the large column diameters and the strut members; however bridge geometry of the model results in more flexible behavior after hinge formation. Modal analysis of the model revealed a first mode natural period of 0.415 seconds in the transverse direction and 0.705 seconds in the longitudinal direction. The third mode natural periods of the fixed version of this bridge resulted in a natural period of 0.133 seconds in the transverse direction and 0.086

seconds in the longitudinal direction. The combination of short, stiff substructure and large span lengths could result in dissimilar behaviors in super and substructure, resulting in possible higher forces at the connection location. Foundation behavior for this bridge is difficult to predict, but a triple column bent should limit foundations rotations in the lateral direction.

3.6.4 Scarham Creek

The Scarham Creek Bridge is two lanes and carries State Route 75 over Scarham Creek in Marshall County. It is a four span bridge with equal span lengths of 130 feet. The 7 inch concrete deck is supported by six BT-72 girders. Each of the six girders rests upon 24.5" x 9" bearing pads. These bearing pads were calculated to slip after an average (0.3 friction coefficient) displacement of 1.336" correlating to a shear of 37.5 kips per bearing pad. The clip-angle/anchor bolt configuration for the transverse connection contained anchor bolts with a diameter of 2.5". These bolts were modeled with a shear capacity of 87 kips. The bridge pier at bents 2 and 4 are 40' x 5.5' x 7.5' and the pier at bent 3 is 40' x 6.5' x 7.5.' Bents 2 and 4 are supported by two circular columns 5 feet in diameter with 3 inches of concrete cover. Bent 3 is supported by two circular columns 6 feet in diameter with 3 inches of concrete cover. All columns are reinforced transversely with #6 hoops at a spacing of 6 inches at the top and bottom hinge zones, and spaced at 12 inches at all other regions. All columns are supported on drilled shafts, which are six inches larger in diameter than the columns. It is assumed that the plastic hinge will form at this transition, so the clear height of the columns is measured from the bottom of the bent cap to the transition between the column and drilled shaft. The average height of columns is 34.02 feet at Bent 2, 59.17 feet at Bent 3, and 32.16 feet at Bent 4. Because of the height of the

columns, struts are provided at approximately mid-height of the columns and span the full length between columns with a thickness of 3.5 feet. The strut at bents 2 and 4 are 6 feet deep and 10 feet deep at bent 3.

This bridge model contained a single connection to represent six girder connections. The selection of a single connection representing six total connections results in the miscalculation of gravity moments imparted into the bent columns in a conservative fashion. Plastic hinges were modeled at the column locations above and below strut locations due to the large depth and stiffness of the struts. Behaviors at these locations are of particular concern during ground motions. The CSiBridge model for this bridge can be seen in Figure 3.16.

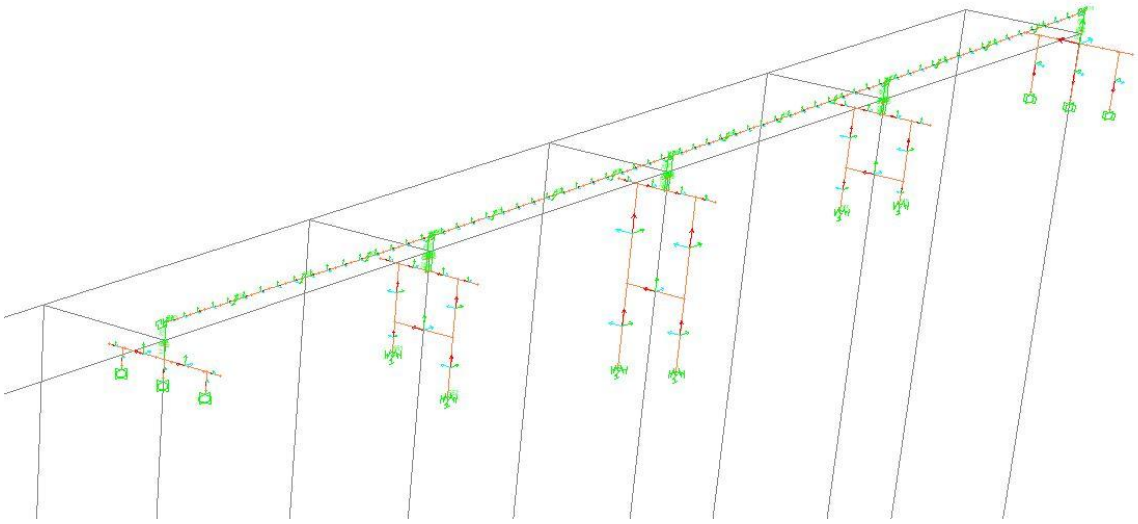

Figure 3.16: Scarham Creek Bridge Model

The overall model of this bridge was found to be initially stiff due to the large column diameters and the strut members; however bridge geometry of the model results in more flexible behavior after hinge formation. Modal analysis of the model revealed a first mode natural period of 0.760 seconds in the transverse direction and 1.080 seconds in the longitudinal direction. The third mode natural periods of the fixed version of this

bridge resulted in a natural period of 0.300 seconds in the transverse direction and 0.340 seconds in the longitudinal direction. The combination of tall substructure and large span lengths could result in similar behaviors in super and substructure, resulting in possible lower forces at the connection location. Foundation behavior for this bridge is difficult to predict, given the unpredictability of this bridges behavior as it enters the inelastic range.

3.6.5 Bent Creek Road

The Bent Creek Road Bridge in Lee County is a five-lane bridge that crosses over Interstate 85 with two spans of 135 feet. Each span is comprised of fifteen modified BT-54 girders spaced approximately 5.33 feet apart that support a 6 inch concrete deck that is 80.75 feet wide. The only bridge pier is 79’ x 4’ x 4.5’ and supported by five square columns 3.5 feet in width. The columns are reinforced longitudinally with 12 #11 bars and transversely with #4 ties uniformly spaced at 9 inches from the bottom of the bent to the top of the pile cap foundation, except for plastic hinge zone region which are reinforced with #4 ties at a spacing of 4 inches. The average clear height of the columns is 20.1 feet. The bridge is supported on driven piles. The pile cap is 8.5’ x 8’ x 4.5’ and each pile cap is supported by 9 HP 12x52 steel piles. Each of the fifteen girders rests upon 24.5” x 9” bearing pads. These bearing pads were calculated to slip after an average (0.3 friction coefficient) displacement of 1.1855” correlating to a shear of 33 kips per bearing pad. The clip-angle/anchor bolt configuration for the transverse connection contained anchor bolts with a diameter of 1.75”. These bolts were modeled with a shear capacity of 61 kips.

This bridge model contained five modeled connections to represent fifteen girder connections. This simplification was chosen due to the bridge bent containing five

columns, instead of a configuration of two columns found in other bridges. A selection of a single connection representing fifteen total connections would result in dramatically miscalculating the gravity loads and moments imparted into the bent columns. The selection of five connections resulted in a more complex model then the other bridges, and it was predicted that analysis problems could arise. The CSIBridge model for this bridge can be seen in Figure 3.17.

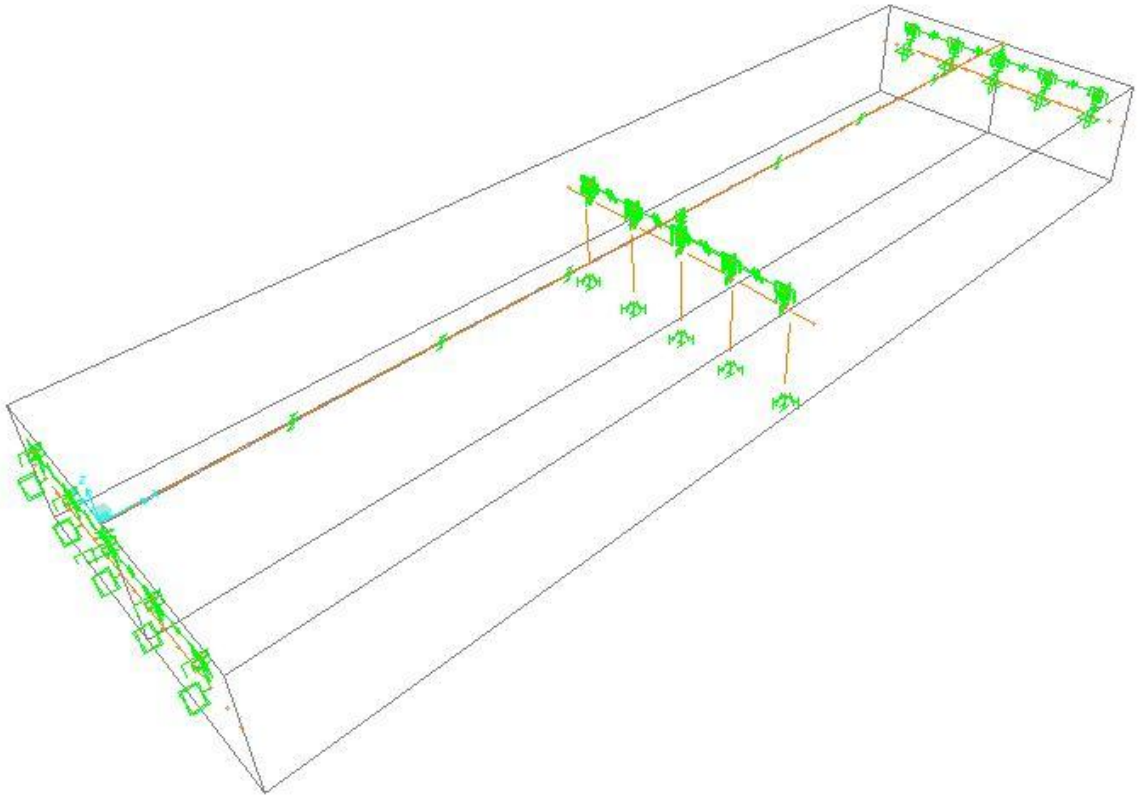

Figure 3.17: Bent Creek Bridge Model

The overall model of this bridge was found to be rather stiff, despite its large mass. Modal analysis of the model revealed a first mode natural period of 0.717 seconds in the transverse direction and 0.933 seconds in the longitudinal direction. The third mode natural periods of the fixed version of this bridge resulted in a natural period of 0.108 seconds in the transverse direction and 0.133 seconds in the longitudinal direction.

The combination of stiff substructure and large superstructure mass could result in large forces at the connection location. Foundation behavior for this bridge may also be inconsistent to the other bridges given a pile cap foundation group located under such a large and stout bridge bent.

3.7 Determination of Capacities

Overall dynamic bridge performance is measured by displacements and internal member forces as they relate to specified capacities. Some of these capacities are specified in design documents and codes, and others vary from project to project. This section will provide details regarding capacities selected for use in this project.

Foundation information provided for this project was analyzed using the geotechnical analysis software FB-Multipier (BSI, 2013). This information included a displacement limit on all foundation degrees of freedom. These limits could not be implemented in the modeling of the bridges, but they are used in the bridge evaluation procedure after analysis. The horizontal displacement and rotation capacities for each foundation are displayed in Table 3.5. Any recorded foundation rotation or displacement exceeding these limits will be classified as a foundation failure.

Table 3.5: Foundation Capacities

	Foundation Displacement and Rotation Limits			
	Transverse Direction		Longitudinal Direction	
	Displacement (in.)	Rotation (rad.)	Displacement (in.)	Rotation (rad.)
Little Bear Creek	0.54	0.005	0.52	0.0054
Norfolk RR	2	0.022	3	0.0072
Scarham (Bent 1 & 3)	0.58	0.002	0.55	0.002
Scarham (Bent 2)	0.71	0.003	0.7	0.003
Oseligee	0.22	0.0032	0.23	0.0033
Bent Creek	1.4	0.035	1.4	0.036

Bearing pad capacity is determined in terms of displacement. Although there exists a limit of shear force that each bearing pad is capable of resisting, this limit does not intrinsically represent a failure criterion of the bearing pads, it simply represents the force in which slipping occurs within the system. The actual capacity that is of concern in this element is the displacement that occurs between the girder and the bearing pad. It was determined that the limit for differential movement between these two elements be set to the dimension of the bearing pad in that direction. Any deflection beyond this limit would result in unseating of the girder.

Bolt strength capacity was conservatively estimated using Equation 3.2. Due to analysis concerns the limit specified for a bolt failure was selected as 95% of the calculated value. This 95% attempts to account for any values not recorded by the analysis software that may trigger failure of the bolt link, and is not meant to account for any loss of strength or safety factor correlated to a failure mode. Failure of the clip angle-anchor rod system does not result in overall structural failure, but its performance was monitored due to its importance in connection behavior. Table 3.6 contains all calculated bolt strengths for the bridge designs selected.

Table 3.6: Calculated Bolt Strengths

	Bolt Shear Capacities
	Individual Bolts (kips)
Little Bear Creek	61
Norfolk RR	48
Scarham	61
Oseligee	78
Bent Creek	87

A commonly recorded criterion of seismic behavior in structures and structural elements is ductility. Ductility in structures can refer to a variety of terms; however, in this analysis, it refers to the degree in which a structure can deform relative to its initial yield. The ductility of bridge bents was selected as an indicator of overall bridge performance. In order to determine the overall ductility of a bridge bent, a state of initial yielding needed to be determined within each bridge bent. A backbone curve was created for each fiber hinge used in the bent columns, and a point of nominal strength was isolated. The rotation that correlated to this point was recorded and used in Equation 3.3 to determine the angle of rotation of the plastic hinges. This calculated angle of rotation was applied at midpoint of each hinge location in each bridge bent, and the overall displacement differential between the center of the bent cap and the foundation was calculated. This displacement was used as a measure of a ductility of 1. A maximum ductility capacity was also determined for each bridge based on pushover analysis performed in a previous task of this project (Law, 2013). The initial ductility displacements and the maximum ductility capacities can be seen in Table 3.7. AASHTO specifies a range of acceptable ductility demands for bents in section 4.9, with a ductility limit of six or less for bents consisting of multiple columns. The lesser of AASHTO and

Law's ductility limit was selected as a maximum capacity for ductility in the bridge bents.

— – — Equation 3.3

Table 3.7: Bent Displacement Limits

	Bent Displacements					
	Transverse Direction			Longitudinal Direction		
	Ductility of 1 (in.)	Pushover Limit (in.)	Ductility Limit	Ductility of 1 (in.)	Pushover Limit (in.)	Ductility Limit
Little Bear Creek (Bent 1)	0.56	2.70	4.82	0.56	1.60	2.85
Little Bear Creek (Bent 2)	0.91	13.5	6.00	0.91	2.52	2.77
Norfolk RR	1.71	4.00	2.32	1.71	6.63	3.89
Scarham (Bent 1 & 3)	1.00	9.80	6.00	2.05	2.20	1.08
Scarham (Bent 2)	3.30	25.6	6.00	5.59	3.60	0.64
Oseligee	0.41	6.75	6.00	0.41	6.30	6.00
Bent Creek	1.79	2.45	1.37	1.79	4.57	2.56

Lastly a serviceability limit was established for the residual displacements of the models. Determining the state of functionality of a bridge after being subjected to a ground motion is a key factor in performance classification. Critical and essential bridges should be open to emergency vehicles and be open for security and defense purposes immediately after the design earthquake, with critical bridges also being open to all traffic (AASHTO 2009). The value for residual span displacements that was selected as an upper limit was one inch in either direction. This value was determined from engineering judgment. A residual displacement exceeding one inch could indicate substructure damage or a localized failure at a connection zone.

This concludes the third Chapter of this thesis. This chapter explained the process of bridge and ground motion selection for use in the Time History analysis that was performed in this research. Ground motion scaling was described and the final scaling

values selected were presented. An overview of the detailing of each bridge was given, along with information used in the modeling process in the form of strength and deflection capacities. Each of these pieces of information were then used to create and analyze bridge models, and the results of these analyses can be found in the next chapter.

Chapter 4: Analysis Results and Discussion

4.1 Introduction

This section will present the results from the time history analyses performed on each bridge model. Some sections will compare the results taken from specific bridges, while other sections will simply provide an overview of observed behaviors and trends. Unique behavior or abnormalities will also be examined. Explanations for observed phenomena will also be provided when necessary. This section will provide insight into the bridges analyzed as well as the ground motions used in the analysis.

4.1.1 Description of Results Presented

Each of the five bridges was analyzed in four ways. Each bridge was modeled as an upper limit bearing pad configuration (coefficient of friction of 0.4), and a lower limit bearing pad configuration (coefficient of friction of 0.2). Each bridge model incorporated soil interaction springs that provide foundation flexibility. Both of these bridge models were then analyzed using ten design-level ground motions and seven MCE-level ground motions, applied in both the longitudinal and transverse direction. The results of each analysis have been recorded and graphed using MathCAD (PTC, 2007). Maximum span and bent displacements are recorded for each bridge analysis, as well as maximum foundation displacements and rotations. Bolt shears and bearing displacements are also recorded at each connection location, with the largest value being used to calculate demand capacity ratios. Each response history analysis performed is categorized based

on the results recorded. Analyses that did not result in completion were rerun using altered analysis constraints in an effort to eliminate numerical instabilities that occur during analysis. After numerous iterations of attempted analysis, motions that did not result in completion are recorded in their state of farthest completion. The analysis is classified as one of the following: 1) Complete: indicating that the entire analysis was completed, 2) Numerical: indicating that no elements appeared to have failed but the analysis could not be completed due to numerical convergence issues and 3) Failure: indicating a numerical failure that either results from a structural failure within the model, or a set of recorded results that indicated possible future structural failure of the model during continued analysis. Data taken from analyses deemed "Numerical" is excluded from statistical analysis of each bridge due to the unknown behaviors of the model during analysis. Data taken from analyses deemed "Failure" is included in statistical analysis of each bridge given predictable behaviors or data related to failures that have already occurred. All major structural component failures are recorded and highlighted for each analysis. Foundation information is displayed as a demand/capacity value in reference to displacements and rotations. The demand/capacity value is taken from each analysis as the maximum demand/capacity value out of each of the bents for the entirety of each ground motion. The value associated with "Bearing Capacity" represents a demand/capacity value that contains the highest bearing pad lateral or longitudinal displacement recorded from the displacements of every bearing pad in the bridge during the entirety of the ground motion. "Bent Ductility" is a value of the largest differential displacement between bent displacement and its respective foundation displacement. The value representing "Bent Ductility" is the quotient of the aforementioned displacement

divided by the displacement determined as the bent displacement relating to nominal moment capacity occurring at a hinge in that bent. "Bolt Status" indicates the highest shear demand present in all anchor bolts within the model compared to the shear capacity of the anchor bolts in the model. All values indicated in **Bold** font represent values that exceed their acceptable limits.

4.1.2 Limits of Bridge Behaviors

Each bridge is analyzed for the purpose of determining behavior acceptability. This acceptable bridge behavior is based on many different criteria stemming from the limits specified in Section 3.6. The average response of each model is used to determine that models performance. In the event that a model contains numerous numerical failures, a prediction of overall behavior is be made, but recommendations for that bridge are not be made unless further completed analysis is performed.

Each bridge result is checked for failures or exceedance of capacity limits. A classification of each of these results is made in the event of a capacity limit being exceeded. The following behaviors are classified as resulting in structural failure: 1) excessive span or bent deflections (values are dependent on bridges), 2) bearing pad capacities exceeding a value of "1", 3) Bent ductility exceeding the limits specified in Section 3.6. A residual displacement of span or bents that exceeds 1 inch is classified as a failure on the grounds of a serviceability limit being exceeded. Bolt failure is also addressed, but is not considered a structural failure due to the anchor bolts only providing a non-essential barrier to transverse displacement. Bridges that contain multiple instances of structural failures are deemed to have inadequate behavior. Bridges that contain only one or two structural failure analysis cases are classified as having

acceptable behavior. This is deemed allowable due to overall analysis results being evaluated as an average of bridge response, and a small amount of failure cases are allowable in a large number of analyses.

4.2 Bent Creek Road Bridge

Results show that the average behavior of the Bent Creek Road Bridge was favorable for most aspects of the bridge components. No design-level (1,000 year hazard) or MCE-level (2,500 year hazard) events resulted in specific structural failures; however, one event may lead to possible structural failures. Foundation failures occurred in six of the design-level longitudinal events; however, the occurrence of these failures is not consistent with other structural behavior during the events. Substructure behavior appears to be adequate at column and bent locations with the exception of foundation displacement capacities in the longitudinal direction of the bridge. Bolt failure was the most frequent behavioral occurrence in the connection during transverse motion. An additional observation regarding the analysis of this bridge is the large number of numerical failures present in the data. This result is thought to have occurred due to the complexity of the bridge model. Judgments needed to be made regarding the inclusion or exclusion of these results. A more in-depth analysis of each set of analysis results is provided in the next sections.

4.2.1 Transverse Motion

The transverse analysis for this bridge resulted in stout, stiff structural behavior. See Table 4.1 and Table 4.2 for an overview of the design-level transverse results. Bolt failure and low bent displacements indicate a stiff substructure able to transfer large loads

to the connection. Both frictions models responded similarly to the design-level transverse ground motions, showing low foundation rotations and low residual displacements. Overall design-level bent ductility did not exceed a value of 1, likely due to the stiff bridge bent. Thirteen of the twenty design-level ground motions ran successfully with this bridge model, with a larger number of incomplete analyses occurring in the upper limit friction model. Six of the seven design-level ground motions that did not run successfully were classified as numerical failures. No data examined from these six ground motions indicated a structural failure before the analysis ceased. The one design-level analysis failure that was classified as such displayed bolt failure prior to the onset of larger ground motions during the Coalinga record. It was estimated that larger shaking, given the existing bolt failure, may result in larger displacements of deck sections. These displacements could result in failure of the structure, or at least a suspension of serviceability. Another numerical failure (Imperial Valley) displayed similar bolt status to the Coalinga event, but had already withstood the majority of its associated ground motion, and was not classified as a "failure" analysis. Successful design-level analysis results and the single "failure" event were used to classify the design-level behavior of this model.

Table 4.1: Results Overview for Lower Limit Friction Bent Creek Transverse Model

Bent Creek	Friction ".2"											
Transverse Motion	Ground Motion	Run Status	Run Time	Foundation Capacity (D/R)		Bearing Capacity	Bent Ductility	Bolt Status	Max Span Disp. (in.)	Max Bent Disp. (in.)	Residual Span Disp. (in.)	Residual Bent Disp. (in.)
San Fernando 1	Design	Comp.	48.00	0.086	0.0006	0.090	0.623	**0.994**	1.170	1.009	0.048	0.105
San Fernando 2	Design	Comp.	50.00	0.034	0.0000	0.022	0.191	0.535	0.367	0.294	0.002	0.000
Imperial Valley	Design	Num.	38.32	0.067	0.0001	0.065	0.470	**0.966**	0.877	0.750		
Coalinga	Design	Fail.	16.25	0.058	0.0016	0.091	0.471	**0.987**	1.183	0.759		
North Palm Springs	Design	Comp.	40.00	0.069	0.0000	0.065	0.464	**0.996**	0.872	0.732	0.001	0.001
Landers	Design	Comp.	70.00	0.040	0.0000	0.027	0.235	0.659	0.452	0.364	0.001	0.001
Little Skull Mountain	Design	Comp.	132.00	0.032	0.0000	0.022	0.191	0.542	0.374	0.296	0.000	0.001
Kocaeli 1	Design	Num.	36.06	0.006	0.0000	0.004	0.033	0.093	0.064	0.051		
Kocaeli 2	Design	Comp.	48.00	0.106	0.0001	0.138	0.984	**0.999**	1.815	1.608	0.401	0.392
Kobe	Design	Comp.	60.00	0.051	0.0000	0.036	0.316	0.885	0.607	0.493	0.042	0.026

Mean	0.0595	0.0003	0.0614	0.4345	0.8246	0.8549	0.6943	0.0706	0.0752
Standard Deviation	0.0261	0.0006	0.0424	0.2705	0.2103	0.5100	0.4485	0.1472	0.1448
Relative Stand Deviation	43.87%	**191.63%**	69.07%	62.25%	25.51%	59.66%	64.60%	**208.29%**	**192.41%**

Table 4.2: Results Overview for Upper Limit Friction Bent Creek Transverse Model

Bent Creek	Friction ".4"											
Transverse Motion	Ground Motion	Run Status	Run Time	Foundation Capacity (D/R)		Bearing Capacity	Bent Ductility	Bolt Status	Max Span Disp. (in.)	Max Bent Disp. (in.)	Residual Span Disp. (in.)	Residual Bent Disp. (in.)
San Fernando 1	Design	Comp.	48.00	0.083	0.0001	0.094	0.677	**0.931**	1.247	1.097	0.121	0.059
San Fernando 2	Design	Comp.	50.00	0.034	0.0000	0.022	0.191	0.535	0.367	0.294	0.001	0.001
Imperial Valley	Design	Num.	26.18	0.067	0.0001	0.065	0.470	**0.966**	0.877	0.750		
Coalinga	Design	Comp.	52.00	0.070	0.0001	0.096	0.654	**0.999**	1.332	1.137	0.071	0.005
North Palm Springs	Design	Num.	6.50	0.005	0.0000	0.003	0.029	0.082	0.057	0.045		
Landers	Design	Comp.	70.00	0.040	0.0000	0.027	0.235	0.659	0.452	0.364	0.001	0.001
Little Skull Mountain	Design	Comp.	132.00	0.032	0.0000	0.022	0.191	0.542	0.374	0.296	0.001	0.001
Kocaeli 1	Design	Num.	36.06	0.006	0.0000	0.004	0.033	0.093	0.064	0.051		
Kocaeli 2	Design	Comp.	48.00	0.086	0.0001	0.095	0.679	**0.999**	1.266	1.092	0.108	0.024
Kobe	Design	Num.	18.28	0.049	0.0001	0.036	0.316	0.885	0.612	0.495		

Mean	0.0576	0.0000	0.0593	0.4379	0.7774	0.8397	0.7132	0.0504	0.0152
Standard Deviation	0.0292	0.0000	0.0377	0.2560	0.3546	0.4879	0.4279	0.0567	0.0233
Relative Stand Deviation	50.62%	**100.57%**	63.56%	58.47%	45.61%	58.10%	59.99%	**112.47%**	**153.50%**

A total of fourteen MCE-level events were applied to this bridge model. See Table 4.3 and Table 4.4 for an overview of the MCE-level transverse results. Overall bent ductility did not exceed a value of 1.2, likely due to the stiff bridge bent. Ten of the

Fourteen MCE-level ground motions ran successfully with this bridge model, with an equal number of incomplete analyses occurring in both friction models. Three of the four ground motions that did not run successfully were classified as numerical failures. No data examined from these three ground motions indicated a significant structural failure before the analysis ceased. The one analysis failure that was classified as such displayed bolt failure prior to the onset of larger ground motions during the first Kocaeli record. It was estimated that larger shaking, given the existing bolt failure, may result in larger displacements of deck sections. These displacements could result in failure of the structure, or at least a suspension of serviceability. Successful analysis results and the single "failure" event design-level ground motions were used to classify the MCE-level behavior of this model. All successful analyses resulted in acceptable bridge behavior in the transverse direction of loading, however the complexity of the model makes it difficult to analyze and thus state any solid conclusions regarding overall bridge behavior. A solution to this would be to continue simplifying the model by reducing the number of modeled connections.

Table 4.3: MCE-Level Results Overview for Lower Limit Friction Bent Creek Transverse Model

Bent Creek	Friction ".2"											
Transverse Motion	Ground Motion	Run Status	Run Time	Foundation Capacity (D/R)		Bearing Capacity	Bent Ductility	Bolt Status	Max Span Disp.	Max Bent Disp.	Residual Span Disp.	Residual Bent Disp.
San Fernando 1	MCE	Comp.	48.00	0.072	0.0000	0.071	0.512	**0.964**	0.958	0.814	0.044	0.036
San Fernando 2	MCE	Comp.	50.00	0.043	0.0000	0.029	0.257	0.722	0.494	0.399	0.000	0.000
Imperial Valley	MCE	Num.	30.00	0.082	0.0001	0.089	0.627	**0.968**	1.162	1.004		
Landers	MCE	Comp.	70.00	0.104	0.0002	0.155	1.104	**0.962**	2.091	1.924	0.672	0.600
Kocaeli 1	MCE	Fail.	99.14	0.129	0.0001	0.153	1.111	**0.988**	2.017	1.801		
Kocaeli 2	MCE	Comp.	48.00	0.149	0.0001	0.163	1.193	**0.965**	2.156	1.920	0.162	0.203
Kobe	MCE	Comp.	60.00	0.139	0.0000	0.158	1.154	**0.989**	2.079	1.864	0.525	0.449
Mean				0.1026	0.0001	0.1170	0.8513	0.9367	1.5651	1.3894	0.2806	0.2576
Standard Deviation				0.0389	0.0001	0.0533	0.3782	0.0955	0.6796	0.6356	0.3007	0.2609
Relative Stand Deviation				37.89%	90.03%	45.57%	44.43%	10.20%	43.42%	45.74%	**107.14%**	**101.29%**

Table 4.4: MCE-Level Results Overview for Upper Limit Friction Bent Creek Transverse Model

Bent Creek	Friction ".4"											
Transverse Motion	Ground Motion	Run Status	Run Time	Foundation Capacity (D/R)		Bearing Capacity	Bent Ductility	Bolt Status	Max Span Disp.	Max Bent Disp.	Residual Span Disp.	Residual Bent Disp.
San Fernando 1	MCE	Comp.	48.00	0.072	0.0000	0.071	0.511	**0.964**	0.955	0.812	0.002	0.001
San Fernando 2	MCE	Comp.	50.00	0.043	0.0000	0.029	0.257	0.722	0.494	0.399	0.001	0.001
Imperial Valley	MCE	Num.	17.23	0.107	0.0001	0.122	0.894	**0.968**	1.642	1.446		
Landers	MCE	Comp.	70.00	0.096	0.0001	0.143	1.102	**0.991**	2.064	1.850	0.002	0.068
Kocaeli 1	MCE	Num.	30.64	0.008	0.0000	0.005	0.047	0.131	0.089	0.071		
Kocaeli 2	MCE	Comp.	48.00	0.141	0.0001	0.159	1.168	**0.965**	2.141	1.887	0.585	0.456
Kobe	MCE	Comp.	60.00	0.112	0.0002	0.129	0.940	**0.984**	1.743	1.522	0.133	0.013
Mean				0.0828	0.0001	0.0942	0.7028	0.8179	1.3041	1.1410	0.1445	0.1077
Standard Deviation				0.0450	0.0001	0.0595	0.4349	0.3175	0.7997	0.7188	0.2528	0.1967
Relative Stand Deviation				54.39%	**117.48%**	63.18%	61.88%	38.82%	61.32%	62.99%	**174.94%**	**182.68%**

4.2.2 Longitudinal Motion

Analysis of the Bent Creek Bridge under longitudinal ground motions provided mixed behavioral results. Table 4.5 and Table 4.6 provide an overview of Bent Creek's design-level longitudinal analysis. Both friction models exhibited numerical failures (nine in total) as well as conflicting completed results. Six of the eleven completed design-level analyses exhibited large foundation displacements. This foundation behavior does not seem to be supported by forces within the recorded model data however, and its existence may be the result of errors propagated within the analysis. The remaining successful design-level analyses indicate very small displacements; however, the overall behavior of the structure may not be adequately described with the results obtained.

Table 4.5: Results Overview for Lower Limit Friction Bent Creek Longitudinal Model

Bent Creek	Friction ".2"										
Longitudinal Motion	Ground Motion	Run Status	Run Time	Foundation Capacity (D/R)		Bearing Capacity	Bent Ductility	Max Span Disp. (in.)	Max Bent Disp. (in.)	Residual Span Disp. (in.)	Residual Bent Disp. (in.)
San Fernando 1	Design	Comp.	48.00	**6.702**	0.0436	0.297	5.213	1.363	0.995	0.492	0.164
San Fernando 2	Design	Comp.	50.00	**2.846**	0.0416	0.216	2.246	0.982	0.664	0.719	0.072
Imperial Valley	Design	Num.	5.82	0.048	0.0081	0.053	0.038	0.240	0.121		
Coalinga	Design	Comp.	52.00	**6.590**	0.0603	0.341	5.526	1.565	1.020	0.694	0.139
North Palm Springs	Design	Num.	7.29	0.048	0.0176	0.100	0.110	0.453	0.263		
Landers	Design	Num.	11.15	0.048	0.0045	0.025	0.075	0.114	0.067		
Little Skull Mountain	Design	Comp.	132.00	0.048	0.0000	0.000	0.038	0.001	0.000	0.001	0.000
Kocaeli 1	Design	Num.	21.70	0.048	0.0276	0.150	0.204	0.681	0.431		
Kocaeli 2	Design	Comp.	48.00	0.803	0.0740	0.376	0.708	1.736	1.179	0.767	0.107
Kobe	Design	Comp.	60.00	0.219	0.0299	0.175	0.365	0.799	0.602	0.613	0.017
Mean				**2.8681**	0.0416	0.2341	2.3492	1.0742	0.7432	0.5477	0.0832
Standard Deviation				**3.0916**	0.0256	0.1371	2.4607	0.6321	0.4263	0.2847	0.0658
Relative Stand Deviation				**107.79%**	61.55%	58.55%	**104.75%**	58.84%	57.36%	51.98%	79.07%

Table 4.6: Results Overview for Upper Limit Friction Bent Creek Longitudinal Model

Bent Creek	Friction ".4"										
Longitudinal Motion	Ground Motion	Run Status	Run Time	Foundation Capacity (D/R)		Bearing Capacity	Bent Ductility	Max Span Disp. (in.)	Max Bent Disp. (in.)	Residual Span Disp. (in.)	Residual Bent Disp. (in.)
San Fernando 1	Design	Comp.	48.00	**5.781**	0.0651	0.372	4.666	1.719	1.302	0.819	0.181
San Fernando 2	Design	Num.	34.28	0.186	0.0416	0.229	0.447	1.044	0.728		
Imperial Valley	Design	Num.	5.82	0.048	0.0081	0.053	0.038	0.240	0.121		
Coalinga	Design	Comp.	52.00	**5.937**	0.0760	0.419	4.773	1.949	1.524	0.985	0.184
North Palm Springs	Design	Num.	7.29	0.048	0.0176	0.100	0.110	0.453	0.263		
Landers	Design	Num.	11.15	0.048	0.0045	0.025	0.075	0.114	0.067		
Little Skull Mountain	Design	Comp.	132.00	0.048	0.0001	0.000	0.038	0.002	0.001	0.001	0.000
Kocaeli 1	Design	Num.	21.70	0.048	0.0276	0.150	0.204	0.681	0.431		
Kocaeli 2	Design	Comp.	48.00	**3.431**	0.0743	0.382	2.807	1.773	1.313	0.787	0.185
Kobe	Design	Comp.	60.00	0.132	0.0282	0.176	0.357	0.800	0.605	0.055	0.109
Mean				**3.0658**	0.0487	0.2698	2.5284	1.2489	0.9490	0.5294	0.1318
Standard Deviation				**2.8923**	0.0334	0.1780	2.2695	0.8280	0.6335	0.4643	0.0804
Relative Stand Deviation				94.34%	68.47%	65.97%	89.76%	66.30%	66.75%	87.70%	60.98%

A total of fourteen MCE-level events were applied to this bridge model. See Table 4.7 and Table 4.8 for an overview of the MCE-level longitudinal results. Bent ductility was inconsistent throughout the analysis, with large and small values being recorded at the MCE-level. Eight of the fourteen MCE-level ground motions ran successfully with this bridge model, with an equal number of incomplete analyses occurring in both friction models. All of the ground motions that did not run successfully

were classified as numerical failures. No data examined from these ground motions indicated a large structural failure before the analysis ceased. One case of residual deformation exceedance was recorded, and seven cases of foundation displacement exceedance were recorded. These large foundation displacements were recorded as a result of unexpected and sudden foundation movement. These displacements could result in failure of the structure, or at least a suspension of serviceability.

Table 4.7: MCE-Level Results Overview for Lower Limit Friction Bent Creek Longitudinal Model

Bent Creek	Friction ".2"										
Longitudinal Motion	Ground Motion	Run Status	Run Time	Foundation Capacity (D/R)		Bearing Capacity	Bent Ductility	Max Span Disp.	Max Bent Disp.	Residual Span Disp.	Residual Bent Disp.
San Fernando 1	MCE	Comp.	48.00	0.730	0.0430	0.263	0.570	1.204	0.911	0.409	0.198
San Fernando 2	MCE	Num.	1.58	0.048	0.0025	0.013	0.053	0.060	0.028		
Imperial Valley	MCE	Num.	6.60	0.048	0.0207	0.116	0.188	0.527	0.284		
Landers	MCE	Comp.	70.00	**7.468**	0.0534	0.595	6.080	2.589	1.893	0.802	0.323
Kocaeli 1	MCE	Num.	20.52	0.048	0.0132	0.073	0.150	0.329	0.200		
Kocaeli 2	MCE	Comp.	48.00	**3.009**	0.1098	0.545	2.423	2.591	1.837	0.741	0.014
Kobe	MCE	Comp.	60.00	**3.551**	0.0436	0.375	2.941	1.733	1.223	**1.033**	0.175
Mean				2.1289	0.0409	0.2829	1.7722	1.2905	0.9108	0.7463	0.1775
Standard Deviation				2.7764	0.0355	0.2307	2.2320	1.0488	0.7744	0.2576	0.1269
Relative Stand Deviation				**130.41%**	86.89%	81.54%	**125.95%**	81.27%	85.03%	34.52%	71.51%

Table 4.8: MCE-Level Results Overview for Upper Limit Friction Bent Creek Longitudinal Model

Bent Creek	Friction ".4"										
Longitudinal Motion	Ground Motion	Run Status	Run Time	Foundation Capacity (D/R)		Bearing Capacity	Bent Ductility	Max Span Disp.	Max Bent Disp.	Residual Span Disp.	Residual Bent Disp.
San Fernando 1	MCE	Comp.	48.00	**3.309**	0.0564	0.372	2.634	1.725	1.273	0.737	0.036
San Fernando 2	MCE	Num.	1.58	0.048	0.0025	0.013	0.053	0.060	0.028		
Imperial Valley	MCE	Num.	6.60	0.048	0.0207	0.116	0.188	0.527	0.284		
Landers	MCE	Comp.	70.00	**13.604**	0.0726	0.769	11.112	2.586	1.702	0.509	0.068
Kocaeli 1	MCE	Num.	20.52	0.048	0.0132	0.073	0.150	0.329	0.200		
Kocaeli 2	MCE	Comp.	48.00	**8.072**	0.0944	0.484	6.492	2.278	1.600	0.888	0.205
Kobe	MCE	Comp.	60.00	**7.092**	0.0525	0.429	5.688	2.001	1.530	0.826	0.074
Mean				4.6031	0.0446	0.3223	3.7596	1.3580	0.9451	0.7400	0.0958
Standard Deviation				5.2149	0.0337	0.2707	4.2040	1.0275	0.7398	0.1660	0.0747
Relative Stand Deviation				**113.29%**	75.47%	83.97%	**111.82%**	75.67%	78.28%	22.43%	78.04%

4.3 Scarham Creek Bridge

Results show that the average behavior of the Scarham Creek Bridge was favorable for design-level events. This behavior does not carry over to the MCE-level behaviors. Design-level events resulted in behaviors typical with flexible bridges, including larger span displacements and bent deflections. Foundation performance for this bridge was mixed, and dependent on event direction. All design-level analyses performed for this bridge succeeded in completing except for the second San Fernando ground motion applied to the upper limit friction model in the longitudinal direction. Substructure behavior appears to be adequate at column, strut and bent cap locations with the exception of foundation displacement capacities in the longitudinal direction of the bridge. Connection behavior also appears to be adequate from the results of each design-level analysis. Bearing pad slippage was minimal in both directions of loading, and did not approach levels indicative of unseating. A more in-depth analysis of each bridge model's results is proved in the next sections.

4.3.1 Transverse Motion

The transverse analysis for this bridge resulted in flexible structural behavior. See Table 4.9 and Table 4.10 for an overview of the design-level transverse results. High bent displacements are indicative of a flexible substructure able to accommodate large deflections. This behavior is in keeping with tall column bridge bents, like the ones present in the Scarham Bridge. Excessive deflections were a concern for the transverse motion of this bridge, in both span and bent locations. A hallmark of long period structures is large deflections, especially during certain ground motions. Results from both friction models indicated design-level deflections that were within acceptable limits

for this bridge, however the magnitude of these deflections may not be acceptable for other bridges in this project. All transverse design-level analyses of the Scarham Creek Bridge ran successfully. One very important observation of the recorded data from both friction models of this bridge is the fact that every single data point is the same for the transverse direction motions. The only difference between both bridge models is the change in bearing pad friction factor. Both models behave in exactly the same manner during events that do not allow friction slips to occur. This information points to a variety of possible conclusions. The first conclusion assumes a very flexible bearing pad in use at each connection, one that is able to accommodate all connection motion without reaching a slipping point. A second conclusion could be made indicating that the stiffness of both the substructure and superstructure were so similar that the resulting differential movement between the two at the connection zones was minimal and did not cause slipping. This second conclusion is not supported by shear bolt behavior however; which did carry a significant load at the connection location. Results seem to favor the first conclusion, but the lack of slipping is still noted.

Table 4.9: Results Overview for Lower Limit Friction Scarham Creek Transverse Model

Scarham	Friction ".2"												
Transverse Motion	Ground Motion	Run Status	Run Time	Foundation Capacity (D/R)		Bearing Capacity	Bent Ductility	Bolt Status	Max Column Shear	Max Span Disp. (in.)	Max Bent Disp. (in.)	Residual Span Disp. (in.)	Residual Bent Disp. (in.)
San Fernando 1	Design	Comp.	48.00	0.286	0.4461	0.023	2.322	0.848	1761.905	4.341	3.742	0.015	0.008
San Fernando 2	Design	Comp.	50.00	0.255	0.3800	0.023	1.877	0.746	1735.696	3.652	3.104	0.031	0.039
Imperial Valley	Design	Comp.	60.00	0.134	0.1747	0.020	0.905	0.565	1379.593	1.676	1.367	0.010	0.007
Coalinga	Design	Comp.	52.00	0.190	0.2618	0.020	1.408	0.696	1626.783	2.798	2.381	0.034	0.027
North Palm Springs	Design	Comp.	40.00	0.144	0.2140	0.020	1.071	0.567	1430.486	2.049	1.669	0.012	0.009
Landers	Design	Comp.	70.00	0.317	0.5033	0.024	2.643	**0.943**	1853.291	4.846	4.235	0.041	0.017
Little Skull Mountain	Design	Comp.	132.00	0.055	0.0750	0.018	0.376	0.184	1174.141	0.736	0.597	0.011	0.008
Kocaeli 1	Design	Comp.	170.00	0.335	0.5500	0.026	2.823	**0.991**	2010.688	5.219	4.549	0.104	0.041
Kocaeli 2	Design	Comp.	48.00	0.256	0.3700	0.022	1.864	0.768	1759.118	3.541	3.018	0.017	0.014
Kobe	Design	Comp.	60.00	0.111	0.1638	0.020	0.733	0.308	1327.181	1.413	1.185	0.013	0.010
Mean				0.2084	0.3139	0.0215	1.6023	0.6615	1605.8882	3.0270	2.5846	0.0288	0.0181
Standard Deviation				0.0950	0.1593	0.0025	0.8366	0.2610	265.8816	1.5342	1.3605	0.0286	0.0130
Relative Stand Deviation				45.57%	50.74%	11.48%	52.21%	39.46%	16.56%	50.68%	52.64%	99.35%	71.50%

Table 4.10: Results Overview for Upper Limit Friction Scarham Creek Transverse Model

Scarham	Friction ".4"												
Transverse Motion	Ground Motion	Run Status	Run Time	Foundation Capacity (D/R)		Bearing Capacity	Bent Ductility	Bolt Status	Max Column Shear	Max Span Disp. (in.)	Max Bent Disp. (in.)	Residual Span Disp. (in.)	Residual Bent Disp. (in.)
San Fernando 1	Design	Comp.	48.00	0.286	0.4461	0.023	2.322	0.848	1761.905	4.341	3.742	0.015	0.008
San Fernando 2	Design	Comp.	50.00	0.255	0.3800	0.023	1.877	0.746	1735.696	3.652	3.104	0.031	0.039
Imperial Valley	Design	Comp.	60.00	0.134	0.1747	0.020	0.905	0.565	1379.593	1.676	1.367	0.010	0.007
Coalinga	Design	Comp.	52.00	0.190	0.2618	0.020	1.408	0.696	1626.783	2.798	2.381	0.034	0.027
North Palm Springs	Design	Comp.	40.00	0.144	0.2140	0.020	1.071	0.567	1430.486	2.049	1.669	0.012	0.009
Landers	Design	Comp.	70.00	0.317	0.5033	0.024	2.643	**0.943**	1853.291	4.846	4.235	0.041	0.017
Little Skull Mountain	Design	Comp.	132.00	0.055	0.0750	0.018	0.376	0.184	1174.141	0.736	0.597	0.011	0.008
Kocaeli 1	Design	Comp.	170.00	0.335	0.5500	0.026	2.823	**0.991**	2010.688	5.219	4.549	0.430	0.315
Kocaeli 2	Design	Comp.	48.00	0.256	0.3700	0.022	1.864	0.768	1759.118	3.541	3.018	0.017	0.014
Kobe	Design	Comp.	60.00	0.111	0.1638	0.020	0.733	0.308	1327.181	1.413	1.185	0.013	0.010
Mean				0.2084	0.3139	0.0214	1.6023	0.6615	1605.8882	3.0270	2.5846	0.0614	0.0455
Standard Deviation				0.0950	0.1593	0.0023	0.8366	0.2610	265.8816	1.5342	1.3604	0.1300	0.0952
Relative Stand Deviation				45.57%	50.74%	10.91%	52.21%	39.46%	16.56%	50.68%	52.64%	**211.69%**	**209.21%**

A total of fourteen MCE-level events were applied to this bridge model. All transverse MCE-level analyses of the Scarham Creek Bridge ran successfully. Only one case of limit exceedance was reported and the results can be found in Table 7.11 and Table 7.12. Results between the two friction models are the same with the exception of the Landers MCE event. This event in the upper friction limit model results in a high foundation rotation case similar to the cases recorded for longitudinal motion. All residual displacements are below the 1" limit, indicating acceptable serviceability of the structure post event.

Table 4.11: MCE-Level Results Overview for Lower Limit Friction Scarham Creek Transverse Model

Scarham	Friction ".2"												
Transverse Motion	Ground Motion	Run Status	Run Time	Foundation Capacity (D/R)		Bearing Capacity	Bent Ductility	Bolt Status	Max Column Shear	Max Span Disp.	Max Bent Disp.	Residual Span Disp.	Residual Bent Disp.
San Fernando 1	MCE	Comp.	48.00	0.306	0.4732	0.024	2.536	**0.926**	1785.350	4.746	4.068	0.017	0.010
San Fernando 2	MCE	Comp.	50.00	0.318	0.5100	0.024	2.553	**0.967**	1921.752	4.897	4.183	0.023	0.027
Imperial Valley	MCE	Comp.	60.00	0.190	0.2381	0.021	1.305	0.793	1520.694	2.387	1.956	0.008	0.006
Landers	MCE	Comp.	70.00	0.305	0.4258	0.025	2.565	**0.983**	1953.014	5.384	4.390	0.615	0.727
Kocaeli 1	MCE	Comp.	170.00	0.308	0.4700	0.027	2.585	**0.994**	1714.110	5.025	4.215	0.438	0.351
Kocaeli 2	MCE	Comp.	48.00	0.335	0.4067	0.027	3.095	**0.979**	2172.828	5.808	5.009	0.200	0.103
Kobe	MCE	Comp.	60.00	0.172	0.2382	0.021	1.152	0.496	1462.366	2.090	1.775	0.016	0.012
Mean				0.2762	0.3946	0.0241	2.2558	0.8769	1790.0164	4.3338	3.6565	0.1881	0.1766
Standard Deviation				0.0661	0.1120	0.0025	0.7300	0.1816	250.3800	1.4756	1.2623	0.2462	0.2724
Relative Stand Deviation				23.93%	28.38%	10.43%	32.36%	20.71%	13.99%	34.05%	34.52%	**130.89%**	**154.25%**

Table 4.12: MCE-Level Results Overview for Upper Limit Friction Scarham Creek Transverse Model

Scarham	Friction ".4"												
Transverse Motion	Ground Motion	Run Status	Run Time	Foundation Capacity (D/R)		Bearing Capacity	Bent Ductility	Bolt Status	Max Column Shear	Max Span Disp.	Max Bent Disp.	Residual Span Disp.	Residual Bent Disp.
San Fernando 1	MCE	Comp.	48.00	0.306	0.4732	0.024	2.536	**0.926**	1785.350	4.746	4.068	0.017	0.010
San Fernando 2	MCE	Comp.	50.00	0.318	0.5100	0.024	2.553	**0.967**	1921.752	4.897	4.183	0.023	0.027
Imperial Valley	MCE	Comp.	60.00	0.190	0.2381	0.021	1.305	0.793	1520.694	2.387	1.956	0.008	0.006
Landers	MCE	Comp.	70.00	0.363	**1.5600**	0.058	4.863	**0.997**	1848.441	7.307	5.368	0.293	0.640
Kocaeli 1	MCE	Comp.	170.00	0.308	0.6367	0.028	2.585	**0.957**	1928.681	7.244	5.558	0.754	0.428
Kocaeli 2	MCE	Comp.	48.00	0.335	0.4233	0.025	3.095	**0.979**	2172.574	5.809	5.007	0.557	0.349
Kobe	MCE	Comp.	60.00	0.172	0.2382	0.021	1.152	0.496	1462.366	2.090	1.775	0.016	0.012
Mean				0.2845	0.5828	0.0287	2.5841	0.8738	1805.6941	4.9257	3.9878	0.2382	0.2103
Standard Deviation				0.0735	0.4543	0.0132	1.2346	0.1798	246.4877	2.0954	1.5536	0.3078	0.2601
Relative Stand Deviation				25.83%	77.95%	46.08%	47.78%	20.58%	13.65%	42.54%	38.96%	**129.22%**	**123.71%**

4.3.2 Longitudinal Motion

The longitudinal analysis for this bridge resulted in fairly consistent design-level results. See Table 4.13 and Table 4.14 for an overview of the design-level transverse results. Maximum span displacements of about 2.5 inches occurred for most ground motions in each bridge model, and bent displacements hovered around 2 inches. These results are to be expected in bridges with such tall columns. Bent ductility appears to remain below the established maximum for the second and fourth bent (1.076 inches), with only one design-level ground motion, (San Fernando 2) causing a ductility in excess of this limit. Foundation capacity for this bridge exceeds the displacement limit set by geotechnical data. This foundation displacement is present in all design-level events, and is thus a conclusive failure in the longitudinal direction of this bridge. These deformations at foundation-level are a result of shear forces carried by the substructure, and not a product of excessive moments or structural failures.

Table 4.13: Results Overview for Lower Limit Friction Scarham Creek Longitudinal Model

Scarham	Friction ".2"											
Longitudinal Motion	Ground Motion	Run Status	Run Time	Foundation Capacity (D/R)		Bearing Capacity	Bent Ductility	Max Column Shear	Max Span Disp. (in.)	Max Bent Disp. (in.)	Residual Span Disp. (in.)	Residual Bent Disp. (in.)
San Fernando 1	Design	Comp.	48.00	**1.685**	0.2917	0.278	0.787	968.259	2.927	2.459	0.413	0.355
San Fernando 2	Design	Comp.	50.00	**1.868**	0.3976	0.239	1.081	1046.208	3.682	3.174	0.453	0.267
Imperial Valley	Design	Comp.	60.00	**1.698**	0.2767	0.195	0.714	973.824	2.729	2.453	0.372	0.250
Coalinga	Design	Comp.	52.00	**1.692**	0.2185	0.182	0.695	971.426	2.341	1.900	0.405	0.275
North Palm Springs	Design	Comp.	40.00	**1.648**	0.1456	0.125	0.520	952.760	1.535	1.249	0.062	0.060
Landers	Design	Comp.	70.00	**1.703**	0.2891	0.234	0.765	975.806	3.013	2.445	0.211	0.131
Little Skull Mountain	Design	Comp.	132.00	**1.600**	0.0814	0.042	0.385	932.183	0.689	0.592	0.172	0.050
Kocaeli 1	Design	Comp.	170.00	**1.744**	0.3006	0.223	0.782	993.502	3.023	2.638	0.240	0.123
Kocaeli 2	Design	Comp.	48.00	**1.718**	0.2314	0.206	0.657	982.143	2.620	2.002	0.050	0.002
Kobe	Design	Comp.	60.00	**1.663**	0.2282	0.180	0.672	958.920	2.380	1.971	0.296	0.178
Mean				**1.7019**	0.2461	0.1905	0.7058	975.5031	2.4938	2.0882	0.2674	0.1691
Standard Deviation				0.0706	0.0878	0.0663	0.1819	30.0148	0.8453	0.7362	0.1448	0.1152
Relative Stand Deviation				4.15%	35.66%	34.80%	25.77%	3.08%	33.90%	35.25%	54.17%	68.11%

Table 4.14: Results Overview for Upper Limit Friction Scarham Creek Longitudinal Model

Scarham	Friction ".4"											
Longitudinal Motion	Ground Motion	Run Status	Run Time	Foundation Capacity (D/R)		Bearing Capacity	Bent Ductility	Max Column Shear	Max Span Disp. (in.)	Max Bent Disp. (in.)	Residual Span Disp. (in.)	Residual Bent Disp. (in.)
San Fernando 1	Design	Comp.	48.00	**1.722**	0.3486	0.207	0.889	984.097	3.294	2.961	0.010	0.002
San Fernando 2	Design	Fail	4.45	**1.640**	0.4037	0.235	1.108	949.414	3.950	3.342		
Imperial Valley	Design	Comp.	60.00	**1.744**	0.2974	0.215	0.959	993.480	3.203	2.680	0.131	0.094
Coalinga	Design	Comp.	52.00	**1.690**	0.2340	0.135	0.764	970.624	2.328	2.038	0.217	0.129
North Palm Springs	Design	Comp.	40.00	**1.653**	0.1456	0.119	0.520	954.562	1.535	1.247	0.174	0.051
Landers	Design	Comp.	70.00	**1.757**	0.3303	0.211	0.962	998.828	3.277	2.847	0.112	0.061
Little Skull Mountain	Design	Comp.	132.00	**1.600**	0.0814	0.042	0.385	932.183	0.689	0.592	0.172	0.050
Kocaeli 1	Design	Comp.	170.00	**1.787**	0.3242	0.210	0.976	1011.495	3.447	2.837	0.022	0.063
Kocaeli 2	Design	Comp.	48.00	**1.707**	0.2398	0.174	0.701	977.714	2.592	2.165	0.103	0.022
Kobe	Design	Comp.	60.00	**1.726**	0.2342	0.167	0.904	985.809	2.727	2.054	0.165	0.081
Mean				**1.7026**	0.2639	0.1714	0.8168	975.8206	2.7042	2.2762	0.1229	0.0614
Standard Deviation				0.0575	0.0975	0.0587	0.2248	24.4181	0.9780	0.8447	0.0700	0.0376
Relative Stand Deviation				3.38%	36.94%	34.26%	27.53%	2.50%	36.17%	37.11%	56.94%	61.27%

A total of fourteen MCE-level events were applied to this bridge model. See Table 4.15 and Table 4.16 for an overview of the MCE-level longitudinal results. Only six of the fourteen analyses were completed with all incomplete analyses showing signs of possible structural failure. It is difficult to classify the MCE-level of behavior for this bridge as acceptable given the large amount of unknowns found in the results. Conservative estimates would suggest that this bridge's behavior is unsuitable for an MCE-level event, however the classification of "Failure" in many of these results stems

from the conservative judgment, rather than an observed failure. Additional study of taller bent bridges at the MCE-level may be required in order to gather more information on cases similar to this analysis case.

Table 4.15: MCE-Level Results Overview for Lower Limit Friction Scarham Creek Longitudinal Model

Scarham	Friction ".2"											
Longitudinal Motion	Ground Motion	Run Status	Run Time	Foundation Capacity (D/R)		Bearing Capacity	Bent Ductility	Max Column Shear	Max Span Disp.	Max Bent Disp.	Residual Span Disp.	Residual Bent Disp.
San Fernando 1	MCE	Comp.	48.00	**1.697**	0.3033	0.280	0.840	973.314	3.198	2.698	0.431	0.348
San Fernando 2	MCE	Fail	4.39	**1.647**	0.3700	0.315	0.844	952.314	3.820	3.299		
Imperial Valley	MCE	Comp.	60.00	**1.721**	0.3089	0.233	0.829	983.621	3.118	2.701	0.170	0.150
Landers	MCE	Comp.	70.00	**1.770**	0.3303	0.291	0.835	1004.557	3.215	2.864	0.437	0.278
Kocaeli 1	MCE	Fail	24.36	**1.802**	0.5199	0.809	2.462	1018.009	3.559	5.110		
Kocaeli 2	MCE	Fail	7.62	**1.819**	0.3119	0.323	0.757	1025.210	3.409	2.812		
Kobe	MCE	Comp.	60.00	**1.668**	0.2864	0.247	0.792	960.924	3.037	2.475	0.049	0.075
Mean				1.7320	0.3472	0.3568	1.0514	988.2784	3.3366	3.1369	0.2718	0.2128
Standard Deviation				0.0666	0.0806	0.2021	0.6230	28.2847	0.2768	0.9056	0.1938	0.1231
Relative Stand Deviation				3.84%	23.21%	56.62%	59.25%	2.86%	8.30%	28.87%	71.30%	57.86%

Table 4.16: MCE-Level Results Overview for Upper Limit Friction Scarham Creek Longitudinal Model

Scarham	Friction ".4"											
Longitudinal Motion	Ground Motion	Run Status	Run Time	Foundation Capacity (D/R)		Bearing Capacity	Bent Ductility	Max Column Shear	Max Span Disp.	Max Bent Disp.	Residual Span Disp.	Residual Bent Disp.
San Fernando 1	MCE	Comp.	48.00	**1.761**	0.8685	0.451	1.797	1000.505	3.425	3.805	**1.139**	0.622
San Fernando 2	MCE	Fail	3.87	**1.641**	0.2634	0.161	0.829	949.502	2.515	2.217		
Imperial Valley	MCE	Fail	10.55	**1.760**	0.3517	0.231	1.026	1000.349	3.719	2.879		
Landers	MCE	Fail	22.89	**1.740**	0.3578	0.208	1.222	991.567	3.595	3.160		
Kocaeli 1	MCE	Fail	22.52	**1.779**	0.5199	0.706	1.061	1008.230	3.529	2.960		
Kocaeli 2	MCE	Fail	7.11	**1.666**	0.3272	0.223	1.062	960.427	3.806	3.219		
Kobe	MCE	Comp.	60.00	**1.740**	0.3058	0.205	0.957	991.848	3.224	2.652	0.076	0.042
Mean				1.7268	0.4278	0.3121	1.1363	986.0612	3.4017	2.9846	0.6075	0.3320
Standard Deviation				0.0523	0.2103	0.1976	0.3146	22.2177	0.4350	0.4951	0.7517	0.4101
Relative Stand Deviation				3.03%	49.17%	63.30%	27.68%	2.25%	12.79%	16.59%	**123.73%**	**123.53%**

4.4 Norfolk Southern Railroad Bridge

Results show that the average behavior of the Norfolk Southern Bridge was favorable for design and MCE-level events. Design-level events resulted in behaviors typical with stiff elastic bridges, including smaller span displacements and bent deflections. Foundation performance for this bridge was acceptable in both directions of

motion. All design-level analysis performed for this bridge succeeded in completing in the lateral direction. Three design-level analyses performed in the longitudinal direction failed to result in completion. Substructure behavior appears to be adequate at column and bent cap locations. Connection behavior also appears to be adequate from the results of each analysis with anchor bolts failing, but no cases of unseating. Bearing pad slippage was minimal in both directions of loading, and did not approach levels indicative of unseating. A more in-depth analysis of each bridge model's results is proved in the next sections.

4.4.1 Transverse Motion

The transverse analysis for this bridge resulted in stiff structural behavior. See Table 4.17 and Table 4.18 for an overview of the design-level transverse results. Lower bent displacements are indicative of a stiff substructure. This behavior is in keeping with triple column bridge bents, like the ones present in the Norfolk Southern Railroad Bridge. Design-level results from both friction models indicated residual deflections that were within acceptable limits for this bridge. All transverse design-level analyses of the Norfolk Southern Railroad Bridge ran successfully. Many anchor bolt failures can be observed in the transverse analyses. These failures are a result of high levels of forces being transferred between the super and substructure of the bridge. This is more common in bridges with stiffer substructures, since the superstructure of each bridge is simply supported with long span lengths and generally behaves in a more flexible manner. Overall these results are in keeping with the predicted behaviors of this bridge.

Table 4.17: Results Overview for Lower Limit Friction Norfolk Southern Railroad Transverse Model

Norfolk	Friction ".2"												
Transverse Motion	Ground Motion	Run Status	Run Time	Foundation Capacity (D/R)		Bearing Capacity	Bent Ductility	Bolt Status	Max Column Shear	Max Span Disp. (in.)	Max Bent Disp. (in.)	Residual Span Disp. (in.)	Residual Bent Disp. (in.)
San Fernando 1	Design	Comp.	48.00	0.124	0.0095	0.115	0.768	**0.981**	28.022	0.973	0.941	0.049	0.162
San Fernando 2	Design	Comp.	50.00	0.083	0.0004	0.040	0.554	0.798	17.716	0.810	0.717	0.020	0.018
Imperial Valley	Design	Comp.	60.00	0.125	0.0143	0.146	0.816	**0.982**	19.424	1.221	1.019	0.066	0.181
Coalinga	Design	Comp.	52.00	0.124	0.0005	0.049	0.768	**0.986**	20.088	1.000	0.942	0.017	0.052
North Palm Springs	Design	Comp.	40.00	0.115	0.0007	0.050	0.715	**0.997**	18.315	0.985	0.877	0.019	0.000
Landers	Design	Comp.	70.00	0.141	0.0101	0.160	0.869	**0.990**	23.942	1.305	1.070	0.060	0.183
Little Skull Mountain	Design	Comp.	132.00	0.014	0.0005	0.011	0.133	0.221	17.246	0.223	0.185	0.019	0.014
Kocaeli 1	Design	Comp.	170.00	0.147	0.0148	0.194	0.950	**0.991**	32.714	1.769	1.193	0.326	0.153
Kocaeli 2	Design	Comp.	48.00	0.138	0.0173	0.216	0.861	**0.990**	20.060	1.748	1.059	0.070	0.198
Kobe	Design	Comp.	60.00	0.092	0.0007	0.042	0.612	0.846	18.093	0.849	0.768	0.030	0.027

Mean	0.1104	0.0069	0.1024	0.7046	0.8782	21.5621	1.0882	0.8771	0.0676	0.0988
Standard Deviation	0.0394	0.0070	0.0732	0.2332	0.2412	5.1289	0.4567	0.2817	0.0932	0.0826
Relative Stand Deviation	35.65%	**101.77%**	71.47%	33.10%	27.47%	23.79%	41.97%	32.12%	**137.84%**	83.53%

Table 4.18: Results Overview for Upper Limit Friction Norfolk Southern Railroad Transverse Model

Norfolk	Friction ".4"												
Transverse Motion	Ground Motion	Run Status	Run Time	Foundation Capacity (D/R)		Bearing Capacity	Bent Ductility	Bolt Status	Max Column Shear	Max Span Disp. (in.)	Max Bent Disp. (in.)	Residual Span Disp. (in.)	Residual Bent Disp. (in.)
San Fernando 1	Design	Comp.	48.00	0.124	0.0088	0.107	0.768	**0.983**	27.118	0.973	0.941	0.010	0.049
San Fernando 2	Design	Comp.	50.00	0.083	0.0004	0.040	0.554	0.798	17.716	0.810	0.717	0.020	0.018
Imperial Valley	Design	Comp.	60.00	0.125	0.0119	0.121	0.816	**0.982**	22.432	1.120	1.019	0.013	0.031
Coalinga	Design	Comp.	52.00	0.124	0.0005	0.049	0.768	**0.986**	20.088	1.000	0.942	0.017	0.052
North Palm Springs	Design	Comp.	40.00	0.115	0.0007	0.050	0.715	**0.997**	18.315	0.985	0.877	0.018	0.001
Landers	Design	Comp.	70.00	0.539	0.0054	0.136	3.173	**0.993**	37.700	1.481	3.837	**1.014**	3.602
Little Skull Mountain	Design	Comp.	132.00	0.014	0.0005	0.011	0.133	0.221	17.246	0.223	0.185	0.019	0.014
Kocaeli 1	Design	Comp.	170.00	0.112	0.0160	0.176	0.747	**0.991**	28.415	1.496	0.949	0.021	0.103
Kocaeli 2	Design	Comp.	48.00	0.118	0.0114	0.150	0.754	**0.990**	29.420	1.407	0.952	0.032	0.023
Kobe	Design	Comp.	60.00	0.092	0.0007	0.042	0.612	0.846	18.093	0.849	0.768	0.030	0.027

Mean	0.1446	0.0056	0.0881	0.9039	0.8787	23.6542	1.0343	1.1187	0.1194	0.3920
Standard Deviation	0.1425	0.0060	0.0563	0.8216	0.2415	6.7916	0.3814	0.9850	0.3144	1.1282
Relative Stand Deviation	98.51%	**105.47%**	63.86%	90.90%	27.48%	28.71%	36.87%	88.05%	**263.32%**	**287.78%**

A total of fourteen MCE-level events were analyzed with this bridge model. See Table 4.19 and Table 4.20 for an overview of the MCE-level transverse results. A majority of these MCE results indicated lower bent displacements and span displacements with a single exception. This behavior is in keeping with triple column bridge bents, like the ones present in the Norfolk Southern Railroad Bridge. The Landers event for the lower friction limit model resulted in behavior that is indicative of span

unseating. A high bearing pad displacement was recorded as well as a high residual displacement. High residual displacement was also recorded in the upper bound friction model during the same ground motion. All transverse design-level analyses of the Norfolk Southern Railroad Bridge ran successfully. Many anchor bolt failures were observed in the MCE-level transverse analyses. This is more common in bridges with stiffer substructures, since the superstructure of each bridge is simply supported with long span lengths and generally behaves in a more flexible manner. Overall these results are in keeping with the predicted behaviors of this bridge, and the average behavior of these models indicates acceptable behavior at the MCE-level.

Table 4.19: MCE-Level Results Overview for Lower Limit Friction Norfolk Southern Railroad Transverse Model

Norfolk	Friction ".2"												
Transverse Motion	Ground Motion	Run Status	Run Time	Foundation Capacity (D/R)		Bearing Capacity	Bent Ductility	Bolt Status	Max Column Shear	Max Span Disp.	Max Bent Disp.	Residual Span Disp.	Residual Bent Disp.
San Fernando 1	MCE	Comp.	48.00	0.128	0.0092	0.109	0.783	**0.979**	26.267	0.974	0.954	0.043	0.148
San Fernando 2	MCE	Comp.	50.00	0.124	0.0138	0.173	0.771	**0.978**	30.382	1.441	0.947	0.051	0.017
Imperial Valley	MCE	Comp.	60.00	0.222	0.0088	0.195	1.383	**0.996**	22.689	2.006	1.699	0.411	0.420
Landers	MCE	Comp.	70.00	0.434	0.0542	**1.492**	2.977	**0.986**	34.799	14.166	6.326	**13.606**	**5.907**
Kocaeli 1	MCE	Comp.	170.00	0.240	0.0263	0.274	1.506	**0.910**	30.369	2.176	1.882	0.883	0.050
Kocaeli 2	MCE	Comp.	48.00	0.271	0.0053	0.219	1.624	**0.993**	20.615	2.161	1.986	0.516	0.525
Kobe	MCE	Comp.	60.00	0.189	0.0054	0.164	1.165	**0.947**	21.888	1.610	1.439	0.337	0.370
Mean				0.2295	0.0176	0.3750	1.4584	0.9698	26.7156	3.5048	2.1762	2.2639	1.0624
Standard Deviation				0.1055	0.0177	0.4950	0.7481	0.0310	5.3084	4.7212	1.8762	5.0097	2.1450
Relative Stand Deviation				45.97%	**100.84%**	**132.00%**	51.30%	3.20%	19.87%	**134.70%**	86.21%	**221.29%**	**201.89%**

Table 4.20: MCE-Level Results Overview for Upper Limit Friction Norfolk Southern Railroad Transverse Model

Norfolk	Friction ".4"												
Transverse Motion	Ground Motion	Run Status	Run Time	Foundation Capacity (D/R)		Bearing Capacity	Bent Ductility	Bolt Status	Max Column Shear	Max Span Disp.	Max Bent Disp.	Residual Span Disp.	Residual Bent Disp.
San Fernando 1	MCE	Comp.	48.00	0.128	0.0084	0.102	0.783	**0.979**	25.533	0.974	0.954	0.003	0.069
San Fernando 2	MCE	Comp.	50.00	0.124	0.0147	0.198	0.833	**0.978**	31.423	1.828	1.080	0.281	0.115
Imperial Valley	MCE	Comp.	60.00	0.178	0.0059	0.163	1.129	**0.996**	24.991	1.721	1.402	0.018	0.081
Landers	MCE	Comp.	70.00	0.353	0.0053	0.402	1.267	**0.971**	34.230	4.577	1.618	**3.399**	0.348
Kocaeli 1	MCE	Comp.	170.00	0.293	0.0064	0.243	1.847	**0.995**	40.217	2.582	2.276	0.096	0.283
Kocaeli 2	MCE	Comp.	48.00	0.234	0.0125	0.208	1.452	**0.993**	28.246	2.028	1.812	0.097	0.123
Kobe	MCE	Comp.	60.00	0.173	0.0126	0.175	1.085	**0.963**	27.853	1.627	1.342	0.148	0.048
Mean				0.2117	0.0094	0.2130	1.1994	0.9821	30.3562	2.1911	1.4978	0.5775	0.1524
Standard Deviation				0.0862	0.0038	0.0942	0.3683	0.0129	5.4184	1.1564	0.4513	1.2476	0.1159
Relative Stand Deviation				40.72%	40.62%	44.22%	30.71%	1.31%	17.85%	52.77%	30.13%	**216.05%**	76.00%

4.4.2 Longitudinal Motion

The longitudinal analysis for this bridge resulted in fairly consistent results. See Table 4.21 and Table 4.22 for an overview of the design-level longitudinal results. Maximum span displacements of about 1 inch occurred for most design-level ground motions in each bridge model, and bent displacements hovered around 1.1 inches. These results are to be expected in bridges with such stiff substructure. Bent ductility appears to remain well below the established maximum (3.89). Foundation capacity for this bridge does not exceed the displacement limit set by geotechnical data. Recorded column shears for this model appear to be incorrectly recorded due to very small recorded values when compared to every other analysis performed in the chapter. Three of the design-level analyses performed on the models resulted in analysis failure, with the Kocaeli 1 event resulting in possible structural failure. The results from this event only last for 22.52 seconds of the applied ground motion, but they already exhibit reasonable bridge response before the largest accelerations are even applied. A judgment was made to classify these results as a possible structural failure. Despite this, overall behavior of this bridge appears to be sufficient in the design-level longitudinal direction.

Table 4.21: Results Overview for Lower Limit Friction Norfolk Southern Longitudinal Model

Norfolk	Friction ".2"											
Longitudinal Motion	Ground Motion	Run Status	Run Time	Foundation Capacity (D/R)		Bearing Capacity	Bent Ductility	Max Column Shear	Max Span Disp. (in.)	Max Bent Disp. (in.)	Residual Span Disp. (in.)	Residual Bent Disp. (in.)
San Fernando 1	Design	Num.	17.44	0.061	0.2009	0.180	0.593	3.332	1.564	0.891		
San Fernando 2	Design	Comp.	50.00	0.066	0.3339	0.500	0.670	7.527	2.272	1.263	0.245	0.110
Imperial Valley	Design	Comp.	60.00	0.066	0.1801	0.233	0.382	6.051	1.078	0.595	0.214	0.094
Coalinga	Design	Comp.	52.00	0.065	0.2494	0.405	0.741	6.556	1.749	1.146	0.333	0.191
North Palm Springs	Design	Comp.	40.00	0.063	0.1871	0.276	0.462	3.271	1.155	0.668	0.327	0.194
Landers	Design	Comp.	70.00	0.352	0.2065	0.376	0.762	306.738	1.622	1.073	0.707	0.229
Little Skull Mountain	Design	Comp.	132.00	0.063	0.0379	0.074	0.178	3.079	0.284	0.185	0.044	0.046
Kocaeli 1	Design	Comp.	170.00	0.064	0.2286	0.340	0.560	7.162	1.486	0.835	0.262	0.127
Kocaeli 2	Design	Comp.	48.00	0.064	0.1968	0.318	0.549	8.072	1.367	0.817	0.343	0.176
Kobe	Design	Comp.	60.00	0.063	0.1427	0.278	0.454	4.119	1.169	0.656	0.283	0.157

Mean	0.0963	0.1959	0.3109	0.5288	39.1749	1.3536	0.8043	0.3064	0.1471
Standard Deviation	0.0961	0.0800	0.1196	0.1855	100.3530	0.5458	0.3295	0.1756	0.0577
Relative Stand Deviation	99.79%	40.85%	38.46%	35.08%	**256.17%**	40.32%	40.97%	57.30%	39.19%

Table 4.22: Results Overview for Upper Limit Friction Norfolk Southern Longitudinal Model

Norfolk	Friction ".4"											
Longitudinal Motion	Ground Motion	Run Status	Run Time	Foundation Capacity (D/R)		Bearing Capacity	Bent Ductility	Max Column Shear	Max Span Disp. (in.)	Max Bent Disp. (in.)	Residual Span Disp. (in.)	Residual Bent Disp. (in.)
San Fernando 1	Design	Comp.	48.00	0.063	0.2356	0.295	0.493	3.870	1.259	0.730	0.036	0.028
San Fernando 2	Design	Comp.	50.00	0.275	0.3686	0.536	0.779	285.206	2.425	1.450	0.225	0.276
Imperial Valley	Design	Comp.	60.00	0.065	0.1871	0.250	0.427	6.588	1.099	0.627	0.040	0.037
Coalinga	Design	Comp.	52.00	0.086	0.2910	0.507	0.924	13.648	2.216	1.459	0.214	0.131
North Palm Springs	Design	Num.	8.10	0.061	0.2425	0.346	0.624	2.613	1.515	0.946		
Landers	Design	Comp.	70.00	0.320	0.2647	0.371	1.181	288.173	2.041	1.437	0.486	0.027
Little Skull Mountain	Design	Comp.	132.00	0.063	0.0379	0.074	0.178	3.096	0.284	0.185	0.044	0.046
Kocaeli 1	Design	Fail.	22.52	0.062	0.3298	0.401	0.651	2.690	1.857	1.232		
Kocaeli 2	Design	Comp.	48.00	0.064	0.2217	0.298	0.501	10.761	1.359	0.793	0.025	0.001
Kobe	Design	Comp.	60.00	0.063	0.1690	0.249	0.421	4.074	1.043	0.599	0.041	0.035

Mean	0.0983	0.2171	0.3054	0.5970	41.6123	1.3949	0.8828	0.1389	0.0726
Standard Deviation	0.0900	0.0895	0.1278	0.3175	99.7030	0.6290	0.4512	0.1628	0.0905
Relative Stand Deviation	91.52%	41.24%	41.85%	53.18%	**239.60%**	45.09%	51.11%	**117.21%**	**124.68%**

A total of fourteen MCE-level events were applied to this bridge model. See Table 4.23 and Table 4.24 for an overview of the MCE-level longitudinal results. Ten of the fourteen analyses ran completely. Three of the four that did not result in completion were determined to cause possible failure in the form of eventual span unseating. The displacements of the bearing pads in these analyses were relatively high at the time of analysis failure. This combined with the fact that these analysis ceased before sections of

the largest ground motion accelerations were applied to the models lead to the prediction of possible unseating. This was determined due to high recorded bearing displacements during sections of the ground motion that proceeded larger ground motion accelerations that were never applied in the analysis. The overall behavior of this bridge appears to be acceptable for critical and essential bridges, and the problem of unseating should become reduced due to the adoption of increased seat widths for future designs.

Table 4.23: MCE-Level Results Overview for Lower Limit Friction Norfolk Southern Longitudinal Model

Norfolk	Friction ".2"											
Longitudinal Motion	Ground Motion	Run Status	Run Time	Foundation Capacity (D/R)		Bearing Capacity	Bent Ductility	Max Column Shear	Max Span Disp.	Max Bent Disp.	Residual Span Disp.	Residual Bent Disp.
San Fernando 1	MCE	Comp.	48.00	0.063	0.2425	0.363	0.596	5.178	1.578	0.895	0.051	0.004
San Fernando 2	MCE	Comp.	50.00	0.064	0.3810	0.563	0.811	8.467	2.542	1.505	0.099	0.119
Imperial Valley	MCE	Comp.	60.00	0.065	0.2660	0.361	0.488	6.479	1.639	0.953	0.218	0.109
Landers	MCE	Comp.	70.00	0.350	0.2314	0.439	0.842	316.381	1.924	1.286	0.171	0.360
Kocaeli 1	MCE	Fail.	23.40	0.067	0.3131	0.493	0.861	3.548	2.173	1.352		
Kocaeli 2	MCE	Fail.	6.95	0.061	0.3048	0.370	0.568	2.696	1.721	1.091		
Kobe	MCE	Comp.	60.00	0.063	0.2120	0.364	0.658	4.725	1.565	1.001	0.379	0.230
Mean				0.1046	0.2787	0.4219	0.6890	49.6392	1.8775	1.1548	0.1836	0.1645
Standard Deviation				0.1084	0.0585	0.0801	0.1488	117.6375	0.3651	0.2287	0.1268	0.1354
Relative Stand Deviation				**103.58%**	20.97%	18.99%	21.60%	**236.98%**	19.45%	19.81%	69.04%	82.34%

Table 4.24: MCE-Level Results Overview for Upper Limit Friction Norfolk Southern Longitudinal Model

Norfolk	Friction ".4"											
Longitudinal Motion	Ground Motion	Run Status	Run Time	Foundation Capacity (D/R)		Bearing Capacity	Bent Ductility	Max Column Shear	Max Span Disp.	Max Bent Disp.	Residual Span Disp.	Residual Bent Disp.
San Fernando 1	MCE	Comp.	48.00	0.064	0.2536	0.325	0.538	6.219	1.395	0.820	0.031	0.016
San Fernando 2	MCE	Num.	15.26	0.325	0.3907	0.577	0.848	121.211	2.593	1.569		
Imperial Valley	MCE	Comp.	60.00	0.064	0.2633	0.336	0.550	9.397	1.543	0.943	0.026	0.001
Landers	MCE	Comp.	70.00	**23.185**	0.3575	0.509	27.825	438.334	3.154	1.645	0.556	0.138
Kocaeli 1	MCE	Fail.	21.58	0.063	0.2882	0.372	0.694	2.932	1.638	1.115		
Kocaeli 2	MCE	Comp.	48.00	0.072	0.2536	0.381	0.762	14.259	1.711	1.180	0.108	0.070
Kobe	MCE	Comp.	60.00	0.063	0.2217	0.355	0.613	5.940	1.523	0.925	0.093	0.051
Mean				3.4052	0.2898	0.4078	4.5473	85.4702	1.9366	1.1709	0.1628	0.0552
Standard Deviation				8.7226	0.0616	0.0964	10.2653	161.2800	0.6675	0.3221	0.2228	0.0538
Relative Stand Deviation				**256.15%**	21.24%	23.64%	**225.74%**	**188.70%**	34.47%	27.51%	**136.86%**	97.50%

4.5 Oseligee Creek Bridge

Results show that the average behavior of the Oseligee Creek Bridge was mixed for design and MCE-level events. Design-level events resulted in behaviors typical with flexible bridges, including larger span displacements and bent deflections. These large span deflections and bent deflections also lead to some cases of collapse of the bridge model. Foundation performance for this bridge was also mixed, and varied from event to event. All design and MCE-level analysis performed for this bridge succeeded in completing except for one transverse analysis at each level. Substructure behavior appears to be inadequate at column and foundation locations due to the large scour situation recommended by geotechnical information. Connection behavior appears to be adequate from the results of each analysis, with design-level unseating only occurring in cases of bridge collapse. A more in-depth analysis of each bridge model's results is proved in the next sections.

4.5.1 Transverse Motion

The transverse analysis for this bridge resulted in flexible structural behavior. See Table 4.25 and Table 4.26 for an overview of the design-level transverse results. High bent displacements are indicative of a flexible substructure able to accommodate large deflections. This behavior is in keeping with tall column bridge bents, like the ones present in the 100% scour condition of the Oseligee Creek Bridge. Excessive deflections were a concern for the transverse motion of this bridge, in both span and bent locations. These deflections led to the collapse of the lower limit friction bridge model during the design-level Landers event. A hallmark of long period structures is large deflections, especially during certain ground motions. Results from both friction models indicated a

majority of design-level deflections that were within acceptable limits for this bridge. The ductility for both models exceeds the limit stated in Table 3.7 of Section 3.6 during the second San Fernando event, however the limit established for ductility of this bridge did not incorporate a 100% scour case. This 100% scour case could alter the limits established by the static pushover analysis. All transverse design-level analyses of the Oseligee Creek Bridge ran successfully with the exception of the Landers ground motion applied to the upper limit friction model. This design-level event was assumed to cause a collapse failure due to the results observed from the previous model, as well as the results recorded before the analysis ceased. Excessive foundation rotations were also observed in 14 of the 20 design-level transverse analyses, with a few other recorded rotations approaching the rotational limits. Ground motion analyses that exhibit these large foundation rotations also tended to exhibit bolt failures at the connection locations.

Table 4.25: Results Overview for Lower Limit Friction Oseligee Creek Transverse Model

Oseligee	Friction ".2"												
Transverse Motion	Ground Motion	Run Status	Run Time	Foundation Capacity (D/R)		Bearing Capacity	Bent Ductility	Bolt Status	Max Column Shear	Max Span Disp. (in.)	Max Bent Disp. (in.)	Residual Span Disp. (in.)	Residual Bent Disp. (in.)
San Fernando 1	Design	Comp.	48.00	0.098	**1.0917**	0.245	3.566	**0.985**	492.010	2.087	1.473	0.188	0.073
San Fernando 2	Design	Comp.	50.00	0.120	**1.4006**	0.389	5.342	**0.985**	558.379	3.095	2.205	0.082	0.028
Imperial Valley	Design	Comp.	60.00	0.106	**1.1223**	0.182	3.389	**0.991**	515.962	1.832	1.405	0.068	0.054
Coalinga	Design	Comp.	52.00	0.102	**1.1040**	0.253	3.991	**0.995**	514.999	2.159	1.645	0.071	0.022
North Palm Springs	Design	Comp.	40.00	0.101	**1.0336**	0.196	3.213	**1.000**	509.962	1.858	1.333	0.051	0.009
Landers	Design	Comp.	70.00	0.199	**3.0673**	**79.975**	27.572	**0.999**	1909.399	786.149	11.267	**587.008**	6.838
Little Skull Mountain	Design	Comp.	132.00	0.022	0.1084	0.017	0.455	0.347	361.541	0.320	0.188	0.000	0.000
Kocaeli 1	Design	Comp.	170.00	0.101	**1.0428**	0.050	3.054	**0.996**	498.337	1.710	1.267	0.003	0.002
Kocaeli 2	Design	Comp.	48.00	0.116	**1.2355**	0.220	3.693	**0.997**	521.881	2.198	1.532	0.099	0.042
Kobe	Design	Comp.	60.00	0.085	0.7951	0.034	2.147	0.686	1525.157	1.276	0.891	0.248	0.047
Mean				0.1050	**1.2001**	**8.1561**	5.6422	0.8981	740.7628	80.2684	2.3207	**58.7818**	0.7115
Standard Deviation				0.0430	0.7426	**25.2349**	7.8078	0.2166	525.0808	248.0220	3.1863	**185.5998**	2.1527
Relative Stand Deviation				40.93%	61.88%	**309.40%**	**138.38%**	24.11%	70.88%	**308.99%**	**137.30%**	**315.74%**	**302.55%**

Table 4.26: Results Overview for Upper Limit Friction Oseligee Creek Transverse Model

Oseligee	Friction ".4"												
Transverse Motion	Ground Motion	Run Status	Run Time	Foundation Capacity (D/R)		Bearing Capacity	Bent Ductility	Bolt Status	Max Column Shear	Max Span Disp. (in.)	Max Bent Disp. (in.)	Residual Span Disp. (in.)	Residual Bent Disp. (in.)
San Fernando 1	Design	Comp.	48.00	0.099	**1.1070**	0.148	3.554	**0.986**	495.895	1.819	1.468	0.304	0.188
San Fernando 2	Design	Comp.	50.00	0.088	0.9694	0.359	5.141	**0.979**	517.882	3.138	2.116	0.010	0.002
Imperial Valley	Design	Comp.	60.00	0.107	**1.1193**	0.187	3.389	**0.994**	512.425	1.855	1.406	0.108	0.057
Coalinga	Design	Comp.	52.00	0.104	**1.1162**	0.251	3.719	**0.969**	522.410	2.155	1.539	0.034	0.009
North Palm Springs	Design	Comp.	40.00	0.103	**1.1193**	0.179	3.827	**0.985**	517.922	1.863	1.584	0.038	0.009
Landers	Design	Fail	35.03	0.009	**1.3089**	0.335	2.914	**0.994**	1749.252	3.469	1.188		
Little Skull Mountain	Design	Comp.	132.00	0.022	0.1076	0.017	0.464	0.345	362.162	0.327	0.192	0.000	0.000
Kocaeli 1	Design	Comp.	170.00	0.097	0.9572	0.046	2.909	**0.914**	494.917	1.645	1.204	0.003	0.003
Kocaeli 2	Design	Comp.	48.00	0.115	**1.2538**	0.172	3.691	**0.988**	521.406	2.260	1.531	0.067	0.105
Kobe	Design	Comp.	60.00	0.070	0.5872	0.033	2.050	0.658	452.858	1.194	0.852	0.000	0.004

Mean	0.0813	0.9646	0.1726	3.1658	0.8810	614.7129	1.9726	1.3079	0.0627	0.0419
Standard Deviation	0.0370	0.3606	0.1193	1.2380	0.2145	401.6717	0.8934	0.5105	0.0974	0.0652
Relative Stand Deviation	45.49%	37.38%	69.09%	39.11%	24.35%	65.34%	45.29%	39.03%	**155.43%**	**155.58%**

A total of fourteen MCE-level events were analyzed with this bridge model. See Table 4.27 and Table 4.28 for an overview of the MCE-level transverse results. High bent ductilities can be observed in these results, as well as high foundation rotations. Four of the fourteen analyses resulted in residual displacements in excess of the 1" limit. All of these undesired behaviors result in questions with this bridge's adequacy but it is important to consider the 100% scour condition present in this bridge. A reduction in this scour amount would result in smaller deflections and a more rigid bridge.

Table 4.27: MCE-Level Results Overview for Lower Limit Friction Oseligee Creek Transverse Model

Oseligee	Friction ".2"												
Transverse Motion	Ground Motion	Run Status	Run Time	Foundation Capacity (D/R)		Bearing Capacity	Bent Ductility	Bolt Status	Max Column Shear	Max Span Disp.	Max Bent Disp.	Residual Span Disp.	Residual Bent Disp.
San Fernando 1	MCE	Comp.	48.00	0.088	0.8532	0.370	4.408	**0.984**	488.994	3.041	1.811	0.001	0.004
San Fernando 2	MCE	Comp.	50.00	0.116	**1.3211**	0.623	7.554	**0.986**	589.055	5.049	3.099	0.100	0.033
Imperial Valley	MCE	Comp.	60.00	0.115	**1.2599**	0.257	3.670	**0.995**	525.915	2.209	1.522	0.041	0.013
Landers	MCE	Comp.	70.00	0.114	**1.4343**	0.717	7.496	**0.992**	1674.884	6.938	3.073	**2.127**	**1.554**
Kocaeli 1	MCE	Comp.	170.00	0.194	**2.7278**	0.429	7.303	**0.986**	673.276	3.961	3.019	0.354	0.000
Kocaeli 2	MCE	Comp.	48.00	0.164	**2.1896**	0.342	6.378	**0.986**	636.391	3.338	2.638	0.006	0.023
Kobe	MCE	Comp.	60.00	0.097	**1.1162**	0.260	3.864	**0.980**	492.120	2.100	1.593	0.040	0.016

Mean	0.1269	1.5574	0.4284	5.8103	0.9869	725.8052	3.8051	2.3936	0.3813	0.2348
Standard Deviation	0.0383	0.6608	0.1778	1.7684	0.0050	424.4309	1.7148	0.7246	0.7794	0.5818
Relative Stand Deviation	30.18%	42.43%	41.51%	30.43%	0.51%	58.48%	45.07%	30.27%	**204.44%**	**247.84%**

Table 4.28: MCE-Level Results Overview for Upper Limit Friction Oseligee Creek Transverse Model

Oseligee	Friction ".4"											
Transverse Motion	Ground Motion	Run Status	Run Time	Foundation Capacity (D/R)		Bearing Capacity	Bent Ductility	Bolt Status	Max Column Shear	Max Span Disp.	Max Bent Disp.	Residual Span Disp.	Residual Bent Disp.
San Fernando 1	MCE	Comp.	48.00	0.139	**1.7339**	**1.593**	8.055	**0.997**	1678.787	14.866	3.288	**1.726**	**1.940**
San Fernando 2	MCE	Comp.	50.00	0.173	**2.3180**	0.421	7.154	**0.995**	1901.130	3.984	2.954	**1.679**	0.689
Imperial Valley	MCE	Comp.	60.00	0.112	**1.2263**	0.208	3.942	**0.987**	527.159	2.184	1.631	0.135	0.053
Landers	MCE	Comp.	70.00	0.011	**1.6391**	0.042	0.469	**0.979**	1508.386	0.431	0.192	0.132	0.066
Kocaeli 1	MCE	Comp.	170.00	0.153	**2.0000**	0.422	5.439	**0.980**	1375.549	3.498	2.250	**2.146**	0.265
Kocaeli 2	MCE	Comp.	48.00	0.121	**1.4709**	0.320	5.812	**0.999**	586.393	3.003	2.397	0.054	0.058
Kobe	MCE	Comp.	60.00	0.094	**1.1162**	0.183	3.659	**0.987**	483.933	2.024	1.513	0.009	0.013
Mean				0.1147	1.6435	0.4554	4.9330	0.9893	1151.6196	4.2842	2.0322	0.8401	0.4406
Standard Deviation				0.0527	0.4227	0.5196	2.5246	0.0079	601.7111	4.8077	1.0346	0.9576	0.7024
Relative Stand Deviation				45.96%	25.72%	**114.10%**	51.18%	0.80%	52.25%	**112.22%**	50.91%	**113.98%**	**159.44%**

4.5.2 Longitudinal Motion

The longitudinal analysis for this bridge resulted in fairly consistent results. See Table 4.29 and Table 4.30 for an overview of the design-level transverse results. Maximum span displacements of about 2 inches occurred for most ground motions in each bridge model, and bent displacements hovered around 1 inch. These results are to be expected in bridges with such tall columns. Bent ductility remains below the established maximum (6), with larger ductility occurring in the upper limit friction model. Foundation capacity for some design-level analyses of this bridge exceeds the rotational limit set by geotechnical data. This foundation rotation is present in three design-level events, two of which also cause collapse of the bridge. These collapse events also show span unseating and high residual displacements, both behaviors support the conclusion of bridge collapse.

Table 4.29: Results Overview for Lower Limit Friction Oseligee Creek Longitudinal Model

Oseligee	Friction ".2"											
Longitudinal Motion	Ground Motion	Run Status	Run Time	Foundation Capacity (D/R)		Bearing Capacity	Bent Ductility	Max Column Shear	Max Span Disp. (in.)	Max Bent Disp. (in.)	Residual Span Disp. (in.)	Residual Bent Disp. (in.)
San Fernando 1	Design	Comp.	48.00	0.071	0.5780	0.447	2.122	10.342	2.305	1.170	0.044	0.052
San Fernando 2	Design	Comp.	50.00	0.080	0.6728	0.504	2.512	11.138	2.475	1.549	0.352	0.018
Imperial Valley	Design	Comp.	60.00	0.061	0.4373	0.391	1.588	10.781	1.607	0.887	0.063	0.003
Coalinga	Design	Comp.	52.00	0.063	0.4281	0.320	1.439	10.407	1.453	0.835	0.370	0.028
North Palm Springs	Design	Comp.	40.00	0.055	0.3731	0.272	1.307	10.540	1.417	0.721	0.024	0.039
Landers	Design	Comp.	70.00	0.073	0.5872	0.618	2.242	10.594	3.215	1.281	**1.371**	0.018
Little Skull Mountain	Design	Comp.	132.00	0.037	0.2006	0.147	0.728	10.260	0.724	0.443	0.083	0.015
Kocaeli 1	Design	Comp.	170.00	0.065	0.4587	0.353	2.125	10.701	1.683	1.050	0.056	0.027
Kocaeli 2	Design	Comp.	48.00	0.078	0.6697	0.658	2.673	11.807	3.280	1.584	0.504	0.004
Kobe	Design	Comp.	60.00	0.053	0.3211	0.253	1.138	10.215	1.326	0.694	0.199	0.075
Mean				0.0635	0.4727	0.3964	1.7876	10.6785	1.9487	1.0213	0.3066	0.0279
Standard Deviation				0.0129	0.1540	0.1625	0.6391	0.4830	0.8422	0.3757	0.4097	0.0223
Relative Stand Deviation				20.38%	32.58%	40.98%	35.75%	4.52%	43.22%	36.78%	**133.62%**	79.90%

Table 4.30: Results Overview for Upper Limit Friction Oseligee Creek Longitudinal Model

Oseligee	Friction ".4"											
Longitudinal Motion	Ground Motion	Run Status	Run Time	Foundation Capacity (D/R)		Bearing Capacity	Bent Ductility	Max Column Shear	Max Span Disp. (in.)	Max Bent Disp. (in.)	Residual Span Disp. (in.)	Residual Bent Disp. (in.)
San Fernando 1	Design	Comp.	48.00	0.096	0.8899	0.438	3.299	10.324	2.359	1.779	0.422	0.217
San Fernando 2	Design	Comp.	50.00	0.108	**1.1223**	0.523	3.477	10.903	2.983	2.133	0.224	0.090
Imperial Valley	Design	Comp.	60.00	0.066	0.4954	0.277	1.613	10.402	1.630	1.039	0.063	0.033
Coalinga	Design	Comp.	52.00	0.124	**1.8685**	**3.781**	24.891	117.009	2.912	7.636	**2.912**	**2.512**
North Palm Springs	Design	Comp.	40.00	0.075	0.6391	0.321	1.963	11.240	1.817	1.164	0.030	0.033
Landers	Design	Comp.	70.00	0.112	**1.5291**	**4.392**	37.605	128.021	3.104	8.918	**3.086**	**6.413**
Little Skull Mountain	Design	Comp.	132.00	0.038	0.2100	0.124	0.728	10.255	0.756	0.449	0.080	0.010
Kocaeli 1	Design	Comp.	170.00	0.105	**1.0917**	0.422	3.137	12.322	2.579	1.583	0.029	0.006
Kocaeli 2	Design	Comp.	48.00	0.093	0.9602	0.657	3.747	11.664	3.211	2.347	0.033	0.013
Kobe	Design	Comp.	60.00	0.066	0.5015	0.292	1.453	10.214	1.488	0.863	0.155	0.048
Mean				0.0883	0.9308	**1.1227**	8.1913	33.2353	2.2839	2.7911	0.7034	0.9375
Standard Deviation				0.0263	0.5034	**1.5754**	12.5551	47.1309	0.8248	2.9636	**1.2166**	**2.0739**
Relative Stand Deviation				29.79%	54.08%	**140.33%**	**153.27%**	**141.81%**	36.11%	**106.18%**	**172.96%**	**221.22%**

A total of fourteen MCE-level events were applied to this bridge model. See Table 4.31 and Table 4.32 for an overview of the MCE-level longitudinal results. All MCE-level analyses of this bridge were completed, and most resulted in acceptable bridge behavior. Four cases of residual displacements exceeding the limit of 1" were recorded, including three cases of bridge collapse. An additional case of span unseating

was also recorded. The recorded foundation rotations of the upper limit friction model were also very high in some cases.

Table 4.31: MCE-Level Results Overview for Lower Limit Friction Oseligee Creek Longitudinal Model

Oseligee	Friction ".2"											
Longitudinal Motion	Ground Motion	Run Status	Run Time	Foundation Capacity (D/R)		Bearing Capacity	Bent Ductility	Max Column Shear	Max Span Disp.	Max Bent Disp.	Residual Span Disp.	Residual Bent Disp.
San Fernando 1	MCE	Comp.	48.00	0.071	0.5810	0.449	3.155	10.215	2.295	1.243	0.189	0.037
San Fernando 2	MCE	Comp.	50.00	0.089	0.8043	0.831	3.112	11.794	3.922	1.783	0.382	0.010
Imperial Valley	MCE	Comp.	60.00	0.073	0.6116	0.444	2.321	10.783	2.217	1.278	0.473	0.070
Landers	MCE	Comp.	70.00	0.082	0.6728	**4.054**	29.851	272.679	3.436	8.247	**2.855**	**3.916**
Kocaeli 1	MCE	Comp.	170.00	0.083	0.7523	0.666	3.435	10.853	3.242	1.491	0.147	0.055
Kocaeli 2	MCE	Comp.	48.00	0.080	0.6575	0.945	4.628	11.131	4.439	2.114	0.262	0.050
Kobe	MCE	Comp.	60.00	0.061	0.4281	0.401	1.911	10.212	2.154	1.146	**1.030**	0.064
Mean				0.0772	0.6439	1.1129	6.9161	48.2381	3.1005	2.4716	0.7626	0.6002
Standard Deviation				0.0093	0.1225	1.3137	10.1500	98.9707	0.9058	2.5694	0.9693	1.4623
Relative Stand Deviation				12.07%	19.02%	**118.05%**	**146.76%**	**205.17%**	29.21%	**103.96%**	**127.11%**	**243.61%**

Table 4.32: MCE-Level Results Overview for Upper Limit Friction Oseligee Creek Longitudinal Model

Oseligee	Friction ".4"											
Longitudinal Motion	Ground Motion	Run Status	Run Time	Foundation Capacity (D/R)		Bearing Capacity	Bent Ductility	Max Column Shear	Max Span Disp.	Max Bent Disp.	Residual Span Disp.	Residual Bent Disp.
San Fernando 1	MCE	Comp.	48.00	0.100	**1.0183**	0.511	3.539	10.655	2.555	1.915	0.718	0.191
San Fernando 2	MCE	Comp.	50.00	0.129	**1.4740**	0.563	3.733	14.612	3.284	1.831	0.266	0.140
Imperial Valley	MCE	Comp.	60.00	0.102	**1.0550**	0.408	3.091	11.482	2.314	1.480	0.159	0.081
Landers	MCE	Comp.	70.00	**1.473**	**1.8135**	**4.667**	41.169	125.317	3.367	9.459	**3.177**	**7.235**
Kocaeli 1	MCE	Comp.	170.00	0.277	**4.8746**	**5.097**	39.118	379.941	3.423	8.910	**3.261**	**8.900**
Kocaeli 2	MCE	Comp.	48.00	0.121	**1.4037**	**1.005**	4.924	14.827	4.769	3.130	0.020	0.021
Kobe	MCE	Comp.	60.00	0.085	0.7951	0.362	2.122	10.212	2.004	1.177	0.169	0.088
Mean				0.3267	1.7763	1.8017	13.9564	81.0067	3.1022	3.9859	1.1100	2.3794
Standard Deviation				0.5097	1.4076	2.1181	17.9181	138.3884	0.9228	3.6063	1.4574	3.9157
Relative Stand Deviation				**156.01%**	79.24%	**117.56%**	**128.39%**	**170.84%**	29.75%	90.48%	**131.29%**	**164.56%**

4.6 Little Bear Creek Bridge

Results show that the average behavior of the Little Bear Creek Bridge was favorable for design and MCE-level events. Super and substructure behaviors of this bridge were found to have acceptable behavior. Foundation performance for this bridge was mixed, and dependent on event direction. Most design-level analysis performed for

this bridge succeeded in completing except for four ground motions applied in the transverse direction. Substructure behavior appears to be adequate at column, strut and bent cap locations with the exception of foundation displacement capacities in the transverse direction of the bridge. Connection behavior also appears to be adequate from the results of each analysis with one design-level case of unseating being recorded. This bridge had three separate models analyzed in the transverse direction, two of which contain a newly designed anchor bolt configuration, while the third contains a previously designed anchor bolt configuration. A more in-depth analysis of each bridge model's results is proved in the next sections.

4.6.1 Transverse Motion

The transverse analysis for this bridge resulted in stiff structural behavior. See Table 4.33, Table 4.34 and table 4.35 for an overview of the design-level transverse results. Each of the three connection details used in this model behaved in an acceptable manner during all design-level ground motions. No bolt failure was recorded, and the old bolt configuration consists of smaller anchor bolts than the new configuration. This old configuration results in a connection that is less stiff, and some behavioral effects of this stiffness change can be observed. The model containing the old configuration experienced higher bent displacements, higher span displacement and higher bolt demands then that of the newer bolt configuration. Higher residual displacements were also observed in the older bolt configuration. These results make sense given that structures with less strength and/or stiffness have a tendency for higher displacements. Results from all transverse models indicated design-level deflections that were within acceptable limits for this bridge. Small residual displacements occurred in each ground

motion as a result of the survival of the anchor bolts as well as the lower levels of ductility that occurred during each ground motion. Transverse design-level analyses of the Little Bear Creek Bridge ran successfully with the exception of the Landers event. There was also an analysis failure in the upper limit friction model containing the new bolt configuration. This failure occurred during the first San Fernando event. Large foundation deformations were recorded in the transverse direction for every design event except the Little Skull Mountain event. This Little Skull Mountain event has generally resulted in lower bridge response throughout this project. The exact cause of these large foundation displacements can be assumed to have been caused by weaker foundation capacity and a bridge with a relatively large mass. The inertia of the bridge's components may have caused large forces to develop at the foundation level during motion.

Table 4.33: Results Overview for Lower Limit Friction Little Bear Creek Transverse Model

Little Bear Creek	Friction ".2"												
Transverse Motion	Ground Motion	Run Status	Run Time	Foundation Capacity (D/R)		Bearing Capacity	Bent Ductility	Bolt Status	Max Column Shear	Max Span Disp. (in.)	Max Bent Disp. (in.)	Residual Span Disp. (in.)	Residual Bent Disp. (in.)
San Fernando 1	Design	Comp.	48.00	**2.354**	0.3953	0.024	1.396	0.581	259.906	3.550	2.148	0.003	0.005
San Fernando 2	Design	Comp.	50.00	**2.334**	0.4396	0.022	1.573	0.529	255.101	3.773	2.178	0.001	0.004
Imperial Valley	Design	Comp.	60.00	**1.206**	0.1793	0.012	0.641	0.299	134.007	1.776	1.007	0.005	0.003
Coalinga	Design	Comp.	52.00	**1.651**	0.2475	0.016	0.875	0.380	183.425	2.439	1.418	0.000	0.001
North Palm Springs	Design	Comp.	40.00	**1.251**	0.1812	0.013	0.668	0.322	139.298	1.838	1.046	0.001	0.001
Landers	Design	Num.	27.36	**2.667**	0.5412	0.028	1.805	0.684	295.194	4.332	2.580		
Little Skull Mountain	Design	Comp.	132.00	0.631	0.0977	0.008	0.361	0.201	69.433	0.864	0.508	0.000	0.000
Kocaeli 1	Design	Comp.	170.00	**2.729**	0.4673	0.025	1.593	0.603	300.714	3.969	2.347	0.005	0.012
Kocaeli 2	Design	Comp.	48.00	**2.257**	0.3934	0.024	1.276	0.598	249.961	3.555	1.998	0.003	0.003
Kobe	Design	Comp.	60.00	0.976	0.1433	0.011	0.552	0.257	107.446	1.442	0.827	0.001	0.000
Mean				**1.7100**	0.2827	0.0171	0.9930	0.4189	188.8102	2.5786	1.4974	0.0021	0.0032
Standard Deviation				0.7340	0.1412	0.0065	0.4711	0.1593	80.6738	1.1564	0.6834	0.0019	0.0037
Relative Stand Deviation				42.93%	49.95%	38.03%	47.44%	38.02%	42.73%	44.85%	45.64%	92.69%	**115.54%**

Table 4.34: Results Overview for Upper Limit Friction Little Bear Creek Transverse Model

Little Bear Creek	Friction ".4"												
Transverse Motion	Ground Motion	Run Status	Run Time	Foundation Capacity (D/R)		Bearing Capacity	Bent Ductility	Bolt Status	Max Column Shear	Max Span Disp. (in.)	Max Bent Disp. (in.)	Residual Span Disp. (in.)	Residual Bent Disp. (in.)
San Fernando 1	Design	Num.	22.01	**2.354**	0.3953	0.024	1.395	0.581	259.828	3.544	2.146		
San Fernando 2	Design	Comp.	50.00	**2.333**	0.4396	0.022	1.573	0.528	255.064	3.773	2.178	0.001	0.000
Imperial Valley	Design	Comp.	60.00	**1.208**	0.1790	0.012	0.641	0.299	134.221	1.776	1.008	0.005	0.003
Coalinga	Design	Comp.	52.00	**1.649**	0.2457	0.015	0.877	0.378	183.276	2.437	1.416	0.001	0.003
North Palm Springs	Design	Comp.	40.00	**1.251**	0.1812	0.013	0.669	0.322	139.301	1.838	1.046	0.001	0.001
Landers	Design	Num.	26.81	**2.676**	0.5283	0.028	1.799	0.683	296.308	4.335	2.604		
Little Skull Mountain	Design	Comp.	132.00	0.631	0.0977	0.008	0.361	0.201	69.433	0.864	0.508	0.000	0.000
Kocaeli 1	Design	Comp.	170.00	**2.898**	0.4784	0.026	1.621	0.639	319.989	4.248	2.512	0.044	0.031
Kocaeli 2	Design	Comp.	48.00	**2.258**	0.3934	0.024	1.277	0.598	250.024	3.556	1.998	0.005	0.005
Kobe	Design	Comp.	60.00	0.976	0.1431	0.011	0.552	0.257	107.448	1.442	0.827	0.000	0.000
Mean				**1.4725**	0.2399	0.0151	0.8500	0.3692	162.6811	2.2410	1.2830	0.0019	0.0017
Standard Deviation				0.6405	0.1293	0.0059	0.4300	0.1447	70.3444	1.0823	0.6151	0.0022	0.0018
Relative Stand Deviation				43.50%	53.87%	39.20%	50.59%	39.20%	43.24%	48.29%	47.94%	**116.82%**	**107.99%**

Table 4.35: Results Overview for Upper Limit Friction Little Bear Creek Transverse Model with Old Bolts

Little Bear Creek	Friction ".4"												
Transverse Motion	Ground Motion	Run Status	Run Time	Foundation Capacity (D/R)		Bearing Capacity	Bent Ductility	Bolt Status	Max Column Shear	Max Span Disp. (in.)	Max Bent Disp. (in.)	Residual Span Disp. (in.)	Residual Bent Disp. (in.)
San Fernando 1	Design	Comp.	48.00	**2.221**	0.3639	0.031	1.309	0.639	244.733	3.448	2.027	0.005	0.002
San Fernando 2	Design	Comp.	50.00	**2.356**	0.4581	0.026	1.618	0.633	256.994	3.858	2.228	0.005	0.004
Imperial Valley	Design	Comp.	60.00	**1.283**	0.1884	0.017	0.677	0.428	142.614	1.924	1.086	0.007	0.005
Coalinga	Design	Comp.	52.00	**1.499**	0.2235	0.018	0.835	0.451	166.765	2.286	1.289	0.007	0.004
North Palm Springs	Design	Comp.	40.00	**1.159**	0.1688	0.021	0.621	0.519	129.902	1.927	0.988	0.002	0.002
Landers	Design	Num.	27.01	**2.667**	0.5098	0.033	1.755	0.813	295.667	4.415	2.580		
Little Skull Mountain	Design	Comp.	132.00	0.644	0.0992	0.015	0.368	0.319	70.952	0.904	0.521	0.000	0.000
Kocaeli 1	Design	Comp.	170.00	**2.720**	0.4655	0.035	1.625	0.859	300.356	4.053	2.367	0.002	0.001
Kocaeli 2	Design	Comp.	48.00	**2.207**	0.3879	0.028	1.259	0.683	245.046	3.585	1.974	0.000	0.001
Kobe	Design	Comp.	60.00	0.974	0.1398	0.017	0.526	0.372	107.606	1.449	0.789	0.001	-0.002
Mean				**1.6735**	0.2772	0.0232	0.9821	0.5448	184.9964	2.6037	1.4743	0.0034	0.0020
Standard Deviation				0.7196	0.1418	0.0070	0.4786	0.1727	78.9187	1.1506	0.6819	0.0028	0.0020
Relative Stand Deviation				43.00%	51.17%	30.23%	48.73%	31.70%	42.66%	44.19%	46.26%	80.97%	98.22%

A total of twenty-one MCE-level events were analyzed with this bridge model. See Table 4.36, Table 4.37 and table 4.38 for an overview of the MCE-level transverse results. Each of the three connection details used in this model behaved in an acceptable manner during most MCE-level events. Two cases of collapse and span unseating were recorded for MCE-level events; however these results are taken from analyses that did not result in completion. A total of seven events did not result in a complete analysis,

with three resulting in data that suggests structural failure. Foundation displacement capacity is exceeded in all transverse MCE events, just like the design-level results.

Table 4.36: MCE-Level Results Overview for Lower Limit Friction Little Bear Creek Transverse Model

Little Bear Creek	Friction ".2"											
Lateral Motion	Ground Motion	Run Status	Run Time	Foundation Capacity (D/R)		Bearing Capacity	Bent Ductility	Bolt Status	Max Column Shear	Max Span Disp.	Max Bent Disp.	Residual Span Disp.	Residual Bent Disp.
San Fernando 1	MCE	Num.	14.51	**2.497**	0.4267	0.026	1.490	0.627	275.069	3.766	2.283		
San Fernando 2	MCE	Comp.	50.00	**2.884**	0.6317	0.027	2.186	0.650	316.127	4.799	2.783	0.004	0.005
Imperial Valley	MCE	Comp.	60.00	**1.677**	0.2678	0.017	0.918	0.428	185.918	2.639	1.458	0.033	0.020
Landers	MCE	Num.	22.16	**2.503**	0.4211	0.027	1.487	0.650	277.383	3.773	2.265		
Kocaeli 1	MCE	Comp.	170.00	**3.578**	0.7628	0.036	2.401	0.887	397.417	5.662	3.293	0.091	0.093
Kocaeli 2	MCE	Fail	23.51	**4.331**	**1.2634**	**12.654**	59.610	**0.991**	416.514	12.764	32.495		
Kobe	MCE	Comp.	60.00	**1.298**	0.1939	0.017	0.759	0.415	142.944	2.019	1.140	0.007	0.004
Mean				2.6810	0.5668	1.8291	9.8360	0.6642	287.3388	5.0605	6.5309	0.0336	0.0305
Standard Deviation				1.0452	0.3645	4.7734	21.9565	0.2145	100.8447	3.6108	11.4725	0.0405	0.0423
Relative Stand Deviation				38.98%	64.31%	**260.97%**	**223.23%**	32.30%	35.10%	71.35%	**175.67%**	**120.51%**	**139.01%**

Table 4.37: MCE-Level Results Overview for Upper Limit Friction Little Bear Creek Transverse Model

Little Bear Creek	Friction ".4"											
Lateral Motion	Ground Motion	Run Status	Run Time	Foundation Capacity (D/R)		Bearing Capacity	Bent Ductility	Bolt Status	Max Column Shear	Max Span Disp.	Max Bent Disp.	Residual Span Disp.	Residual Bent Disp.
San Fernando 1	MCE	Num.	12.01	**2.491**	0.4341	0.026	1.497	0.627	274.381	3.767	2.281		
San Fernando 2	MCE	Comp.	50.00	**2.885**	0.6317	0.027	2.186	0.650	316.135	4.799	2.783	0.000	0.012
Imperial Valley	MCE	Comp.	60.00	**1.674**	0.2678	0.017	0.918	0.428	185.575	2.639	1.458	0.022	0.017
Landers	MCE	Fail	39.51	**6.282**	**1.5312**	**10.437**	31.778	**0.947**	680.943	24.092	16.503		
Kocaeli 1	MCE	Comp.	170.00	**3.575**	0.7204	0.036	2.311	0.888	397.610	5.555	3.278	0.055	0.056
Kocaeli 2	MCE	Comp.	48.00	**3.189**	0.7185	0.035	2.243	0.853	349.186	5.305	2.967	0.041	0.004
Kobe	MCE	Comp.	60.00	**1.298**	0.1939	0.017	0.757	0.416	142.918	2.017	1.138	0.007	0.005
Mean				3.0564	0.6425	1.5136	5.9557	0.6870	335.2496	6.8821	4.3440	0.0251	0.0187
Standard Deviation				1.6354	0.4447	3.9350	11.4043	0.2166	176.5650	7.7043	5.4189	0.0229	0.0216
Relative Stand Deviation				53.51%	69.22%	**259.98%**	**191.49%**	31.53%	52.67%	**111.95%**	**124.74%**	91.26%	**115.48%**

Table 4.38: MCE-Level Results Overview for Upper Limit Friction Little Bear Creek Transverse Model with Old Bolts

Little Bear Creek-Old	Friction ".4"											
Lateral Motion	Ground Motion	Run Status	Run Time	Foundation Capacity (D/R)		Bearing Capacity	Bent Ductility	Bolt Status	Max Column Shear	Max Span Disp.	Max Bent Disp.	Residual Span Disp.	Residual Bent Disp.
San Fernando 1	MCE	Num.	24.51	**2.343**	0.3916	0.033	1.396	0.683	258.183	3.663	2.149		
San Fernando 2	MCE	Comp.	50.00	**2.910**	0.6594	0.032	2.222	0.786	319.602	4.874	2.842	0.005	0.001
Imperial Valley	MCE	Comp.	60.00	**1.793**	0.3048	0.027	1.033	0.636	199.631	2.828	1.601	0.005	0.006
Landers	MCE	Fail	22.51	**3.195**	0.9328	0.381	4.242	**1.033**	311.538	6.168	3.567		
Kocaeli 1	MCE	Comp.	170.00	**2.865**	0.5116	0.292	1.958	**0.972**	321.904	5.839	3.055	0.192	0.083
Kocaeli 2	MCE	Comp.	48.00	**3.114**	0.7074	0.037	2.202	**0.914**	344.173	5.323	2.928	0.019	0.006
Kobe	MCE	Comp.	60.00	**1.301**	0.1921	0.025	0.746	0.533	142.812	2.027	1.083	0.004	0.001
Mean				2.5029	0.5285	0.1182	1.9714	0.7936	271.1205	4.3890	2.4610	0.0451	0.0194
Standard Deviation				0.7217	0.2565	0.1514	1.1536	0.1866	74.8786	1.5768	0.8827	0.0824	0.0356
Relative Stand Deviation				28.83%	48.54%	**128.17%**	58.52%	23.51%	27.62%	35.93%	35.87%	**182.64%**	**183.48%**

4.6.2 Longitudinal Motion

The longitudinal analysis for this bridge resulted in fairly consistent results. See Table 4.39 and Table 4.40 for an overview of the design-level transverse results. Maximum span displacements of about 2.5 inches occurred for most ground motions in each bridge model, and bent displacements hovered around 1.5 inches. These results are larger than expected, and may point to possible amplified bridge response. Bent ductility appears to remain below the established maximum for the second bent (2.77), with only one ground motion, (Landers) causing a ductility in excess of this limit. This excess in the upper limit friction model's ductility appears to have been caused due to a collapse of a bridge bent. Results show that this design-level event also contains large foundation displacements and a large case of span end displacements, resulting in unseating. Despite the results of the aforementioned event, all other events appear to behave in an acceptable manner. Foundation behavior in the longitudinal direction appears to suggest low shears and moments within bent columns. Bearing pad displacements also indicate constant movement and slipping, given maximum demand capacity ratios of about 0.4 for each model. Lastly the residual displacements in this direction are below the acceptable limit in all but two cases, the case of collapse and the Coalinga analysis of the lower limit bearing pad model.

Table 4.39: Results Overview for Lower Limit Friction Little Bear Creek Longitudinal Model

Little Bear Creek	Friction ".2"											
Longitudinal Motion	Ground Motion	Run Status	Run Time	Foundation Capacity (D/R)		Bearing Capacity	Bent Ductility	Max Column Shear	Max Span Disp. (in.)	Max Bent Disp. (in.)	Residual Span Disp. (in.)	Residual Bent Disp. (in.)
San Fernando 1	Design	Comp.	48.00	0.008	0.1676	0.345	0.857	149.824	1.313	0.668	0.579	0.218
San Fernando 2	Design	Comp.	50.00	0.008	0.1786	0.559	0.780	144.559	2.345	0.730	0.296	0.204
Imperial Valley	Design	Comp.	60.00	0.005	0.1399	0.415	0.674	130.554	1.638	0.563	0.176	0.197
Coalinga	Design	Comp.	52.00	0.008	0.1995	0.474	0.873	159.838	2.095	0.592	**1.357**	0.179
North Palm Springs	Design	Comp.	40.00	0.006	0.1710	0.357	0.737	115.856	1.308	0.524	0.611	0.194
Landers	Design	Comp.	70.00	0.006	0.1342	0.513	0.754	124.155	2.323	0.720	0.955	0.181
Little Skull Mountain	Design	Comp.	132.00	0.003	0.0531	0.118	0.314	77.611	0.366	0.190	0.153	0.109
Kocaeli 1	Design	Comp.	170.00	0.007	0.1713	0.524	0.729	129.000	2.197	0.706	0.143	0.186
Kocaeli 2	Design	Comp.	48.00	0.006	0.1357	0.477	0.675	116.030	1.844	0.516	0.101	0.215
Kobe	Design	Comp.	60.00	0.005	0.1041	0.287	0.646	105.904	1.002	0.480	0.303	0.190
Mean				0.0062	0.1455	0.4068	0.7039	125.3332	1.6431	0.5688	0.4674	0.1873
Standard Deviation				0.0015	0.0426	0.1338	0.1560	23.6488	0.6472	0.1612	0.4139	0.0305
Relative Stand Deviation				24.86%	29.27%	32.90%	22.16%	18.87%	39.39%	28.34%	88.56%	16.29%

Table 4.40: Results Overview for Upper Limit Friction Little Bear Creek Longitudinal Model

Little Bear Creek	Friction ".4"											
Longitudinal Motion	Ground Motion	Run Status	Run Time	Foundation Capacity (D/R)		Bearing Capacity	Bent Ductility	Max Column Shear	Max Span Disp. (in.)	Max Bent Disp. (in.)	Residual Span Disp. (in.)	Residual Bent Disp. (in.)
San Fernando 1	Design	Comp.	48.00	0.008	0.1212	0.311	0.675	164.178	1.412	0.517	0.162	0.108
San Fernando 2	Design	Comp.	50.00	0.012	0.2992	0.523	1.184	238.002	2.430	0.919	0.374	0.222
Imperial Valley	Design	Comp.	60.00	0.009	0.1736	0.437	0.832	170.966	1.919	0.817	0.065	0.138
Coalinga	Design	Comp.	52.00	0.013	0.2789	0.589	1.191	241.389	2.754	0.989	0.255	0.174
North Palm Springs	Design	Comp.	40.00	0.011	0.2734	0.494	1.118	218.942	2.265	0.851	0.461	0.201
Landers	Design	Comp.	70.00	**1.107**	0.1748	**5.097**	10.408	146.902	28.140	14.851	**4.316**	**1.146**
Little Skull Mountain	Design	Comp.	132.00	0.003	0.0554	0.118	0.314	77.611	0.366	0.190	0.153	0.110
Kocaeli 1	Design	Comp.	170.00	0.011	0.1958	0.441	0.843	201.198	1.966	0.736	0.093	0.156
Kocaeli 2	Design	Comp.	48.00	0.008	0.1368	0.364	0.657	153.498	1.629	0.479	0.331	0.128
Kobe	Design	Comp.	60.00	0.007	0.1185	0.327	0.598	140.905	1.452	0.425	0.153	0.107
Mean				0.1189	0.1828	0.8700	1.7820	175.3592	4.4333	2.0774	0.6363	0.2490
Standard Deviation				0.3473	0.0800	**1.4909**	3.0438	50.5801	8.3557	4.4952	**1.2992**	0.3177
Relative Stand Deviation				**292.04%**	43.77%	**171.37%**	**170.81%**	28.84%	**188.48%**	**216.39%**	**204.19%**	**127.58%**

A total of fourteen MCE-level events were applied to this bridge model. See Table 4.41 and Table 4.42 for an overview of the MCE-level longitudinal results. All of the MCE-level analyses were completed, resulting in acceptable bridge behavior. A single case of residual displacement exceedance was observed in the lower bound friction model during the Landers event.

Table 4.41: MCE-Level Results Overview for Lower Limit Friction Little Bear Creek Longitudinal Model

Little Bear Creek	Friction ".2"											
Longitudinal Motion	Ground Motion	Run Status	Run Time	Foundation Capacity (D/R)		Bearing Capacity	Bent Ductility	Max Column Shear	Max Span Disp.	Max Bent Disp.	Residual Span Disp.	Residual Bent Disp.
San Fernando 1	MCE	Comp.	48.00	0.008	0.1676	0.345	0.857	149.824	1.313	0.668	0.579	0.218
San Fernando 2	MCE	Comp.	50.00	0.009	0.1736	0.704	0.922	178.721	3.010	0.889	0.819	0.200
Imperial Valley	MCE	Comp.	60.00	0.006	0.1470	0.657	0.753	151.814	2.802	0.671	0.469	0.177
Landers	MCE	Comp.	70.00	0.007	0.1550	0.686	0.910	145.619	3.050	0.863	**1.776**	0.118
Kocaeli 1	MCE	Comp.	170.00	0.009	0.2198	0.471	0.896	168.571	1.978	0.799	0.477	0.188
Kocaeli 2	MCE	Comp.	48.00	0.008	0.1457	0.666	0.781	157.187	2.641	0.708	0.239	0.235
Kobe	MCE	Comp.	60.00	0.006	0.1258	0.388	0.745	115.832	1.506	0.577	0.408	0.171
Mean				0.0076	0.1621	0.5595	0.8377	152.5095	2.3286	0.7394	0.6810	0.1867
Standard Deviation				0.0011	0.0299	0.1534	0.0765	19.8633	0.7229	0.1143	0.5140	0.0378
Relative Stand Deviation				14.69%	18.44%	27.42%	9.13%	13.02%	31.05%	15.46%	75.47%	20.22%

Table 4.42: MCE-Level Results Overview for Upper Limit Friction Little Bear Creek Longitudinal Model

Little Bear Creek	Friction ".4"											
Longitudinal Motion	Ground Motion	Run Status	Run Time	Foundation Capacity (D/R)		Bearing Capacity	Bent Ductility	Max Column Shear	Max Span Disp.	Max Bent Disp.	Residual Span Disp.	Residual Bent Disp.
San Fernando 1	MCE	Comp.	48.00	0.008	0.1212	0.311	0.675	164.178	1.412	0.517	0.162	0.108
San Fernando 2	MCE	Comp.	50.00	0.013	0.3085	0.585	1.258	253.462	2.791	1.232	0.330	0.236
Imperial Valley	MCE	Comp.	60.00	0.013	0.2124	0.612	1.143	247.484	2.851	1.119	0.440	0.157
Landers	MCE	Comp.	70.00	0.014	0.2992	0.491	1.209	260.593	2.354	0.910	0.104	0.075
Kocaeli 1	MCE	Comp.	170.00	0.013	0.2881	0.623	1.165	240.275	2.820	1.133	0.053	0.201
Kocaeli 2	MCE	Comp.	48.00	0.011	0.2530	0.535	1.062	206.596	2.541	0.930	0.496	0.205
Kobe	MCE	Comp.	60.00	0.009	0.1623	0.481	0.830	181.152	2.425	0.774	0.138	0.155
Mean				0.0115	0.2350	0.5197	1.0489	221.9626	2.4564	0.9450	0.2461	0.1624
Standard Deviation				0.0021	0.0724	0.1075	0.2159	38.1048	0.5016	0.2456	0.1748	0.0569
Relative Stand Deviation				18.15%	30.80%	20.68%	20.58%	17.17%	20.42%	25.99%	71.01%	35.01%

4.7 Summary of Results

Overall each bridge in these analysis contained some flaw or behavior that will need to be improved upon, but the majority of analyses provided results deemed acceptable. A summary of critical events taken from all design-level analyses can be found in Table 4.43. A summary of critical events taken from all MCE-level analyses can be found in Table 4.44. The Bent Creek Road Bridge consistently produced partially complete analyses, but the few that did result in completion suggested adequate performance. The Scarham Creek Bridge demonstrated expected behaviors in regards to

overall design-level performance, utilizing large displacements as a method of surviving the earthquake. The Scarham model did however present large foundation displacements. The MCE-level behavior for the Scarham Bridge proved to be less than acceptable. Incomplete analyses were present in most MCE-level longitudinal events along with high displacements. These results indicate the need for additional design considerations of tall substructure long span bridges like the Scarham Creek Bridge, design considerations regarding P-delta and stability concerns. The Norfolk Southern Railroad Bridge behaved as a stiff bridge would, results of these analyses include lower displacements and anchor bolt connection failure. Despite this, bridge behavior still remained within the range of acceptable behavior at the design level and MCE-level. The Oseligee Creek Bridge presented the challenge of a 100% scour condition during an earthquake event. Total bent collapse occurred in both directions of motion, at both design and MCE-level events. Special design actions may need to be implemented in order to prevent occurrences like this. The Little Bear Creek Bridge performed acceptably under most ground motions. This bridge was also used to compare old bolt configurations with code specified configurations. The new bolt configurations caused a slight increase in overall bridge performance in that it reduced overall deflections of the structure. This reduction of overall deflection does not necessarily result in better seismic bridge behavior for all bridges, and greater connection stiffness can actually lead to damage in other components of the bridge. The main reason for selection of the new connection anchor bolt is the redundancy that it provides for the connection, as well as an increase in the connection shear capacity. An isolated occurrence of bent collapse was

observed in the design-level analysis of the Little Bear Creek Bridge. Conclusions and design recommendations will be provided in the next chapter of this thesis.

Table 4.43: Summary of Critical Design-Level Analysis Behaviors

Bridge Case	Number of Analyses	Critical Analysis Behaviors
Bent Creek Bridge	40	16 cases of unfinished analysis
		6 cases of foundation displacement exceedance
Scarham Creek Bridge	40	Foundation Displacement exceedance in all longitudinal events
Norfolk Southern Bridge	40	3 cases of unfinished analysis
		1 case of residual displacement exceedance
Oseligee Creek Bridge	40	17 cases of Foundation Rotation exceedance
		3 cases of residual displacement exceedance
		3 cases of bent collapse
Little Bear Creek	50	4 cases of unfinished analysis
		25 cases of foundation displacement exceedance
		1 case of bent collapse
		2 cases of residual displacement exceedance

Table 4.44: Summary of Critical MCE-Level Analysis Behaviors

Bridge Case	Number of Analyses	Critical Analysis Behaviors
Bent Creek Bridge	28	10 cases of unfinished analysis
		1 case of residual displacement exceedance
		7 cases of foundation displacement exceedance
Scarham Creek Bridge	28	Foundation Displacement exceedance in all longitudinal events
		8 cases of unfinished analysis
		1 case of residual displacement exceedance
Norfolk Southern Bridge	28	4 cases of unfinished analysis
		1 case of bent collapse
		1 case of span unseating
		2 cases of residual displacement exceedance
Oseligee Creek Bridge	28	17 cases of Foundation Rotation exceedance
		7 cases of residual displacement exceedance
		4 cases of bent collapse
Little Bear Creek	35	7 cases of unfinished analysis
		21 cases of foundation displacement exceedance
		2 cases of bent collapse
		1 case of residual displacement exceedance

Chapter 5: Summary, Conclusions and Recommendations

5.1 Summary

The Alabama Department of Transportation (ALDOT) is in the process of updating their seismic design procedure by adopting AASHTO's LRFD Bridge Design Specifications and the AASHTO's LRFD Seismic Bridge Design Guide Specification. The use of the Guide Specifications is limited to bridges classified as "non-critical" and "non-essential." Analysis was requested by ALDOT regarding the applicability of the Guide Specifications design on current bridges in the state, and the behavior of these redesigned bridges when subjected to the seismic hazards present in the state. If this analysis was able to conclude that the behavior of these redesigned bridges was adequate for critical and essential bridge performance, then it could be concluded that the Guide Specifications could be adopted for use in the design of critical and essential bridges in the state of Alabama due to the moderate hazard.

In this thesis, analyses were performed on redesigned bridge models in an attempt to determine these bridges behaviors when subjected to seismic hazards found in the state. An initial literature review was performed in order to determine the function and behavior of concrete bridges during seismic events, as well as determine the most critical failure modes and damage associated with seismic loading of bridges. Three main behaviors were selected as the primary cause of bridge failure during seismic events: foundation failure, unseating of spans, and column failure. A suite of five bridges was

selected from a list of bridges designed and constructed in Alabama. These bridges were redesigned according to the Guide Specifications for use in this analysis. Next an analysis of Alabama's seismic hazard was performed, and ground motions were selected and scaled to represent this hazard. Bridges were then modeled in CSIBridge and analyzed using a nonlinear time history analysis. The results of these analysis concluded that the average behavior for most of the bridges is acceptable for use in critical and essential bridges. Design recommendations for each of these bridges are provided in the next section in order to improve overall seismic performance.

5.2 Conclusions

Based on the analysis performed in this project, the following conclusions regarding the performance and implementation of the Guide Specifications design on Alabama bridges were reached:

- Ground Motions that represent the hazard for northern Alabama are difficult to acquire, and scaling of worldwide ground motions is required in order to simulate this hazard.
- The two largest seismic hazards locations in Alabama contain unique hazards that each control different natural period bridges. One hazard location controls longer period bridges (Northwest Alabama), and the other controls shorter period bridges (Northeast Alabama).
- Current connection details at end span locations of highway bridges exhibit adequate strength and ductility for design-level seismic events. Failures of these connections were only observed in cases of excessive bent and span displacements, indicating structural collapse of bridge bents.

- Highway bridges designed with stiffer substructures using the Guide Specifications behave in a manner that is considered safe and result in usability after a seismic event.
- Bridges resting on weaker or scour-able soils will require additional analysis in order to determine lateral foundation and soil capacities, as well as capacities of substructure displacement. Increase in foundation and column sizes may be required if soil cannot provide adequate lateral resistance.
- Bridges with tall substructures will require additional p-delta analysis for larger displacements.
- Critical and Essential bridges can be designed using the AASHTO Guide Specifications in the state of Alabama, with minor additional analysis.

5.3 Recommendations

The following are a few additional tasks that have been recommended for completion after the culmination of the work performed in this thesis:

- The comparison of results obtained from the models described in this thesis with the results obtained from the geotechnical foundation models analyzed and discussed by Kane (2013).
- Performance of a dynamic lateral loading test on a real bridge bent designed to conform to the Guide Specifications. This test would help evaluate inelastic behavior of bridge bents.

References

AASHTO. (2002). *Standard Specifications for Highway Bridges* (17th ed.). Washington DC: American Association of State Highway and Transportation Officials.

AASHTO. (2007). AASHTO Ground Motion Parameters Calculator Version 2.1. Washington DC.

AASHTO. (2009). *LRFD Bridge Design Specifications* (4th ed.). Washington DC: American Association of State Highway and Transportation Officials.

AASHTO. (2011). *Guide Specifications for LRFD Seismic Bridge Design* (2nd ed.). Washington DC: American Association of State Highway and Transportation Officials.

AISC. (2005). *Steel Construction Manual* (13th ed.). United States: American Institute of Steel Construction.

Alabama DOT. (2012, November 30). *ALDOT Standard Details.* Alabama Department of Transportation.

ATC/MCEER Joint Venture. (2003). *Recommended LRFD Guidelines for the Seismic Design of Highway Briges.* Federal Highway Administration.

Barker, R. M., & Puckett, J. A. (2007). *Design of Highway Bridges An LRFD Approach.* Hoboken, NJ: John Wiley & Sons.

BSI. (2013). *FB-MultiPier v4.18.* Gainesville, Florida: BSI.

Caltrans. (1994, June). Bridge Bearings. *Memo to designers 7-1*, pp. 1-12.

Caltrans. (2011, October). *Bridge Design Specifciations: Chapter 1.* Retrieved February 18, 2013, from California Department of Transportation: http://www.dot.ca.gov/hq/esc/techpubs/manual/bridgemanuals/bridge-design-practice/pdf/bdp_1.pdf

Chen, W.-F., & Duan, L. (2000). *Bridge Engineering Seismic Design.* Boca Raton: CRC Press.

Chopra, A. K. (2007). *Dynamics of Structures.* Upper Saddle River, NJ: Pearson Prentice Hall.

Computer and Structures Inc. (2012). *CSI Bridge 15.* Berkely, CA: Computer and Structures, Inc.

Computers & Structures inc. (2012, August 02). Caltrans vs. fiber hinge. Berkley, California, United States of America.

Corporation, P. T. (2007). *Mathcad 14.* Needham, MA: Parametric Technology Corporation.

Coulston, P. J., & Marshall, J. D. (2011). *Influence of the LRFD Bridge Design Specifications on Seismic Design in Alabama.* Auburn University, Auburn, AL.

EERI. (2001, November). Preliminary Observations on the Southern Peru Earthquake of June 23, 2001. *Learning from Earthquakes*, pp. 3-11.

Kane, K. M. (2013). *Response of Deep Foundations to Seismic Loads in Alabama.* Auburn University, Auburn.

Law, J. D. (2013). *Update of Bridge Design Standards in Alabama for AASHTO LRFD Seismic Design Requirements.* Auburn, AL: Auburn University.

Lin, C.-C. J., Hung, H.-H., Liu, K.-Y., & Chai, J.-F. (2008). RECONNAISSANCE REPORT OF 0512 CHINA WENCHUAN. *The 14th World Conference on Earthquake Engineering* (pp. 1-9). Bejing: NCREE.

PEER. (2010). *PEER Ground Motion Database*. Retrieved September 20, 2013, from PEER Ground Motion Database: http://peer.berkeley.edu/peer_ground_motion_database/spectras/21713/unscaled_searches/new

PTC. (2007). Mathcad. Needham, Massachusetts, USA.

Rodriguez-Marek, A. (2007). *DYNAMIC RESPONSE OF BRIDGES TO NEAR-FAULT, FORWARD DIRECTIVITY GROUND MOTIONS.* Pullman: Washington State Transportation Center.

Steelman, J. S., Fahnestock, L. A., Filipov, E. T., LaFave, J. M., Hajjar, J. F., & Foutch, D. A. (2012, April 24). Shear and Friction Response of Non-Seismic Laminated Elastomeric Bridge Bearings Subject to Seismic Demands. *Journal of Bridge Engineering*, pp. 1-15.

StructurePoint. (2012). *spColumn.* StructurePoint, LLC.

Tobias, D. H., Anderson, R. E., Hodel, C. E., Kramer, W. M., Wahab, R. M., & Chaput, R. J. (2008, August). Overview of Earthquake Resisting System Design and Retrofit Strategy for Bridges in Illinois. *Practice Periodical on Structural Design and Construction*, pp. 148-152.

USGS. (2013, May 17). *2008 Interactive Deaggregations*. Retrieved September 17, 2013, from USGS: https://geohazards.usgs.gov/deaggint/2008/

Wight, J. K., & MacGregor, J. G. (2009). *Reinforced Concrete: Mechanics and Design.* Upper Saddle River, NJ: Pearson Prentice Hall.

Wotherspoon, L., Bradshaw, A., Green, R., Wood, C., Palermo, A., Cubrinovski, M., & Bradley, B. (2011). Performance of bridges during the 2010 Darfield and 2011 Christchurch earthquakes. *Seismological Research Letters Volume 82*, 961-962.

Yen, W.-H. P., Chen, G., Buckle, i., Allen, T., Alzamora, D., Ger, J., & Arias, J. G. (2011). *Post-Earthquake Reconnaissance Report on Transportation Infrastructure:*. McLean, VA : U.S. Department of Transportation.

APPENDIX A: GROUND MOTIONS

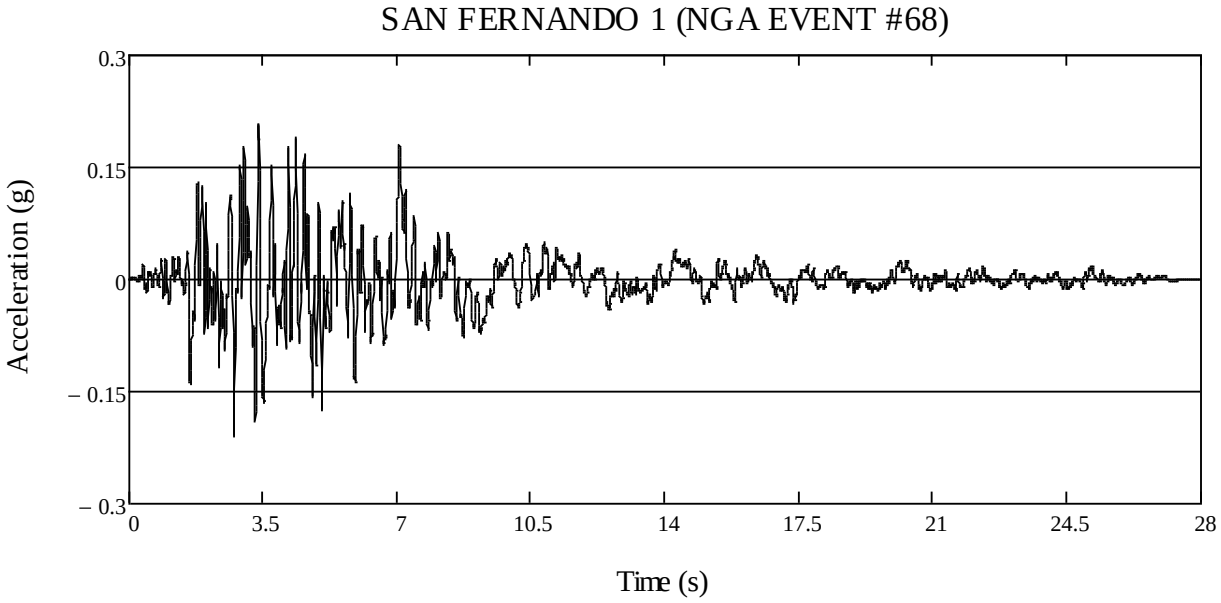

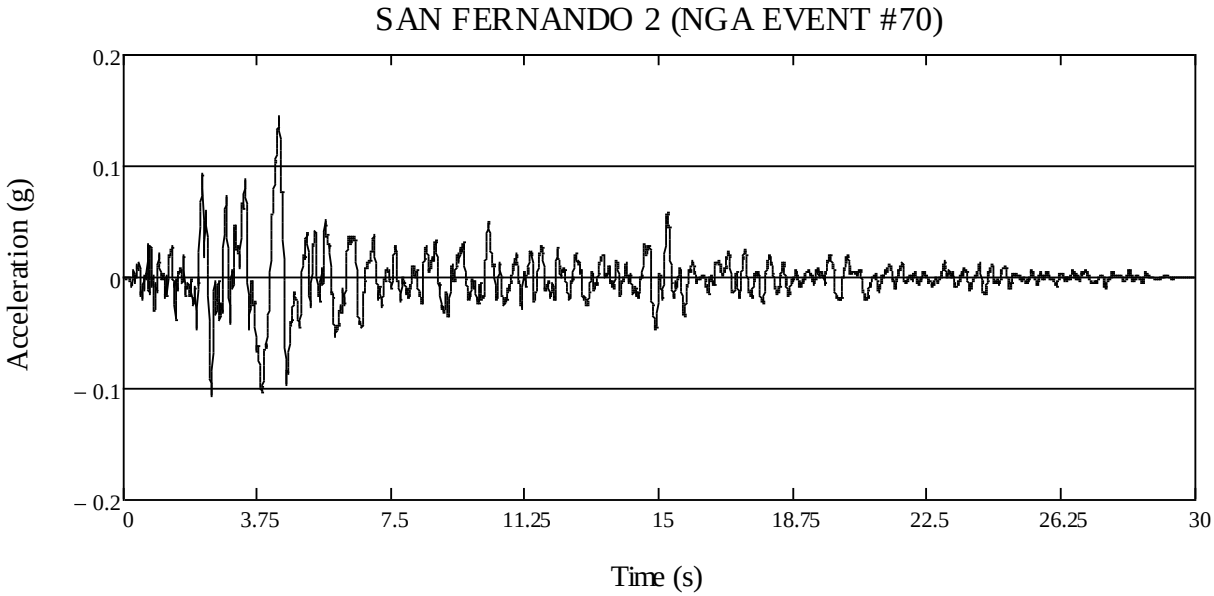

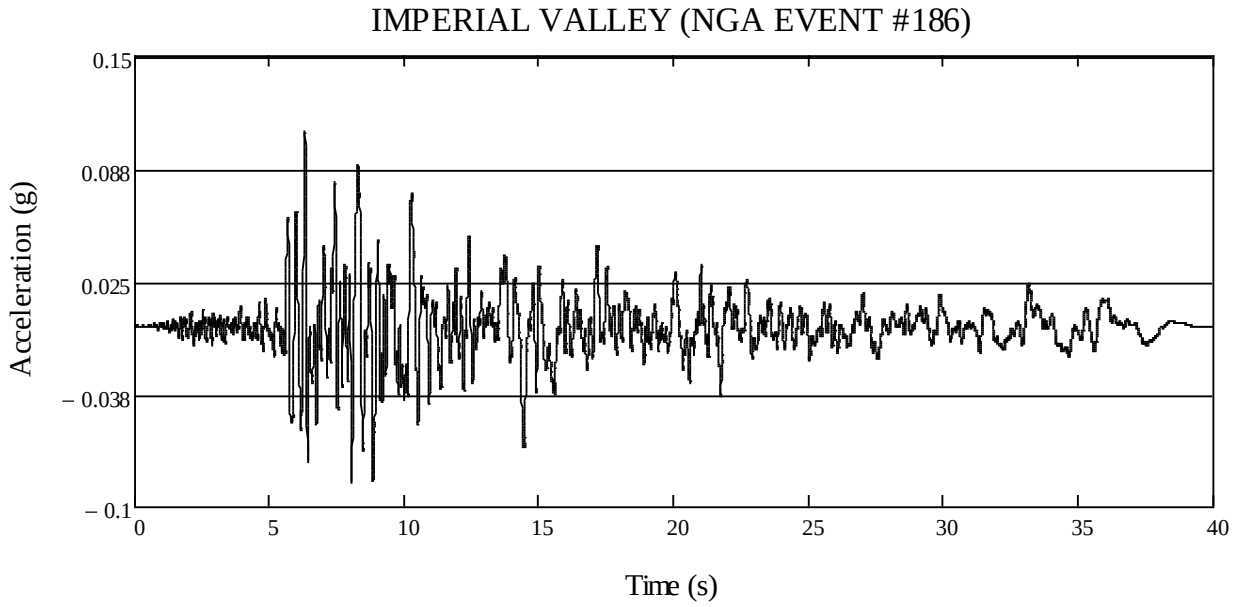
IMPERIAL VALLEY (NGA EVENT #186)
Acceleration (g)
0.15
0.088
0.025
– 0.038
– 0.1
0
5
10
15
20
25
30
35
40
Time (s)

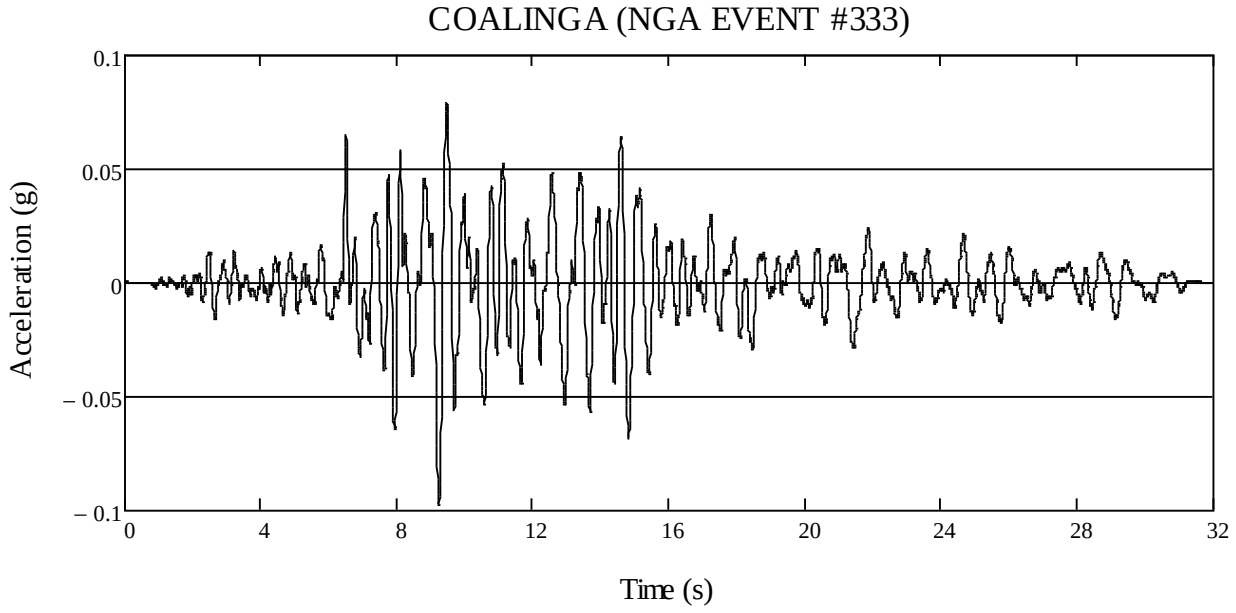
COALINGA (NGA EVENT #333)
Acceleration (g)
0.1
0.05
0
– 0.05
– 0.1
0
4
8
12
16
20
24
28
32
Time (s)

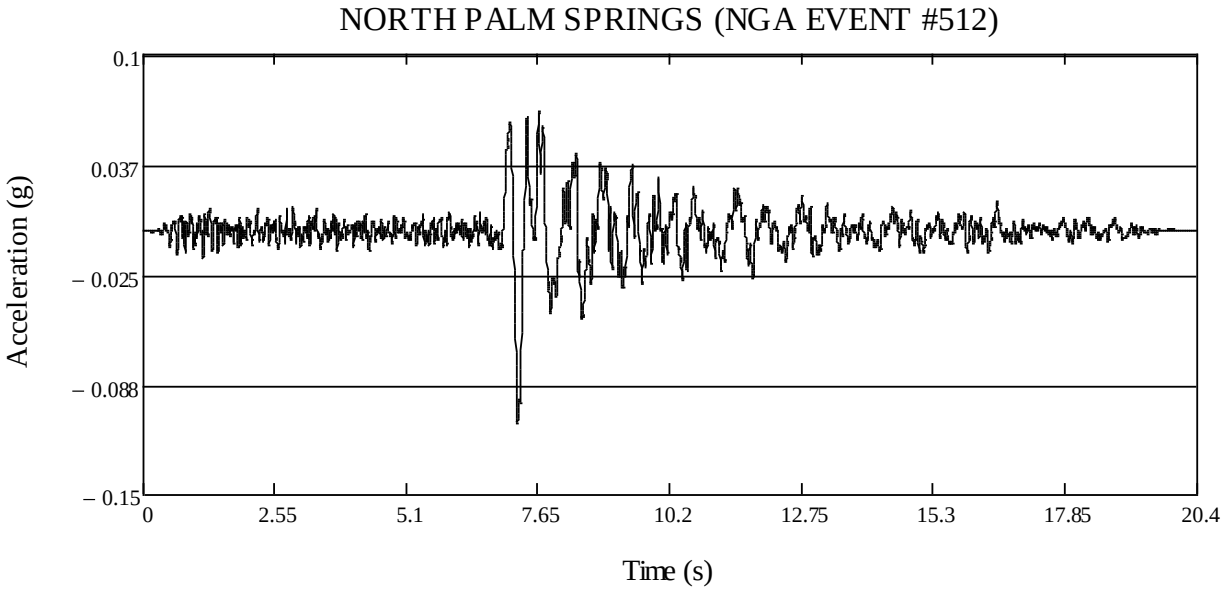
NORTH PALM SPRINGS (NGA EVENT #512)
Acceleration (g)
0.1
0.037
– 0.025
– 0.088
– 0.15
0
2.55
5.1
7.65
10.2
12.75
15.3
17.85
20.4
Time (s)

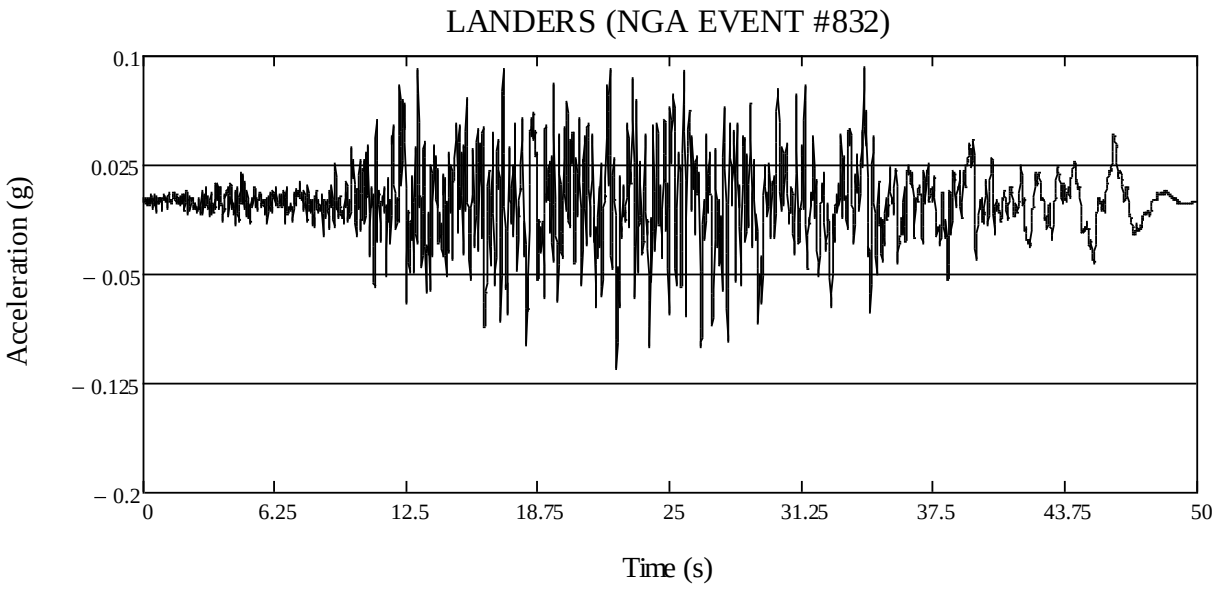
LANDERS (NGA EVENT #832)
Acceleration (g)
0.1
0.025
– 0.05
– 0.125
– 0.2
0
6.25
12.5
18.75
25
31.25
37.5
43.75
50
Time (s)

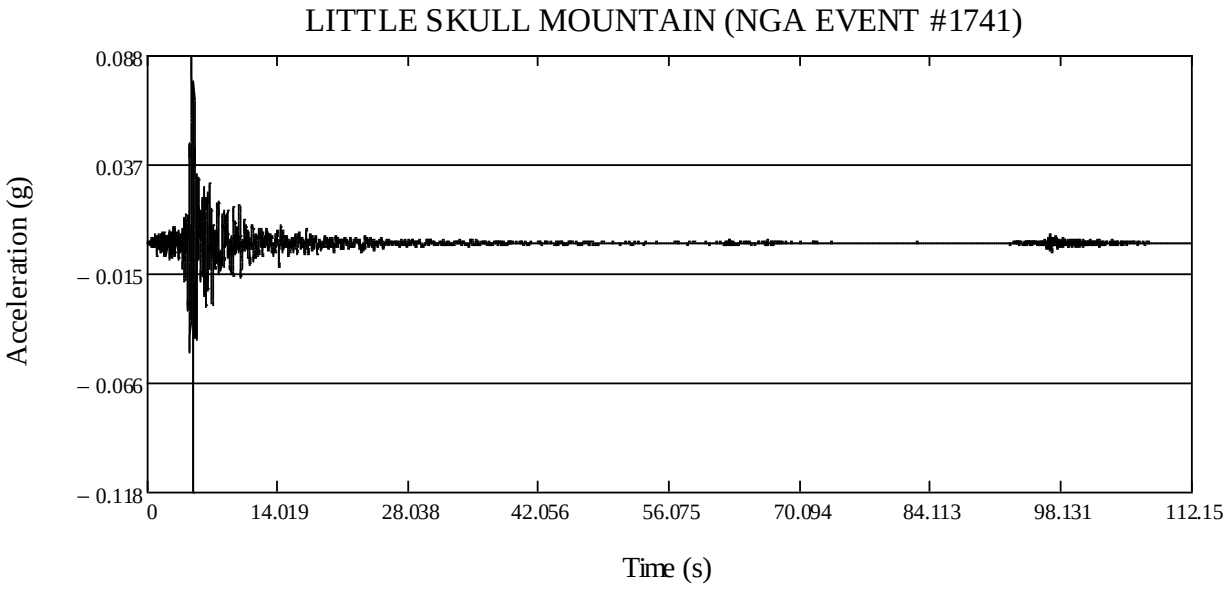
LITTLE SKULL MOUNTAIN (NGA EVENT #1741)
0.088
0.037
– 0.015
– 0.066
– 0.118
Acceleration (g)
0
14.019
28.038
42.056
56.075
70.094
84.113
98.131
112.15
Time (s)

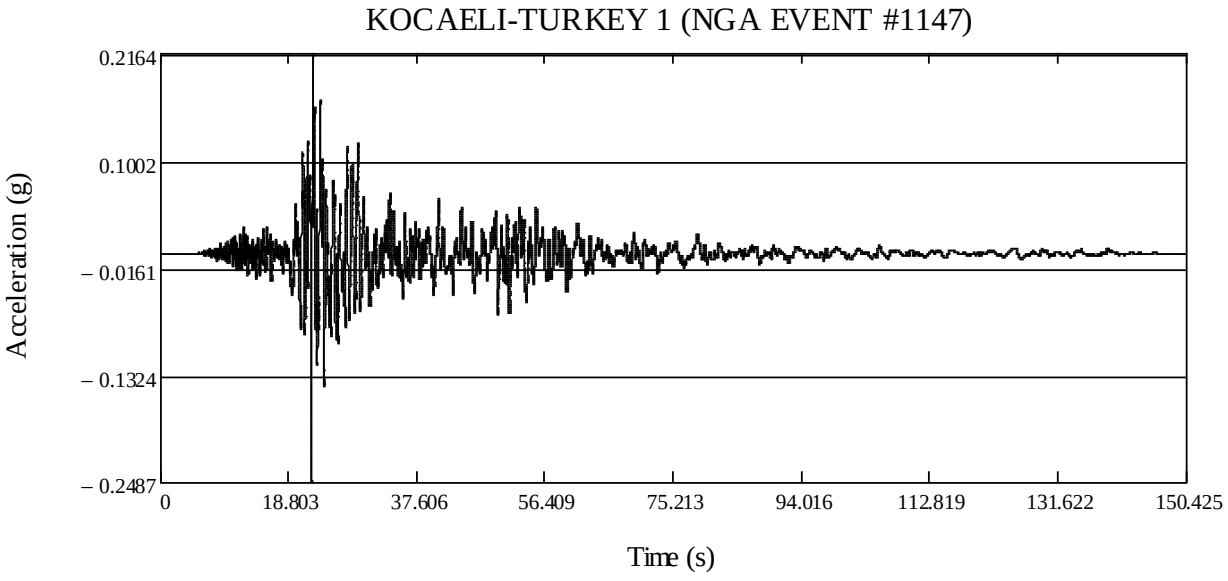
KOCAELI-TURKEY 1 (NGA EVENT #1147)
0.2164
0.1002
– 0.0161
– 0.1324
– 0.2487
Acceleration (g)
0
18.803
37.606
56.409
75.213
94.016
112.819
131.622
150.425
Time (s)

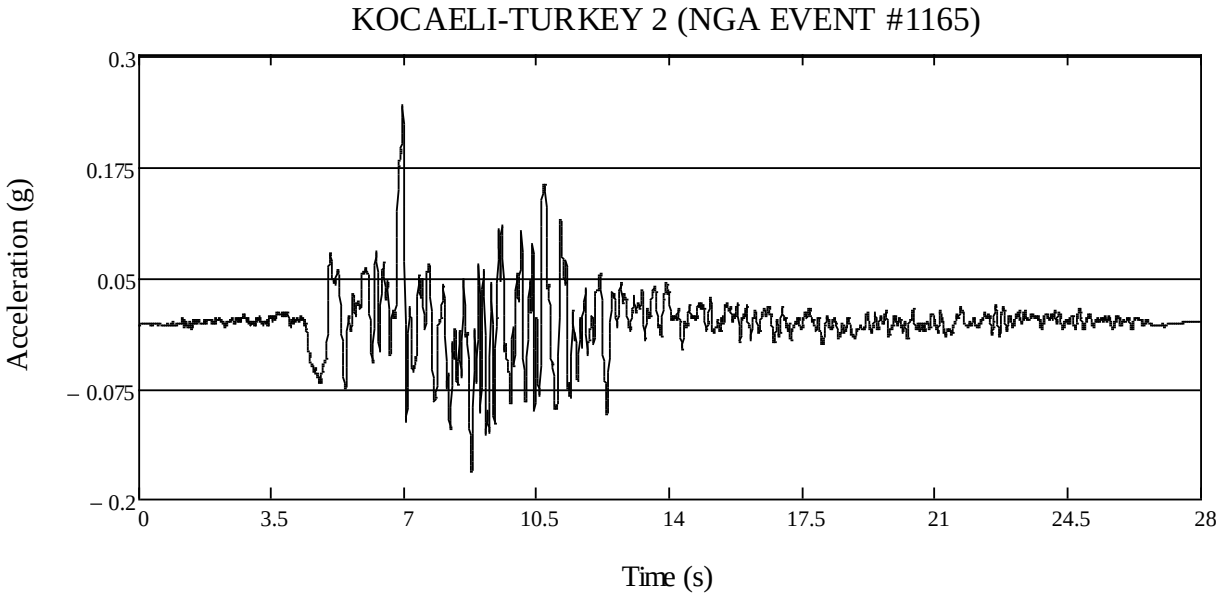
KOCAELI-TURKEY 2 (NGA EVENT #1165)
Acceleration (g)
0.3
0.175
0.05
– 0.075
– 0.2
0
3.5
7
10.5
14
17.5
21
24.5
28
Time (s)

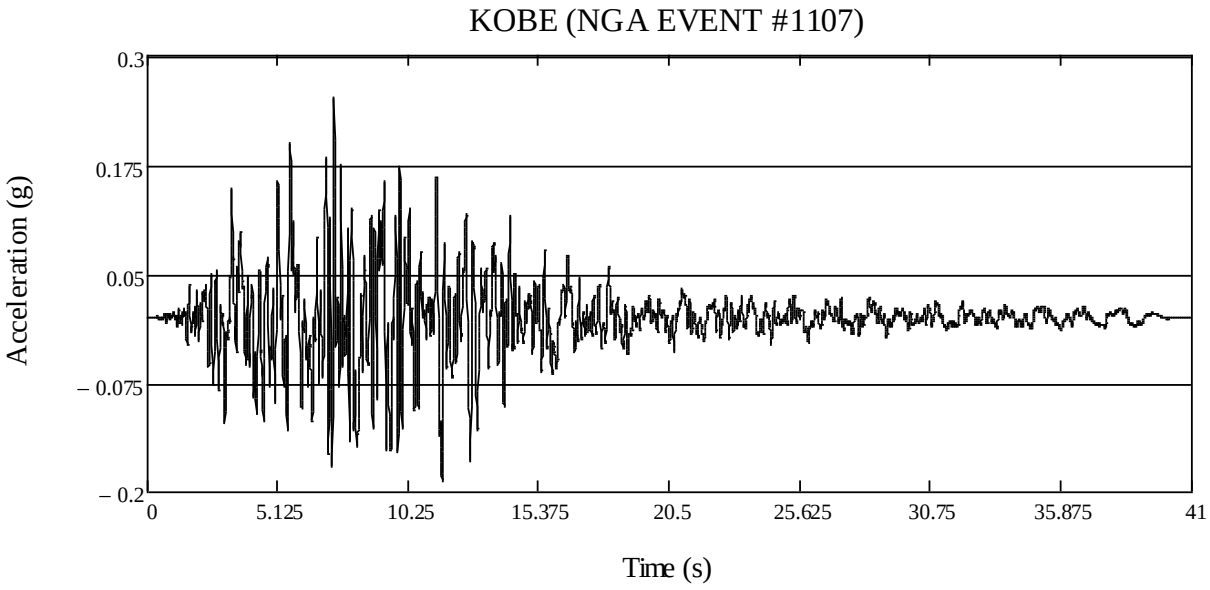
KOBE (NGA EVENT #1107)
Acceleration (g)
0.3
0.175
0.05
– 0.075
– 0.2
0
5.125
10.25
15.375
20.5
25.625
30.75
35.875
41
Time (s)